NASA Technical Memorandum 86785

IN-40199

The Handling Qualities and Flight Characteristics of the Grumman Design 698 Simulated Twin-Engine Tilt Nacelle V/STOL Aircraft

Megan A. Eskey and Samuel B. Wilson, III

June 1986

National Aeronautics and
Space Administration

NASA Technical Memorandum 86785

The Handling Qualities and Flight Characteristics of the Grumman Design 698 Simulated Twin-Engine Tilt Nacelle V/STOL Aircraft

Megan A. Eskey,
Samuel B. Wilson, III, Ames Research Center, Moffett Field, California

June 1986

National Aeronautics and
Space Administration

Ames Research Center
Moffett Field, California 94035

SUMMARY

This paper describes three government-conducted, piloted flight simulations of the Grumman Design 698 vertical and short takeoff and landing (V/STOL) aircraft. Emphasis is placed on the aircraft's handling qualities as rated by various NASA, Navy, and Grumman Aerospace Corporation pilots with flight experience ranging from conventional takeoff and landing (CTOL) to V/STOL aircraft. Each successive simulation incorporated modifications to the aircraft in order to resolve the flight problems which were of most concern to the pilots in the previous simulation. The objective of the first simulation was to assess the basic handling qualities of the aircraft with the noncross-shafted propulsion system. The objective of the second simulation was to examine the effects of incorporating the cross-shafted propulsion system. The objective of the third simulation was to examine single-engine-inoperative characteristics with and without cross-shafted engines.

INTRODUCTION

The purpose of the first simulation (Phase I) was to evaluate the basic handling qualities and flight characteristics of the aircraft (using the noncross-shafted engines) with the objective of identifying areas requiring aerodynamic, propulsion, or flight-control improvements. The objective of the second simulation (Phase II) was to evaluate the handling qualities of the aircraft with the modifications which were added in an attempt to resolve the flight problems which had been of greatest concern to the pilots in the first simulation. An empirical model of the cross-shafted propulsion system, including variable-inlet guide vane effects, was incorporated and preliminary tests were made in preparation for the third simulation. The control system for this and the previous (noncross-shafted) propulsion configuration was refined. The objectives of the third simulation (Phase III) were to evaluate one-engine-inoperative (OEI) characteristics for both the cross-shafted and noncross-shafted configurations and to evaluate a series of proposed flight-control-system configurations. Emphasis was placed on defining a satisfactory, final, control-system configuration for a proposed demonstrator aircraft.

The Grumman Design 698 aircraft is a twin-turbofan-powered vertical short takeoff and landing (V/STOL) aircraft, which the military could utilize as high-altitude, vertical takeoff and landing (VTOL) radar platform (ref. 1). It also has potential for civil applications requiring high-speed short takeoff and vertical landing (STOVL) operations (ref. 2). The Design 698-411 is powered by two standard General Electric TF34-GE-100 high-bypass-ratio turbofans that facilitate both vertical flight and efficient, high-subsonic cruise at altitude. Two CTF-34 engines

(modified versions of the standard TF34-GE-100 engines) are used in the cross-shafted version. Vertical flight is achieved by tilting the engines on an integral structure. Attitude control in the three axes is achieved via the forces and moments produced by the control vanes located in the fan-exhaust flow (fig. 1) (ref. 3). The cross-shafted version uses variable-inlet guide vanes (VIGVs) which modulate thrust by transferring shaft horsepower from one engine to the other, thereby providing an alternate means for roll-attitude control. The mathematical model was based on the wind tunnel tests conducted at NASA Ames Research Center (ARC) (ref. 4) and on other tests conducted by Grumman.

Several features of this airplane are of interest to the U.S. military. The attitude-control vanes in the fan exhaust flow resolve one of the major problems of fixed-wing, jet-lift, V/STOL aircraft: attitude control at speeds below the velocity for minimum control (VMC). The control vanes are the primary stabilization and control effectors when the aircraft is flying below 120 knots. The control vanes can induce a thrust perpendicular to the axis of the engine with a magnitude of up to 30% of the total thrust. This force is generated under the center of mass of the aircraft, so that the pitch and roll attitude is controlled by a moment which is generated by a single unopposed force. When the nacelles are near 5°, the horizontal vanes control pitch and roll, and the vertical vane controls yaw. In the hover mode (when the nacelles are near 90°), the horizontal vanes control pitch and yaw and the vertical vane controls roll. One function of the control system is to coordinate these controls as a function of nacelle angle. The geometric placement of the vanes with respect to the center of gravity provides the proper angular control. However, the force developed by the vane acts in a direction to provide acceleration in the opposite direction to the acceleration provided by the angular motion. This is an effect known as adverse-nonminimum-phase (NMP) acceleration response. The force is in the opposite direction to the desired direction of travel, so a "negative" acceleration is the first result of the pilot's input. This unusual characteristic, which could produce a pilot-induced oscillation (PIO), is much like the effect produced by the elevator on a close-coupled conventional airplane. The advantage of these vanes is that the force is produced without having to bleed the engines or distribute high-pressure air around the airframe, and the thrust loss is less than 1% of the total installed thrust or 6% of the axial thrust (fig. 2). This force-attitude control system can be used with almost any conventional high-bypass-ratio turbofan that can be tilted and operated vertically.

SIMULATION FACILITIES

These simulations were performed on the Vertical Motion Simulator (VMS) at NASA ARC using the Sigma 8 computer and the four-window Singer-Link Computer-Generated Image (CGI) system (ref. 5). The VMS has six degrees of freedom, with the vertical and lateral directions having the most translational capability; there is limited travel in the longitudinal direction (fig. 3). The cab can be easily rotated 90° to provide more travel in the longitudinal direction at the expense of the lateral movement. The interchangeable cab facility makes it possible to change the entire

cab as opposed to changing only the inside layout. This gives the researcher the option of making major cab modifications to duplicate the cockpit of the actual aircraft being simulated without incurring the usual facility downtime. As these were initial simulations, the cockpit layouts were not critiqued by the pilots; nevertheless, they are shown here for completeness (figs. 4a and 4b). The heads-up display (HUD) was based on work done for the Navy by Systems Technology, Inc., during the simulations of medium-speed, "Type A" V/STOL aircraft at ARC (ref. 6). The HUD served as a reference by which the pilot could evaluate his performance (figs. 5a and 5b). The power-management quadrant (figs. 6a and 6b) is one type of V/STOL console refined by simulations at ARC over the past decade (refs. 7-10).

DESCRIPTION

Phase I

The two control systems used in Phase I (the first simulation) consisted of one classical system with single-axis control laws and a second, modern, "space-state," control system, using direct digital design with uncoupled velocity control and attitude control. The classical control system provided individual control of pitch, roll, and yaw using aerodynamic control surfaces, control vanes, and direct control of altitude rate/position (via thrust magnitude) and surge velocity (via nacelle tilt). The modern control system was a direct-digital, integrated flight/propulsion controller designed to provide the pilot with uncoupled flightpath control and attitude control in all axes (ref. 11).

The power-management quadrant shown in figure 6a was used in the first simulation. This quandrant has three levers: one for direct control of the thrust magnitude (the throttle power lever), another for control of the engine position relative to the fuselage (adjusting the nacelle angle), and a third lever (the flightpath controller/velocity command lever) to provide the pilot with discrete control of longitudinal acceleration and vertical velocity. The throttle power lever controlled thrust directly via the power-level angle (PLA) and the nacelle rate-command switch on the lever commanded nacelle angle directly. The paddle switch on this lever was used to disconnect the flightpath lever (FPL) and return the system to direct control. The thumbwheel controlled the nacelle by commanding acceleration and deceleration through a closed acceleration loop-feedback system.

In the the classical control system, the longitudinal stick motion provided pitch control and the lateral stick motion provided roll control. A standard "coolie hat" was provided to effect trim. In the modern system, the momentary on the right top hat selected spot hover or heading command and the proportional top hat commanded longitudinal and lateral accelerations. In both systems, the rudder pedals provided yaw control. A detailed explanation of the classical control system can be found in table 1. The primary response characteristics at 15 knots to stimulus from the stick, rudder pedals, heave-rate control, and surge are shown in appendix A.

The test matrix used in Phase I is shown in table 2. The flight experience of the five evaluation pilots ranged from conventional takeoff and landing (CTOL) to V/STOL aircraft (table 3). The tasks used to evaulate the aircraft included spot turns over a VTOL landing pad and an approach to and landing on an LPH ship (fig. 7). In addition, the pilots landed on a DD-963 destroyer, but because of time limitations, pilot ratings were not recorded for this task. The typical flightpath from fixed-wing flight to touchdown involves mode changes and the use of different control inputs in different regions of flight. Each region contains multiple control modes (see table 1). The regions of flight are labeled as level flight, glide-slope descent, and station-keeping (fig. 8).

The pilots used the Cooper-Harper Handling Qualities Rating (HQR) Scale (fig. 9) (ref. 12) to rate the performance of the aircraft. Level I performance (pilot ratings of 1, 2, or 3) is defined as "satifactory, requiring no improvement and minimal pilot compensation." Level II performance (ratings of 4, 5, or 6) is "unsatisfactory but acceptable, requiring some pilot compensation." Level III flight performance (ratings of 7, 8, or 9) is "unacceptable, requiring significant pilot compensation for control of the vehicle." An HQR of 10 is given if the aircraft is uncontrollable.

Phase II

The control system used in Phase II was the classical system with single-axis control laws. Improvements were made to the control system of the noncross-shafted propulsion system configuration. A similar control system was designed utilizing a cross-shafted propulsion system. For purposes of pilot training and evaluation, all changes made to the control system could be cancelled, thus returning to the baseline Phase I configuration. Because of the changes to the original control system, the power-management quadrant was also modified. The nacelle-angle controller was removed, and all necessary controls were confined to two levers and a center controller-stick (fig. 6b). Minor improvements were made to the HUD (fig. 5b). A detailed explanation of each control mode and its flight condition can be found in table 4. At below 50 knots, the two control modes available are the standard mode and the precision mode. The standard mode control is via the stick, and the precision mode utilizes both the stick and TRC button. Up to 160 knots, flight control options include an automatic flightpath augmentation mode and manual throttle-and-nacelle-tilt mode. At above 160 knots, both heading and altitude holds are available as well as manual throttle.

The test matrix used in this simulation is shown in table 5. The tasks used to evaluate the aircraft performance included spot turns above a VTOL pad, shipboard hover tests over a DD-963-class destroyer, up-and-away flight to station-keeping and partial conversion to landing on an LPH ship, and outbound conversion after vertical lift-off from an LPH. A list of the pilots and a brief description of their past experiences are given in table 3.

Most of the testing was done with the VMS cab rotated 90° for greater motion in the longitudinal direction because the greatest portion of the flight regime included acceleration in both the longitudinal and vertical directions. The VMS is capable of handling the responses (such as the lateral adverse NMP characteristic) even with the cab rotated for maximum longitudinal travel; the lateral acceleration is significant only in hover.

Some unsatisfactory aircraft chracteristics observed in Phase I were an adverse-NMP linear-acceleration response in both the longitudinal and lateral axes, a large thrust-response lag at low power settings, and adverse ground effects. The primary modifications included the use of the vertical-vane deflection as a thrust spoiling method, the addition of the cross-shafted propulsion system model, and the implementation of two velocity- and attitude-control modes (standard and precision) for speeds below 50 knots (13).

The cross-shafted engine included VIGVs, which produced differential thrust with a conservative time constant of 0.2 sec. In the Navy Type A V/STOL simulation investigation at ARC, a VIGV time constant of 0.05 sec was used (14). As a comparison exercise, the time constant of the TF-34 VIGVs was changed to 0.05, which considerably improved the thrust response. In Phase III, the time constant was kept at 0.05 sec for the entire simulation.

The vertical vanes were used as speed brakes (thrust spoilers); they were manually commanded by the pilot before nacelle unlock. The splayed vertical vanes then automatically augmented flightpath control by keeping the throttle or the PLA high, thus reducing the engine-response lag.

In the standard mode, horizontal and vertical vane deflections were used to control roll and pitch. This mode functioned essentially as surge and sway control for the classical system in Phase I. Longitudinal acceleration control was provided through pitch-attitude command on the stick, by manual nacelle tilt in the manual throttle mode, or by using the thumbwheel in the flightpath augmentation mode. Lateral acceleration control was provided through bank-attitude command with the stick. Height was controlled by using either the manual throttle or the vertical velocity control (VVC) button with the heave mode engaged.

The precision mode was available only when the flightpath augmentation mode was also engaged. Surge- and sway-control was provided through the translational rate command (TRC) button which was independent of pitch- and roll-attitude control, or through the stick with minimal pitch- and roll-attitude control (fig. 6b). Longitudinal acceleration was controlled with the thumbwheel; longitudinal velocity was controlled with either the stick or TRC button. The lateral TRC button or the lateral stick was used to control sway. In the precision mode, a combination of nacelle tilt and horizontal vane deflection was used for pitch and surge control. Vertical-vane deflection and differential thrust were used for roll- and sway-control.

Phase III

In order to correct some undesirable flight characteristics identified in Phase II and to more thoroughly examine both the cross-shafted and noncross-shafted configurations, several modifications were made to the mathematical model in the third simulation. A third vertical vane was added to the noncross-shafted configuration to generate larger control moments. The three-vane configuration also permitted vane overtravel (up to 70°) for the investigation of roll-control capabilities following noncross-shafted engine failure. Six roll-control modes were made available in hover and low-speed flight conditions in order to define the most desirable control configuration. The PLA limit schedule was modified to give the pilot the ability to stay within a more realistic transition corridor. The strake angle was allowed to vary in order to isolate the impact of ground effects on the aircraft handling qualities during landing. Flightpath command gains were modified to provide improved flightpath control. Finally, the rates and scheduling of the speedbrakes were modified to reduce pitch and height transients which accompanied a configuration change (15).

Simulation-engine-failure- and pilot-ejection capabilities were added to the model in order to investigate the aircraft's OEI characteristics and the pilot's ejection response. Cross-shafted, single-engine failures were modeled so that the core thrust of the failed engine reduced to zero in approximately 1.0 sec, and the total fan torque available became one-half of its prior value divided between the two fans. Noncross-shafted, single-engine failures were modeled so that all of the propulsive thrust of the failed engine dropped to zero in 1.0 sec. In addition, all accompanying propulsion-induced aerodynamics were modeled.

In the event of an engine failure of either the cross-shafted or noncross-shafted configuration, engine speed brakes were automatically retracted. For noncross-shafted engine failures, the three vertical vanes on the operative engine were automatically programmed to their maximum overtravel positions to counter the rolling moment caused by the loss of thrust of the failed engine. Engine failure logic for the cross-shafted configuration assumed that an engine failure could be detected within 3 sec. For the noncross-shafted configuration, a rapid drop of core RPM exceeding 50% of its starting value triggered the related engine-failure logic to adjust the vertical vanes.

In addition to the motion of the aircraft and visual cues provided by the CGI system, the pilot was provided with an engine failure warning on the HUD. The pilot was instructed to eject by using an ejection ring placed on the seat between his legs if he felt the aircraft could not be safely controlled. Initiation of ejection stopped the aircraft motion and allowed the critical ejection parameters to be recorded.

The control modes used were essentially the same as in Phase II. There were, however, six hover-control modes available (table 6). Modes 1 (cross-shafted configuration) and 2 (noncross-shafted configuration) were the standard modes which used only the vertical vanes to control roll attitude. These modes exhibited the maximum adverse-NMP acceleration behavior. Mode 1P (P for precision) used vertical

vanes and VIGVs for roll-attitude control and mode 2P used vertical vanes and differential engine RPM for roll-attitude control. Both modes reduced the adverse NMP-acceleration behavior and provided lateral gust rejection. The TRC button was available for both modes 1P and 2P. In mode 3 (the cross-shafted configuration), the VIGVs alone controlled roll attitude. There was no adverse NMP-acceleration response. Mode 4 (also with cross-shafting) controlled the roll rate using the VIGVs and also exhibited zero adverse NMP-acceleration. Mode 2P had slower response characteristics than the other modes. The dynamic response characteristics of the longitudinal stick, top hat, and surge wheel with no wind is shown in Appendix B. Also shown are the lateral stick and top hat dynamic-response characteristics for the various control modes in no-wind conditions.

The HUD and the power-management quadrant were satisfactory in Phase II. The speed brake arm button on the second lever became the nacelle arm in Phase III, and the low airspeed and vector display on the HUD were modified for clarity (figs. 5b and 6b).

The test matrix, shown in table 7, was constructed to investigate the OEI characteristics throughout the flight envelope and to evaluate the lateral control modes of hover and low-speed flight. Four tasks were flown with varied combinations of control modes and environmental conditions. The tasks included a complete inbound transition to station keeping on the port side of an LPH, an approach to and landing on an LPH, an approach to and landing on a DD-963 destroyer, and spot turns over a VTOL pad. Figure 8 illustrates the inbound transition profile. The evaluation pilots (table 3) were informed that engine failure could occur at any time during any task. If a failure occurred, they were to attempt to recover the aircraft by converting to a clean configuration (landing gear up, nacelles completely down, and speed brakes stowed). If a pilot felt recovery was not possible, he was to eject.

DISCUSSION OF RESULTS

Phase I

Pilot ratings for the inbound transition and landing on an LPH are shown in table 8 and the ratings for the hover tasks over the VTOL pad are shown in table 9. Pilots rated most of the hover tasks as "adequate," but the spot turns were rated "inadequate" with HQRs as high as 10 ("controllable") in a 25-knot wind. Pilot work load is especially high for the spot turns because the pilot must control the nacelle and throttle position with his left hand while coordinating pitch and roll attitude with his right. Pilots recommended better visual cues on the CGI pad to improve their ability to sense motion in the VMS.

Pilots rated the inbound transition to landing on the deck of an LPH as "essentially adequate with room for improvement." The pilots had the most difficulty descending toward and touching down on the deck, with HQRs ranging from 2 to 8

depending on the control system used and the velocity of the wind over the deck (WOD).

The pilots were asked to achieve a sink rate of 300 ft/min out-of-ground-effect (OGE) and allow the aircraft to settle to the deck. Figure 10 shows the trim requirements as a function of height and nacelle diameter. This high level of sink rate was rarely achieved at touchdown primarily because of the cushioning characteristics of the lift in-ground-effect caused by the fountain which is formed when the two engine exhaust streams merge beneath the fuselage. Reduction of this lifting force could not be successfully countered by reducing engine power either manually through the PLA or automatically in the heave control mode. The lifting force produced a fountain that caused the aircraft to float. In addition, a nose-up pitching moment occurred when the horizontal vanes tried to counteract the attitude change from the fountain effect. The adverse-NMP acceleration caused the vane deflection to product a rearward motion. The pilots had some difficulty landing on either the LPH or the DD-963 because of the strong ground effects of the aircraft. The tendency of the aircraft to float on the cushion of air caused the aircraft to remain in ground effect (IGE) longer, producing the rearward drift identified by the pilots. When the nacelle angle was controlled, either manually or via the surge mode, this drift was countered. However, the precision of the landing could not be controlled to desired accuracy without undue pilot compensation during a normal workload period. The landing distributions are shown in figure 11.

Various control-system characteristics were identified by the pilots as needing improvement. The high-speed aerodynamic spoilers provided sufficient roll, but produced excessive yaw. More precise location of the spoilers in the successive simulations would increase the roll effectiveness by 50% and reduce the "proverse" yaw effectiveness by 40%, providing satisfactory roll performance. This would also improve the spoiler/rudder relationship.

Thrust levels and response characteristics are key factors in the ability of pilots to control the aircraft. The level and response time of the thrust determine the ability to spool down, the ability to spool up, the effect of the gyroscopic moments, the sensitivity of glide-slope control, the amount of ground-effect control, and the sensitivity of the throttle control. Thrust levels are low for most phases of flight other than hover and engine response is slower at low thrust levels (figs. 12 and 13). The thrust behavior could be improved by modulating the trim thrust, predicated on the profile to be flown. The trim thrust could be modulated by using the vertical vanes as speed brakes. This would also desensitize the thrust/nacelle relationship, allowing the pilot to reduce his work load.

The pilots felt that the initial deceleration and acceleration capability via the surge mode (which depends on nacelle tilt) was too low. The capability was then increased from 0.15 to 0.30 g. Although this helped the pilots to decelerate quickly on the glide slope and to make rapid and precise velocity corrections near the ship, the subsequent trim thrust was lowered, thereby reducing the engine-response characteristic. To maintain altitude and stay within the prescribed glide slope, the pilots had to increase power when decelerating. A need was identified for a nacelle-control scheme, which would provide the pilot with proper thrust

behavior while staying within the physical constraints of the aircraft. Implementation of scheduled rate limits and anticipatory cues to the thrust command would probably improve nacelle behavior.

The adverse NMP-acceleration response was noticed by the pilots when executing tight position control of the vehicle while landing or making spot turns. The pilot would bank the aircraft to create a lateral translation, but before the translation was effected by the bank angle, the aircraft accelerated in the opposite direction because of the horizontal force from the vane deflection. The correct translation then occurred as the thrust vector from the bank angle took over. The level of acceleration during the translation was also reduced because of the side force of the vertical vane. To compensate, the pilot would adjust the lateral stick, resulting in PIO. This inherent vehicle characteristic was worsened by the design of the classical control system, which was purposefully designed to be simplistic in nature without correcting for this previously known behavior. In addition, no command filter was tried in Phase I. The NMP acceleration response can be minimized, however, by integrating all control effectors. The use of differential thrust to provide the pure rolling moment in conjunction with the correct vertical vane motion will alleviate the lateral-axis, NMP difficulties, and the integration of the nacelle deflection with the deflection of the horizontal vanes will alleviate the longitudinal-axis NMP difficulties.

PIO occurred out of ground effect (OGE) in the lateral axis, becoming more pronounced when IGE. The PIO can be attributed to a combination of a large time delay in the aircraft's response and to unstable ground-effects. Height control was difficult because of a strong positive lift created by the fountain formed when the two exhaust streams merged beneath the fuselage (ref. 16). Longitudinal position could not be held during hover because of the risk of a nose-up pitching-moment IGE. Pilot-generated, nose-down inputs induced a negative X-force on the vertical vanes, resulting in a rearward aircraft acceleration which compounded the effect.

Phase II

The use of the flightpath augmentor was generally preferred over the manual throttle and nacelle tilt. However, during the inbound transition, the engine-inlet-separation boundary stop was often reached (the scheduled PLA minimum) whether the manual throttle or the flightpath augmentor was used. A computer-controlled stop was implemented to ensure that the pilot never reached the engine-inlet-stall conditions. Each pilot had a preferred method of decelerating; all of the pilots rated the handling qualities at Level II ("unsatisfactory but acceptable, requiring some pilot compensation") when using the manual throttle and at Level I ("satisfactory") with the flightpath augmentor engaged (fig. 14). The VVC improved handling qualities by reducing PIO during low-speed and hover operations. Only during the outbound transition was the manual throttle preferred (fig. 15). The aircraft was unable to effectively hold altitude when the VVC was used during the conversion from hover to forward flight unless the pilot adjusted the flightpath lever.

The precision mode of velocity and attitude control eliminated the adverse NMP response at the aircraft's c.g. by using a combination of automatic nacelle tilt longitudinally and differential engine thrust laterally. In the standard mode, however, only the longitudinal adverse-NMP response was eliminated (using the surge-command system); the lateral adverse-NMP response remained a problem. As the thumb-wheel controlled surge and the lateral stick controlled sway, an additional problem arose with a separation of lateral and longitudinal control.

Although the precision mode eliminated the adverse NMP response, a large time delay (0.1 - 0.2 sec) in the translational response remained. The capabilities of the precision mode were not fully realized, for the pilots tended to automatically use the center stick instead of the TRC button. As a result, improvements in the pilots ratings for the precision mode over the standard mode were not significant.

For the shipboard landing task, each pilot's experience and the technique that was used determined the HQRs given. Pilots with V/STOL experience flew with greater precision (a higher "gain") than CTOL pilots and thereby encountered deficiencies that the CTOL pilots did not encounter. Level II ratings were then given, even with the precision mode engaged (figs. 16-19).

Figure 16 shows the range of HQRs given by each of the pilots who attempted an inbound transition to landing on an LPH. The ratings of 10 were given given by the pilots with V/STOL experience, whereas the ratings below 3 were given by the pilots with CTOL experience. An average of the ratings is shown in figure 17. The individual ratings of each pilot who attempted an inbound transition to landing on a DD-963 destroyer are shown in figure 18, and the averaged values are shown in figure 19. Pilot ratings were essentially equal (a difference of one-half an HQR) for the cross-shafted and noncross-shafted systems. This was the expected result, for the difference in thrust-response time-constants was minimal.

Figure 20 presents the touchdown dispersion results on the LPH deck for each pilot using each control system mode. The pilots were asked to select a touchdown position using any information they perceived and could duplicate based on the CGI visuals. The pilots used the deck markings and the ship's elevator as reference points. Neither an increase in the velocity of the WOD nor an increase in turbulence affected the pilots' performance. A comparison of the touchdown accuracies for each control made coincides with the pilots' ratings for landing on the LPH (fig. 17). The pilots' performances improved with the use of the precision control mode, and remained essentially the same for the cross-shafted and noncross-shafted engine configurations.

The touchdown dispersions for landings on the DD-963 destroyer are shown in figure 21. The pilots used the hangar door and the touchdown markings for visual references. The landing positions were skewed down and to the right along the approach path due to the tendency of pilots to pull away from the hangar door. Also, the pilots centered the aircraft on the pad based on their position, whereas

the aircraft's c.g. (the data reference point) is approximately 12 ft aft of the pilot. As shown in the pilots' ratings (fig. 19), the performance for each control mode is essentially equal.

As expected, use of the vertical vanes as speed brakes improved both the acceleration and deceleration as well as the flightpath-control characteristics of the aircraft. However, pitch and height-coupling transients occurred when the vanes automatically changed position. By increasing the splaying time-constant on the vertical vanes, the transients were partially eliminated.

For spot turns over the VTOL pad, flightpath augmentation was preferred over manual throttle, and the precision mode was preferred over the standard mode. The pilots were not able to maintain position in 25 knot crosswinds; futhermore, only by using full lateral stick could they maintain position in 15-knot crosswinds (fig. 22).

Phase III

The simulated aircraft exhibited no better than Level 2 handling qualities while using any of the control modes. This may have been caused partially by simulator fidelity limitations caused by computational delays, lack of real-world visual cues in the simulated image, and unrealistic motion cues (ref. 17). There was an improvement from Level 3 to Level 2 handling qualities when control modes 1P, 2P, and 3 (with reduced or eliminated adverse-NMP acceleration responses) were used rather than modes 1 and 2 (fig. 23).

Touchdown dispersion results for landings on an LPH ship using control modes 1, 1P, 2, and 2P are shown in figures 24a-d. The pilots were asked to land at their own preferred position on deck using whatever visual cues were available. A scaled figure of a man was placed on deck for some of the earlier runs, and later, more deck markings were added. No combination of extra visual cues seemed to make a difference in the accuracy of the touchdowns, however.

The pilots landed using only the stick using the top hat, and using their own "best way." Since each pilot had his own preferred landing position, the touchdown data points are grouped in clusters.

The use of attitude command (mode 3) over rate command (mode 4) yielded an improvement of approximately one-half an HQR during the day and one HQR at night (fig. 25). Using modes 3 and 4, pilots landed on the LPH in day and night conditions. The touchdown dispersion results are shown in figures 26a-d.

No significant difference in handling qualities between mode 1P (which has an attitude command/translational-rate-command combination) and 3 (pure attitude command) was observed in either sea state 3 or sea state 5 (fig. 27). In addition, a degradation of approximately 1 HQR occurred when operating in high sea states rather

than in moderate sea states using either control mode. Landing distributions on a DD-963 are shown in figures 28a-d. The pilots tended to pull away from the hangar door, skewing the results down and to the right.

In the spot-turn task, desired and adequate performance was defined as keeping the entire aircraft (with a wing span of 40 ft) within an 80-ft or a 120-ft diameter circle. In 15-knot winds, desired performance was achieved with surge on and adequate performance was achieved with surge off (fig. 29). In 25-knot winds, adequate performance was achieved with surge on and unsatisfactory performance was achieved with surge off.

Varying the strake angle provided inconclusive results. However, the ground effects seemed to affect the pilots far less than in the previous simulations. This is probably traceable to pilot technique, as the pilots tended to increase their sink rate and spend less time IGE.

The minimum recovery speed for this aircraft (the lowest airspeed at which a single engine failure can occur and consistent recoveries are possible) is approximately 60 knots with cross-shafted engines (fig. 30). Below that speed, the pilot must eject. For the noncross-shafted configuration, the minimum recovery speed is approximately twice that (117 knots) (fig. 31).

Within the recoverable region, altitude loss following a single engine failure with cross-shafted engines remained consistently below the Grumman prediction which ranged from 600 ft at 60 knots to 100 ft at 160 knots (fig. 32). For the noncross-shafted engine configuration, the altitude loss ranged from 2400 ft at 120 knots to 340 ft at 200 knots (fig. 33).

Following a single-engine failure below the minimum recovery speed, the mean time from failure to ejection initiation was 2.1 sec with cross-shafted engines (fig. 34) and 1.8 sec with noncross-shafted engines (fig. 35). All ejections made following a single-engine failure with cross shafted engines during a nominal inbound transition were performed safely. A safe ejection is defined as an ejection within the safety envelope of the MK.10 ejection seat, which is a typical contemporary ejection seat. Approximately two-thirds of the ejections made following a single-engine failure, with noncross-shafted engines, during a nominal inbound transition were performed within the bank angle, altitude, and sink-rate safety limits.

Following a single-engine failure within recovery limits, recovery was accomplished by converting to a clean configuration. No attempt was made to stabilize at a partially converted configuration.

CONCLUSIONS

Three government-conducted simulations of the Grumman design 698 V/STOL aircraft have been successfully completed. The classical control system was adequate for the tasks attempted, such as landing on a DD-963 destroyer in a moderate-sea state and on an LPH in heavy seas. Although the simulation pilots had diverse backgrounds, all of them mastered the aircraft with the classical control system. The pilots who had no VTOL experience exhibited a steep learning curve. One important addition was the use of engine tilt with pitch command to reduce the adverse-NMP characteristics and to increase the knots per degree of stick input. A second improvement was the addition of VIGVs and cross-shafted engines for OEI operation. This also provided the means for using differential engine thrust for roll control and direct side force for lateral translation.

Based on HQRs, touchdown performance measurements and pilots' comments, a precision mode of flight control architecture would be required on a demonstrator or a production Design 698 configuration. The definition of response type alone, however, would not ensure satisfactory handling qualities. In hover and in low-speed flight, the pilot is primarily concerned with control of relative linear acceleration, velocity, and position. This concern places requirements on both transient and steady-state translational response. As a result, the elimination of the aircraft's characteristic adverse-NMP linear response would be required with any flight control architecture. In addition, selection of either a satisfactory steady-state linear acceleration response or velocity response with an attitude command architecture would be required.

Based primarily on performance results, a surge system is required for hover and low-speed operations. This system, however, does not deliver desired performance in moderate to high winds mainly because of the limit on side-force generation through roll-attitude and vertical vane deflection; a significant degradation in shipboard launch and recovery ability in moderate to high crosswinds may result.

Based on minimum recovery speed, altitude loss, and ejection capability following a single engine failure, any two-engine configuration should incorporate cross-shafting.

During any designated power approach scenario, the pilot should attempt to maximize flight time above the minimum recovery speed and above an altitude greater than the maximum corresponding altitude loss, thus minimizing flight time below these speed and altitude limits.

APPENDIX A

PRIMARY RESPONSE CHARACTERISTICS

The figures in appendix A illustrate the primary response characteristics at 15 KEAS to stimulus from the stick, rudder pedals, heave rate control, and surge. These responses were generated on the GAC 6DOF computer program and were used to verify the NASA Ames model.

ALFA	angle of attack, deg
AXPIL	acceleration at the pilot station, x direction, g
AYPIL	acceleration at pilot station, y direction, g
AZPIL	acceleration at the pilot station, z direction, g
BETA	sideslip angle, deg
DEL ALT	incremental altitude change, ft
DELFWD	incremental forward position of the aircraft, ft
GTH LT	gross thrust, left engine, lb/100
HDOT	rate of change of altitude, ft/s
LT VANEH	left horizontal vane deflection, deg
NACEL LT	left nacelle deflection, deg
P	body angular velocity, deg/s
PHI	Euler bank angle of the aircraft, deg
PSI	Euler heading angle, deg
QDOT	Pitch rate acceleration in body axis, deg/s^2
RR	Yaw rate at body axis, ft/s
RRDOT	Yaw axis acceleration, ft/s^2
THET	pitch attitude, deg

TLEVX/PL	power level angle, deg
VEQUI	equivalent airspeed, knots

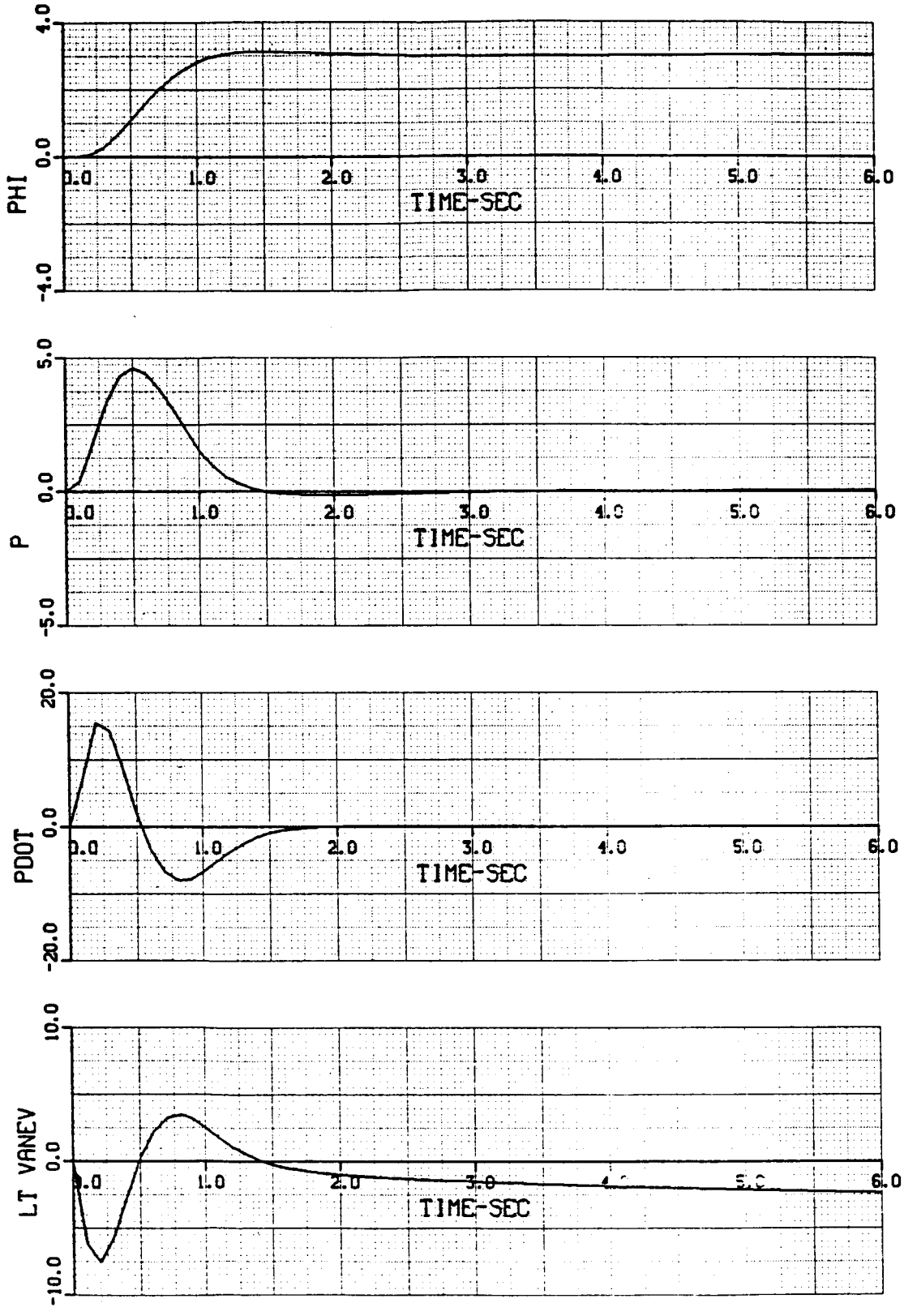

Figure A1.- Lateral stick input.

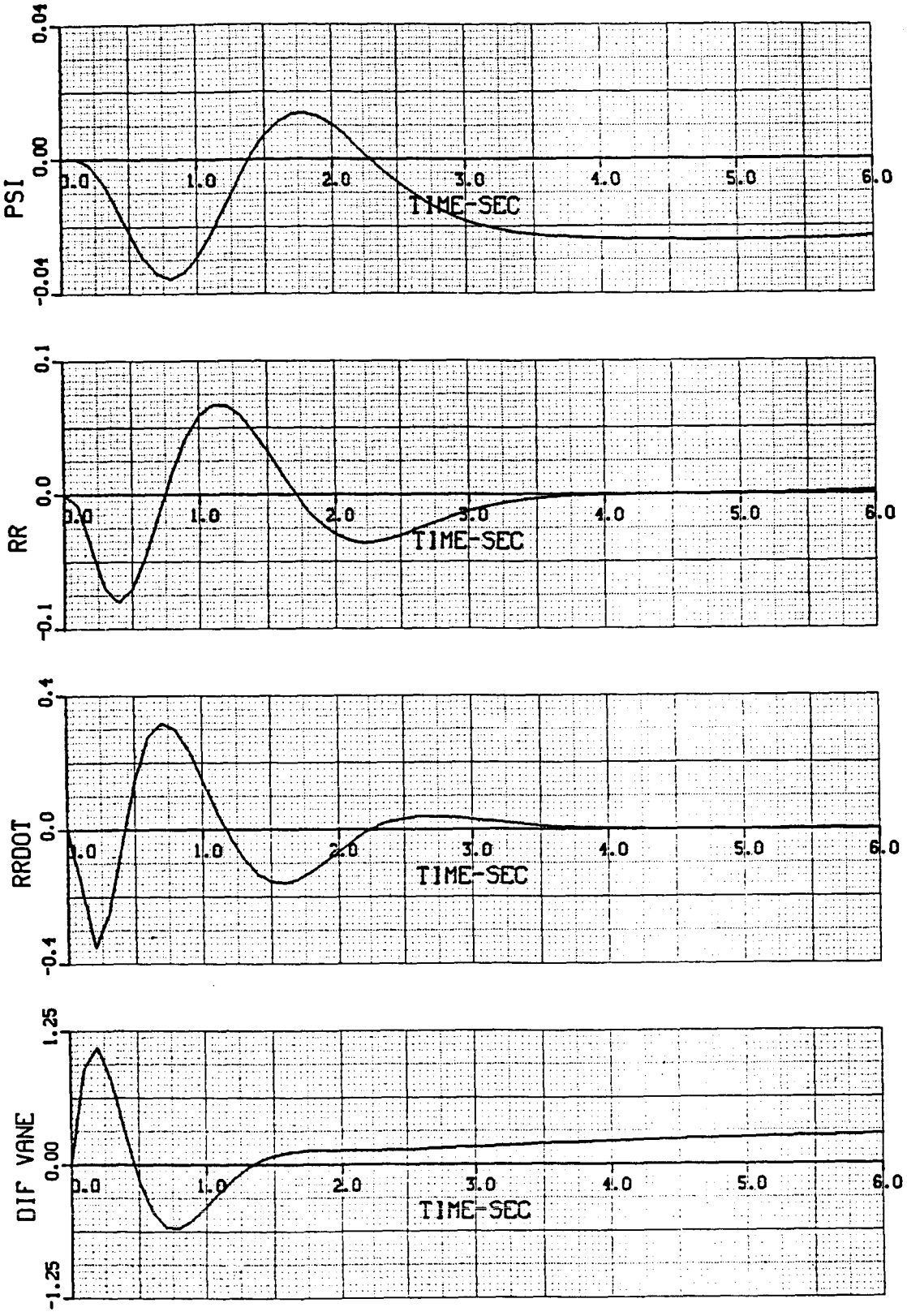

Figure A1.- Continued.

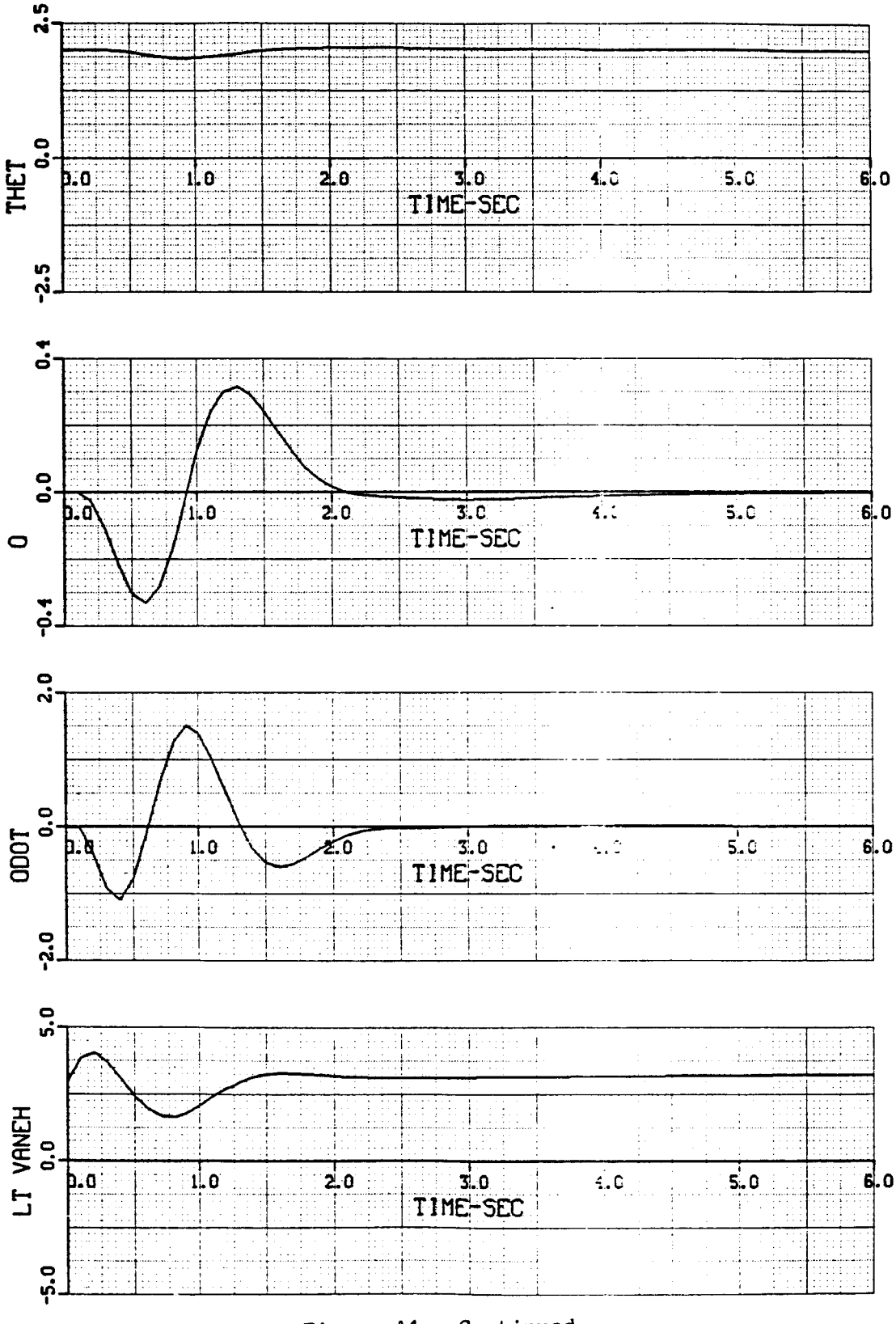

Figure A1.- Continued.

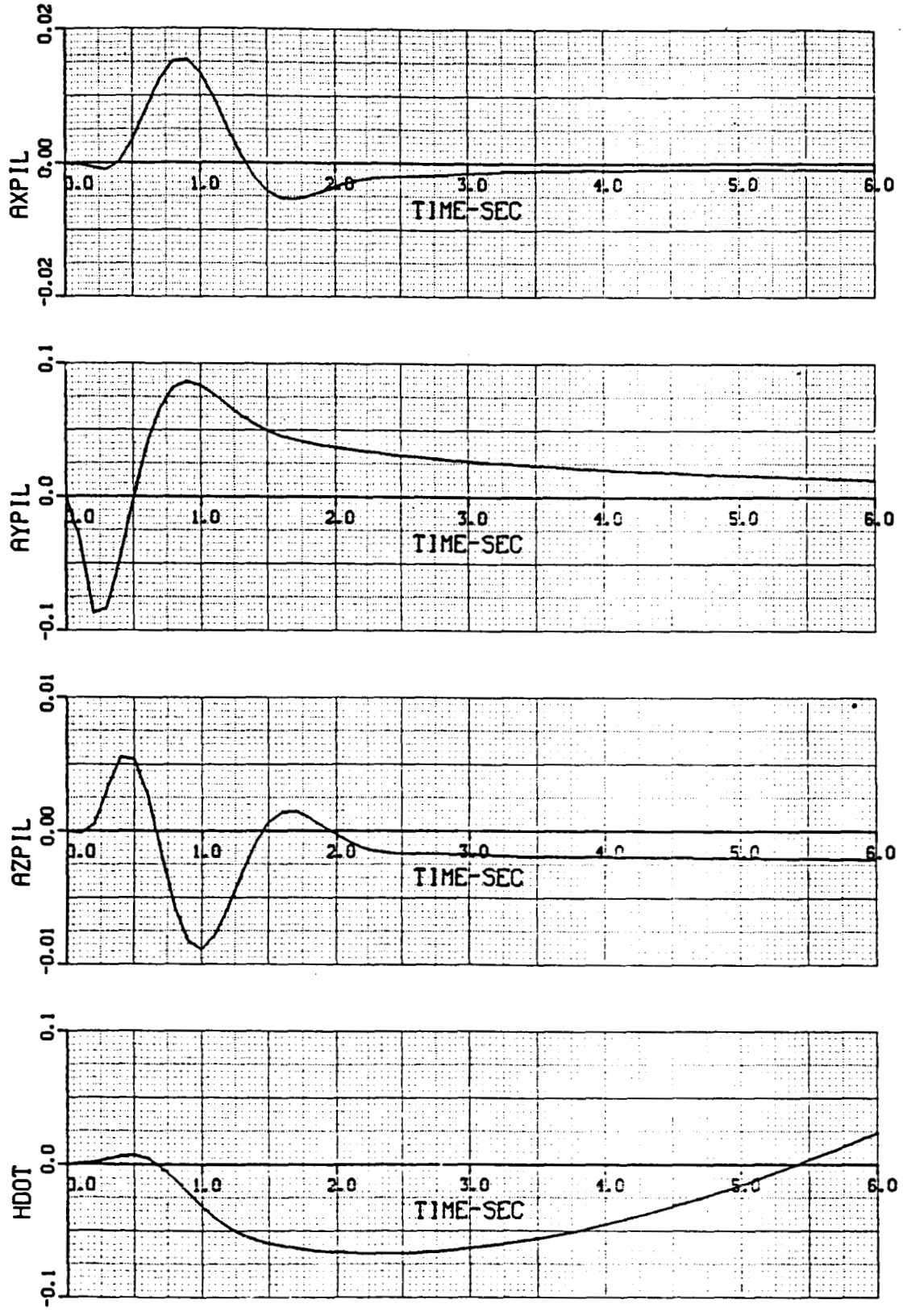

Figure A1.- Continued.

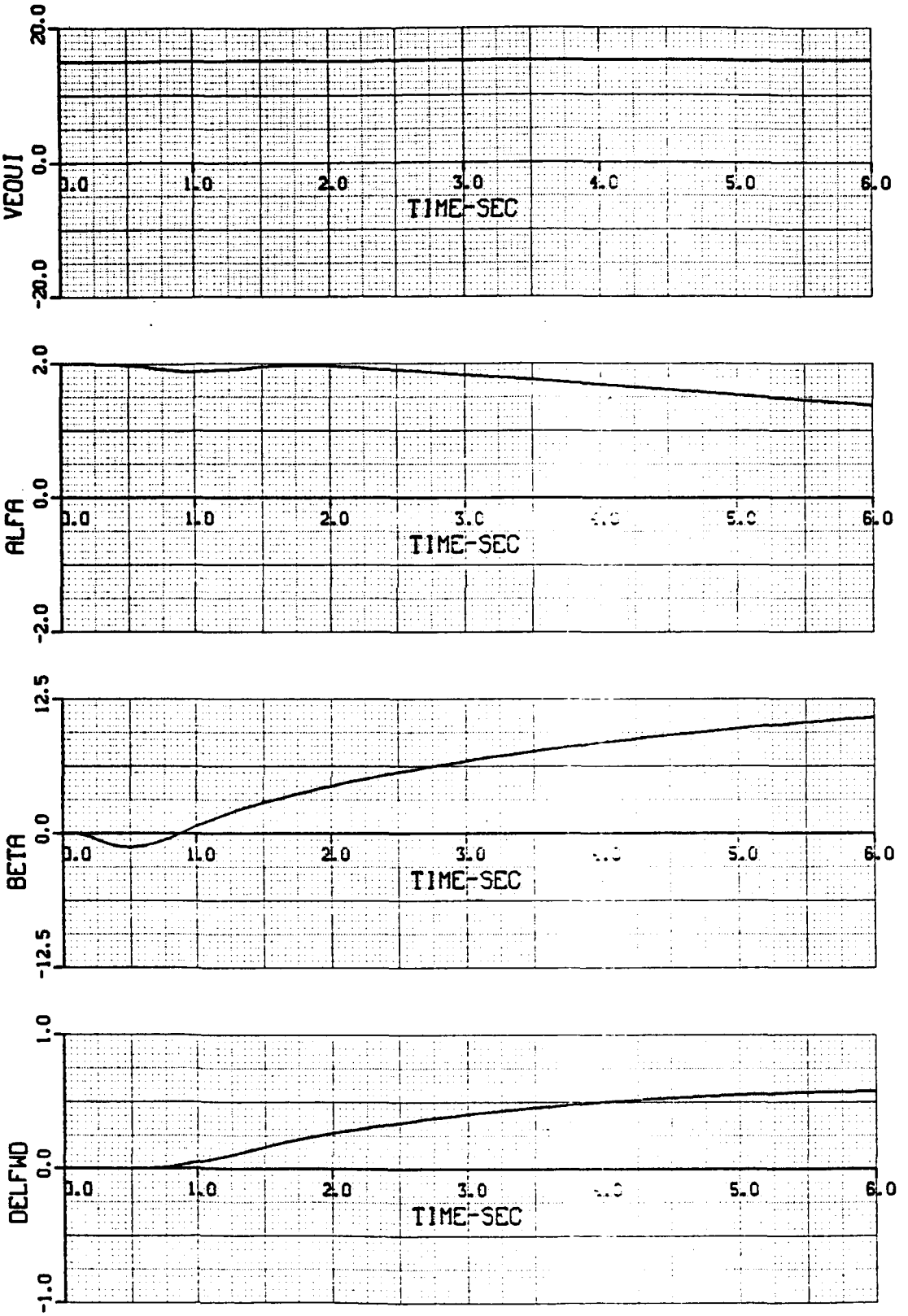

Figure A1.- Continued.

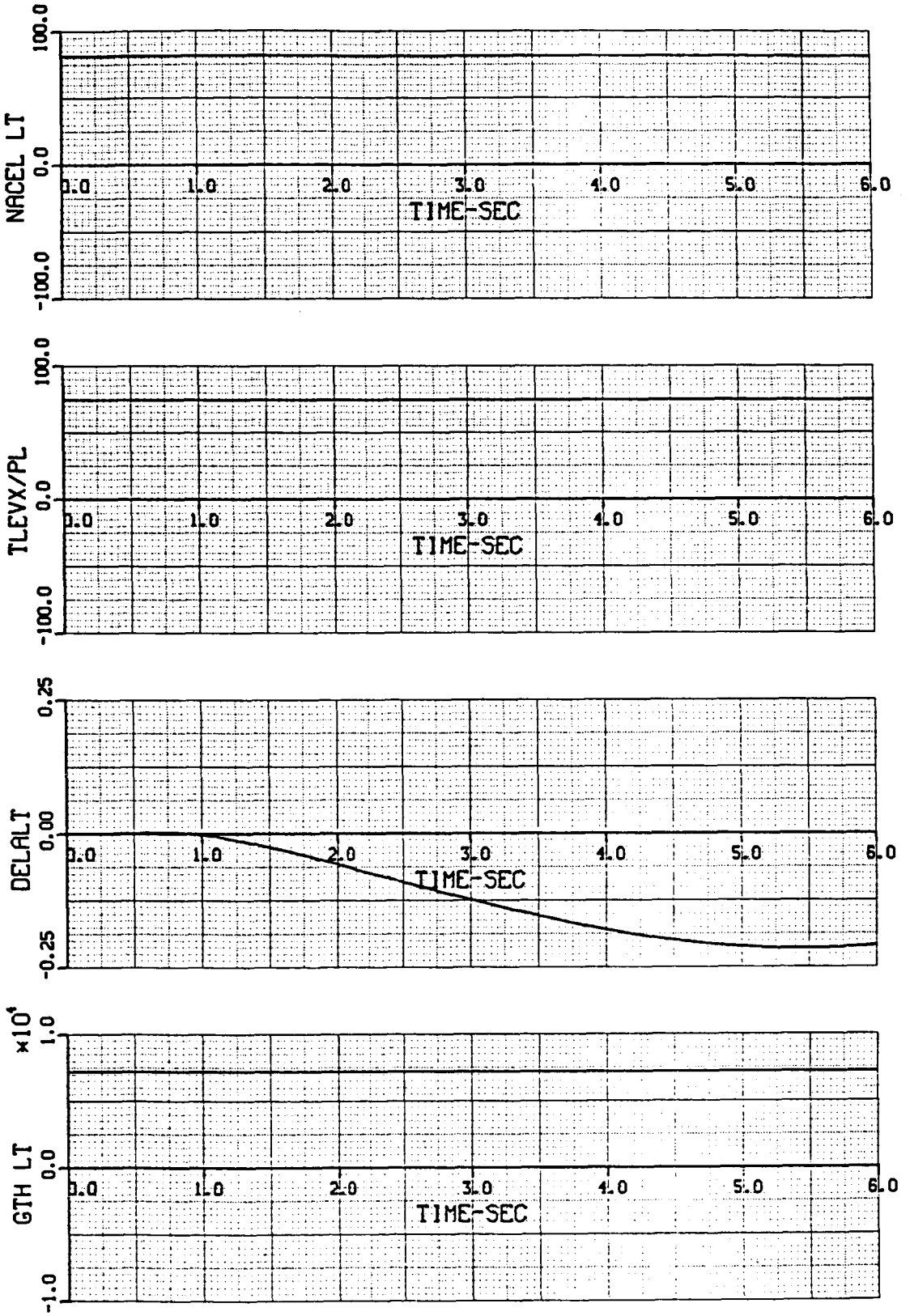

Figure A1.- Continued

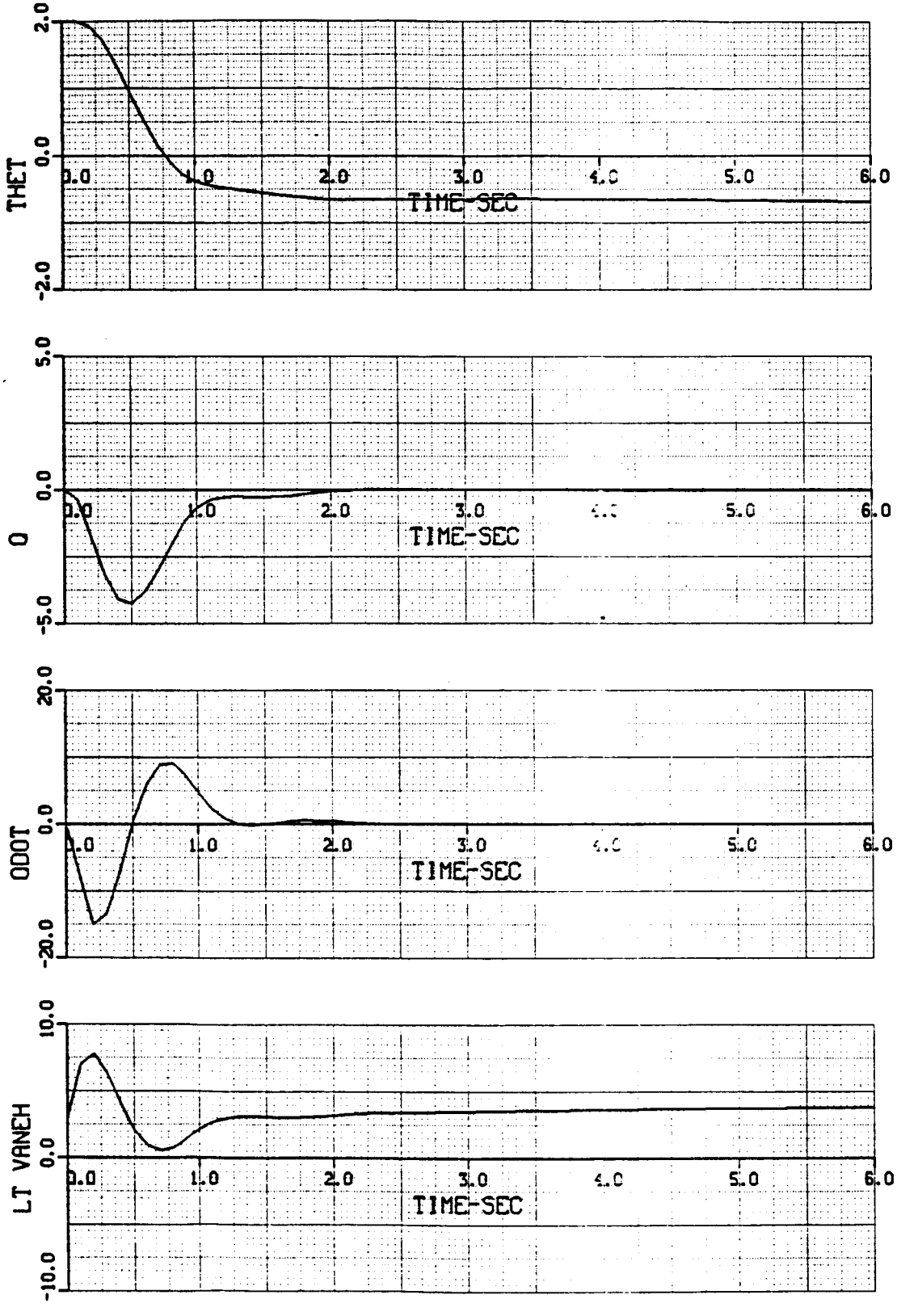

Figure A1.- Continued.

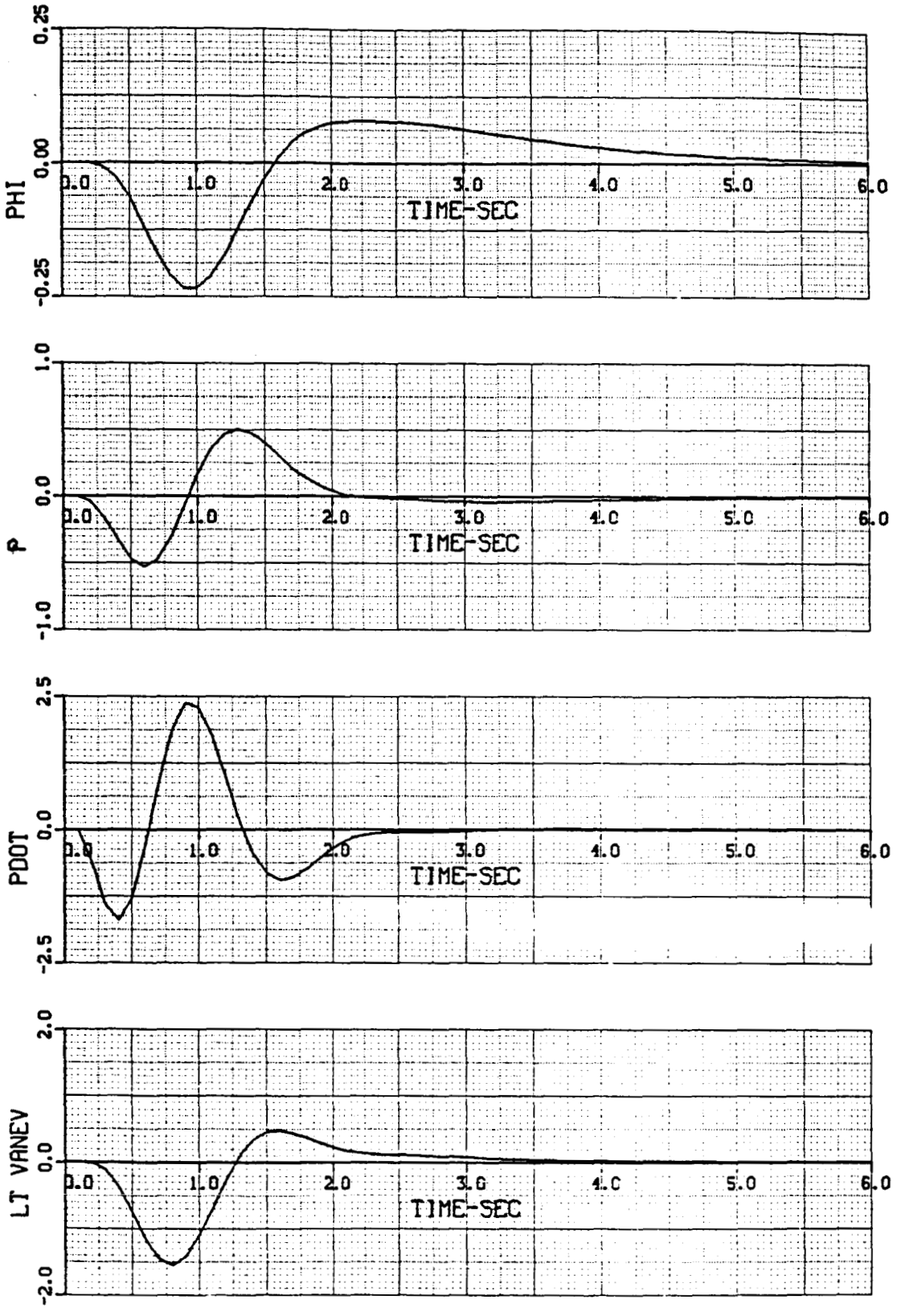

Figure A1.- Continued.

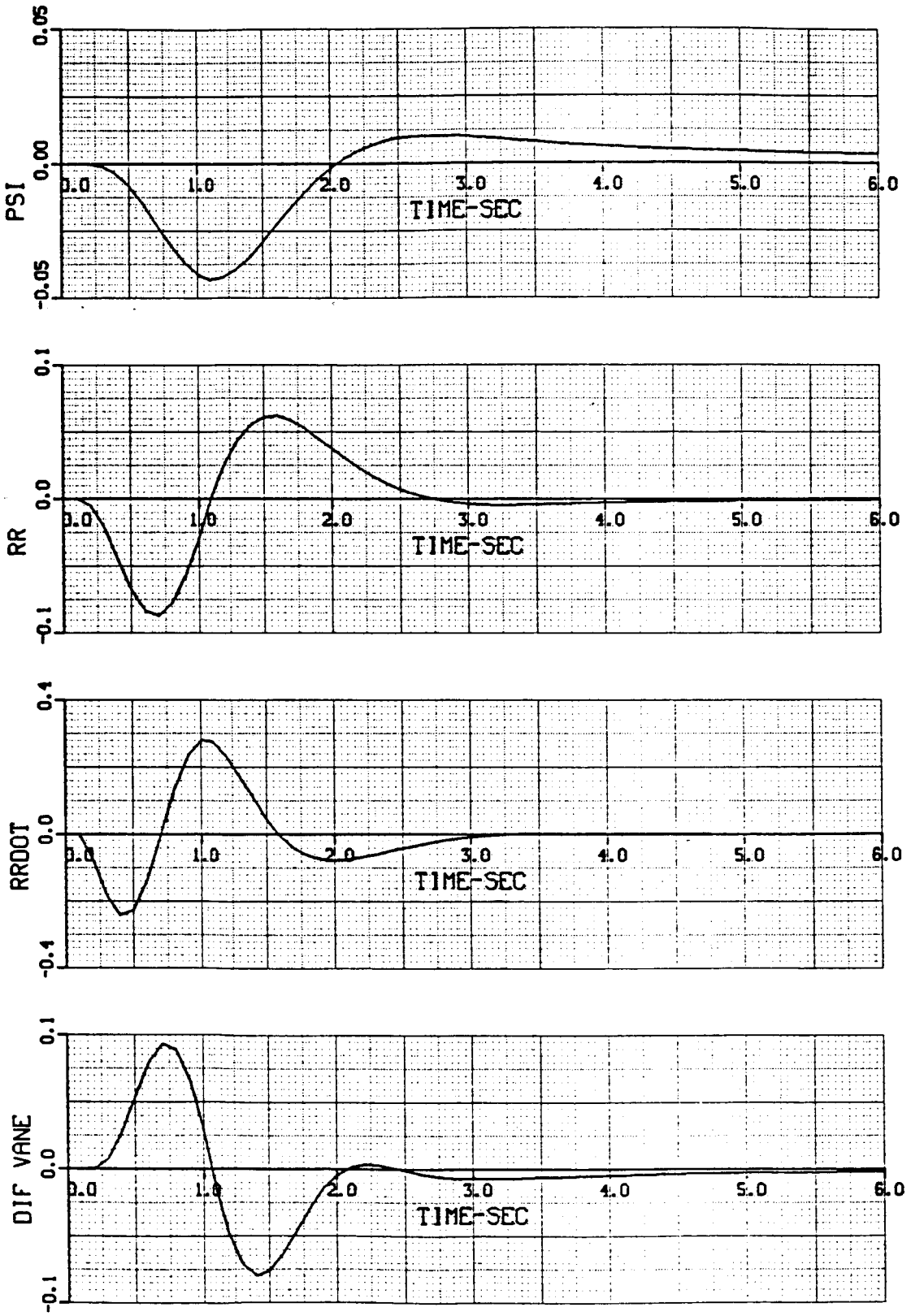

Figure A1.- Continued.

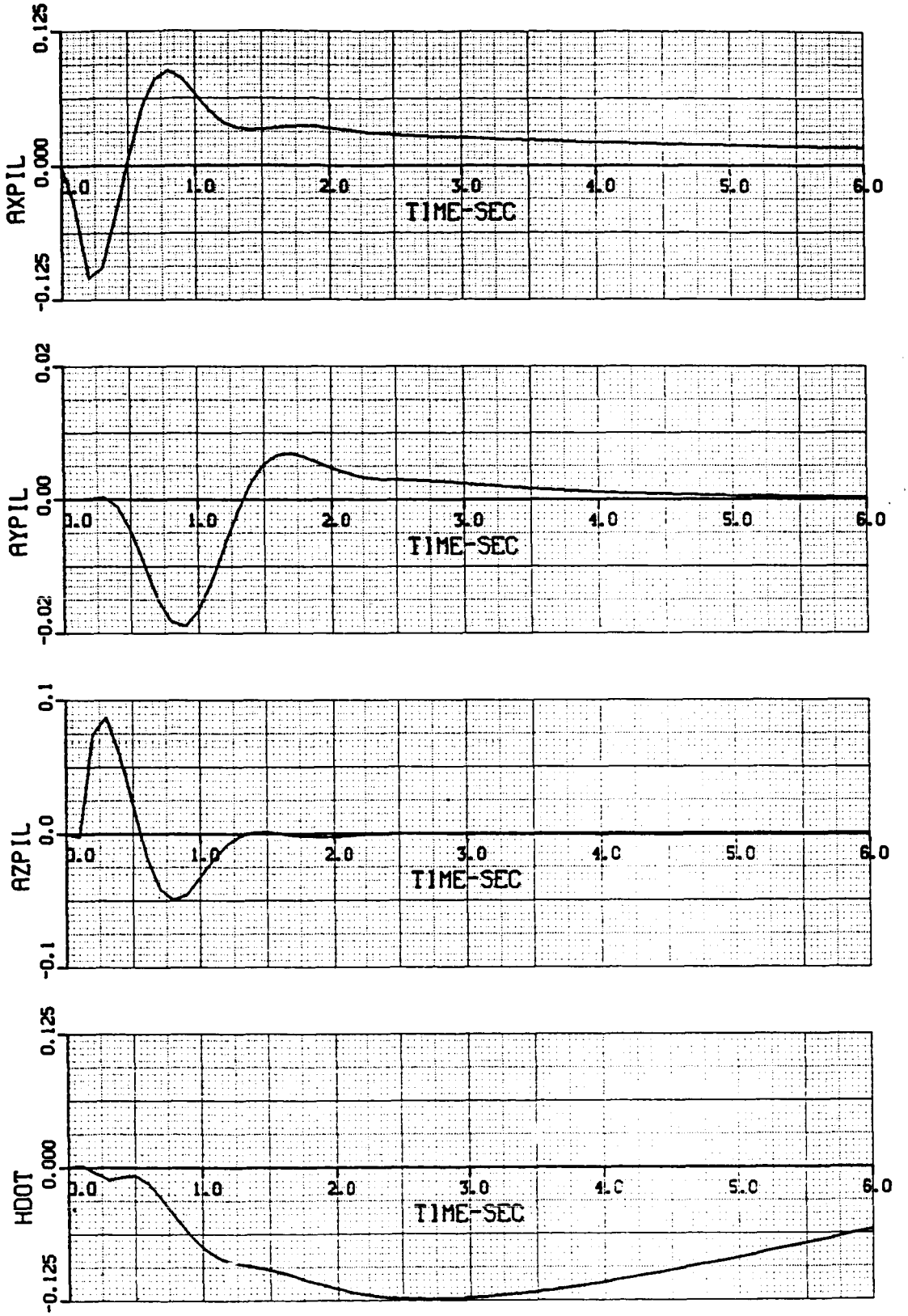

Figure A1.- Continued.

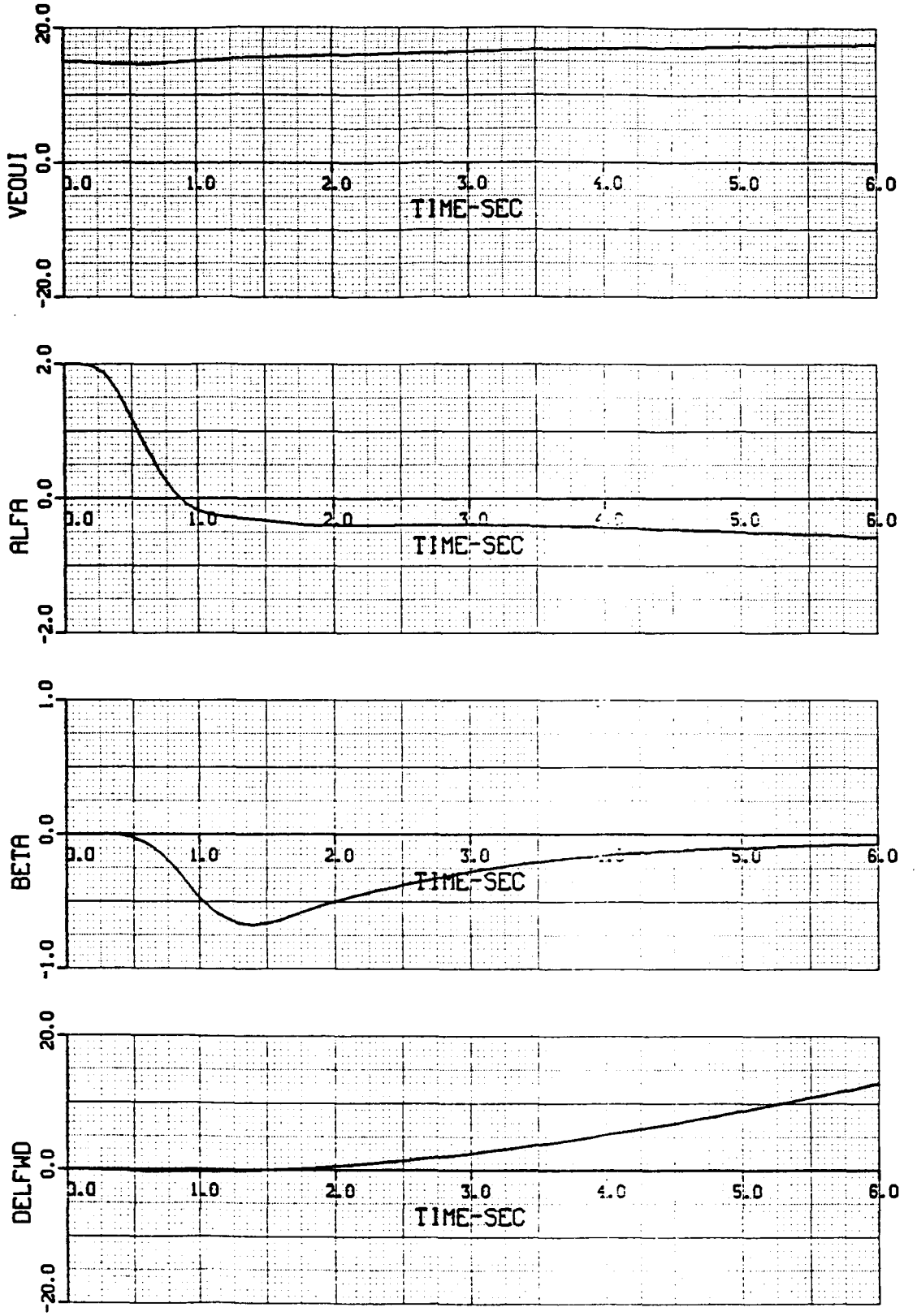

Figure A1.- Continued.

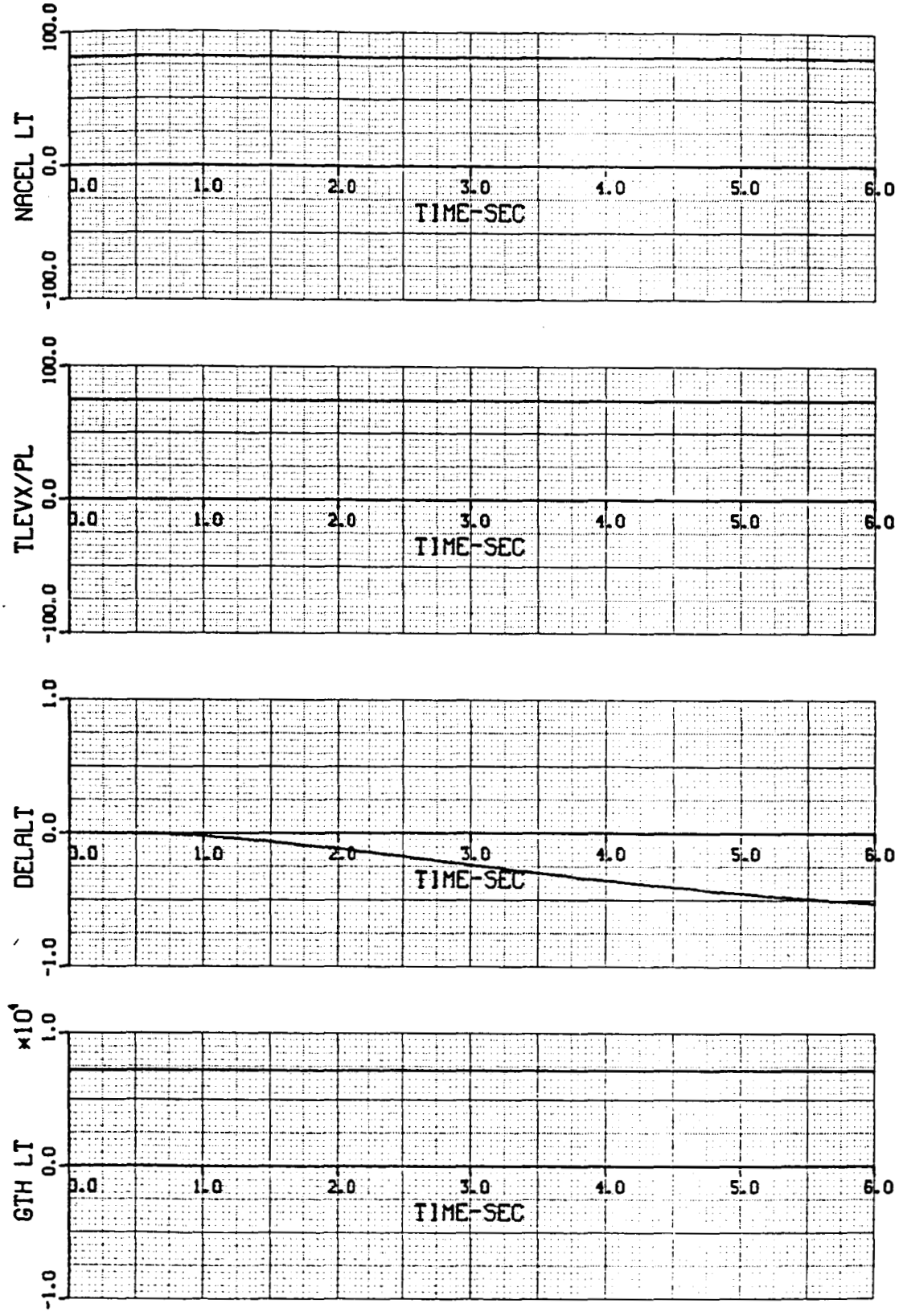

Figure A1.- Concluded.

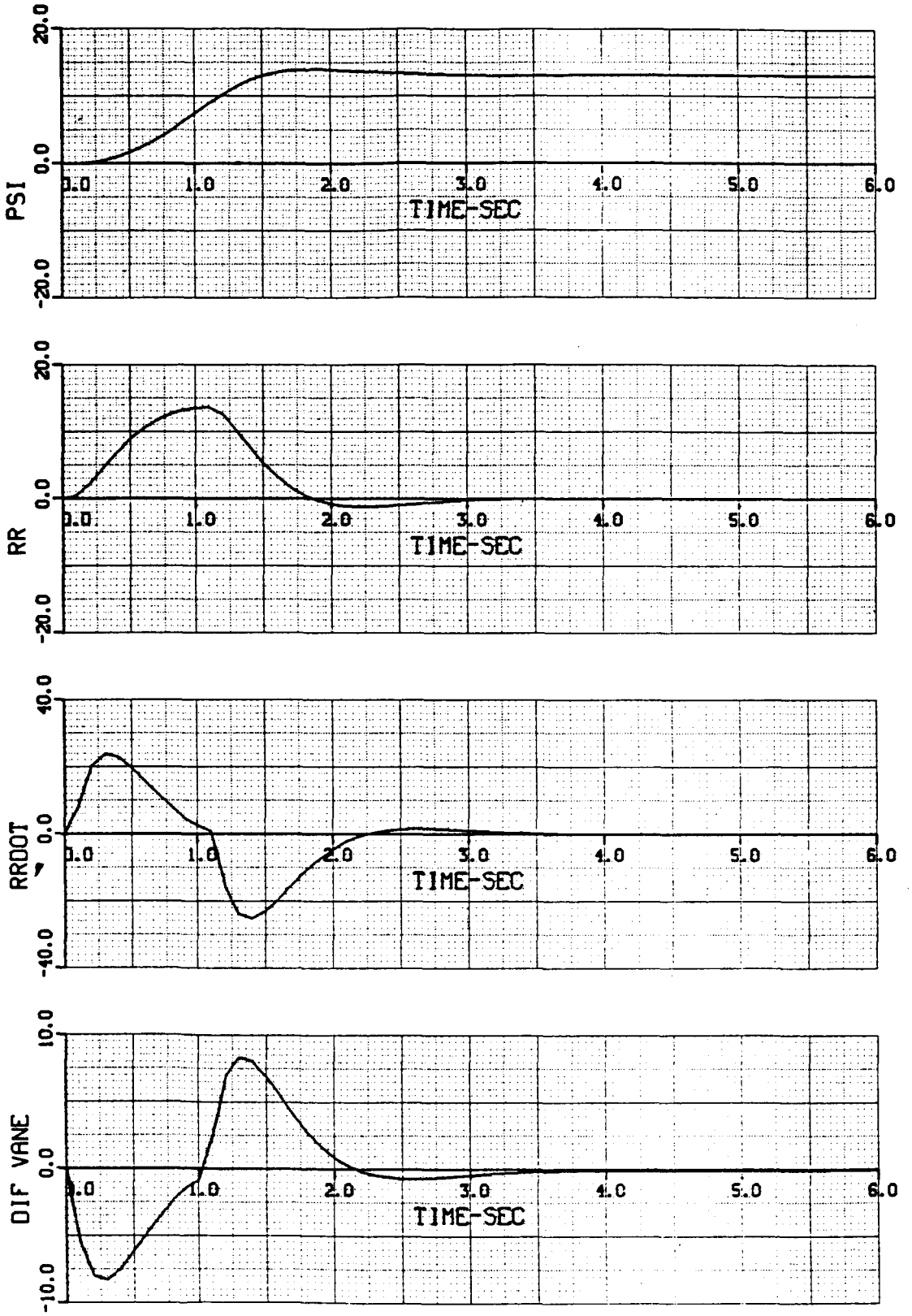

Figure A2.- Rudder pedal input.

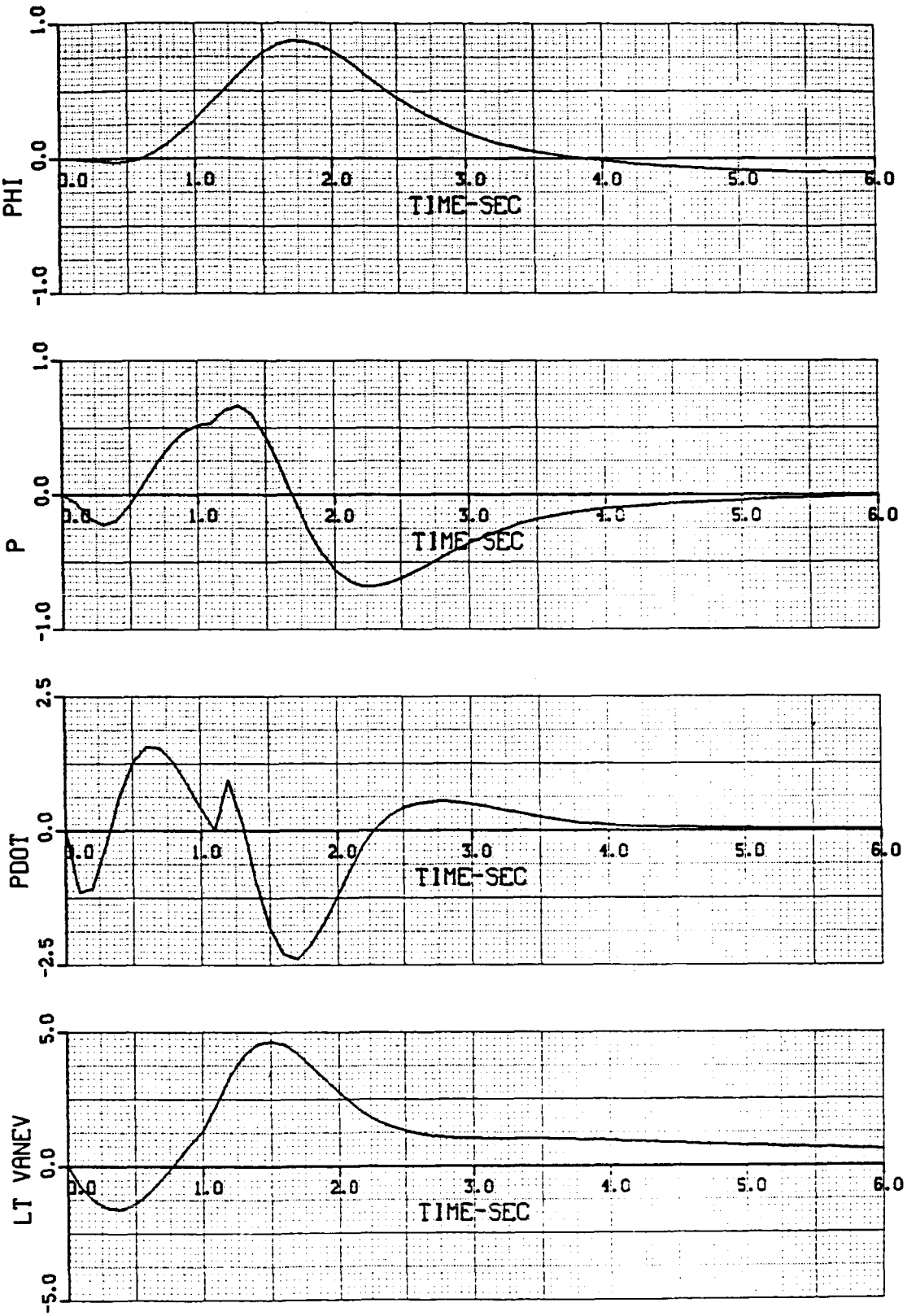

Figure A2.- Continued.

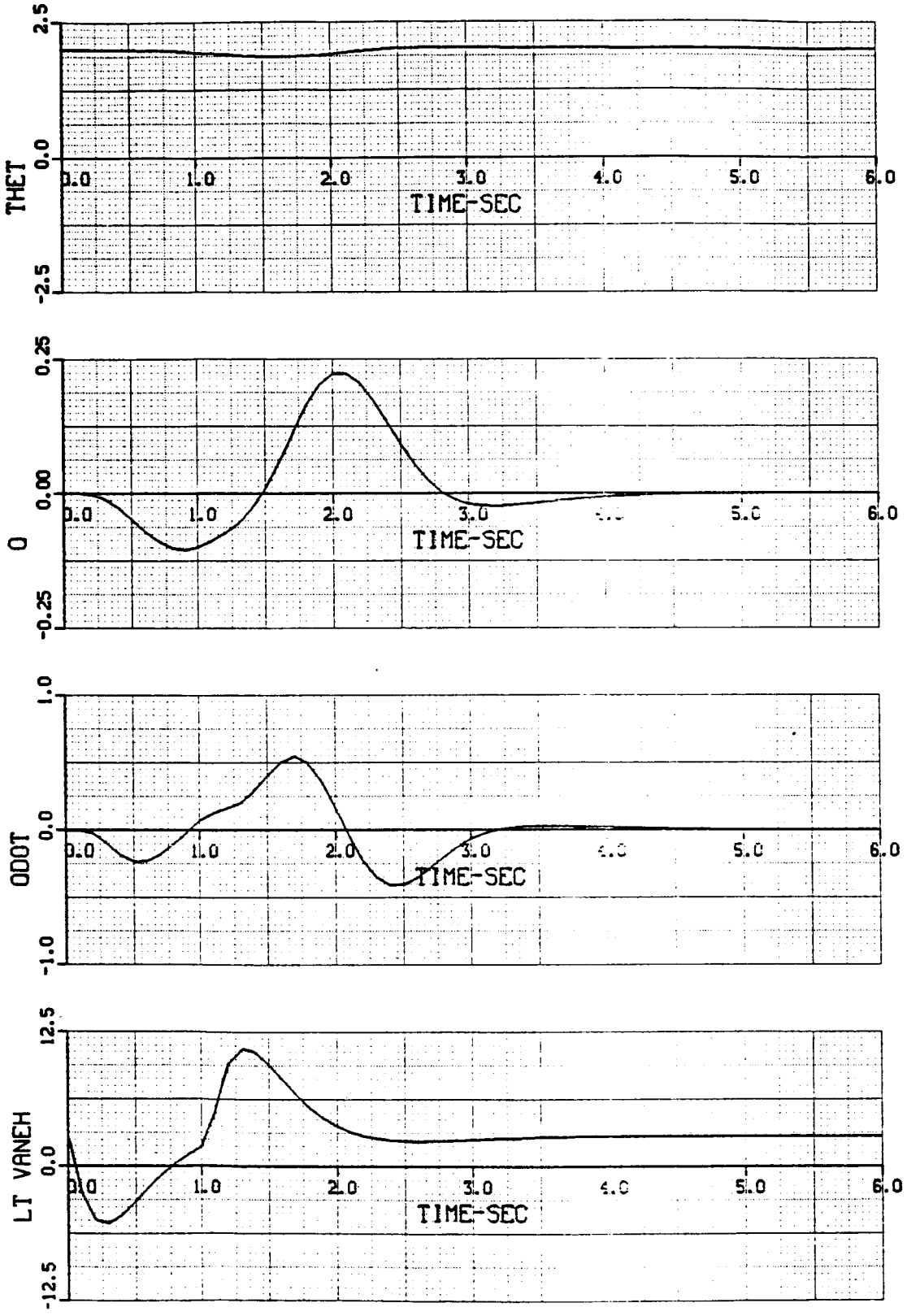

Figure A2.- Continued.

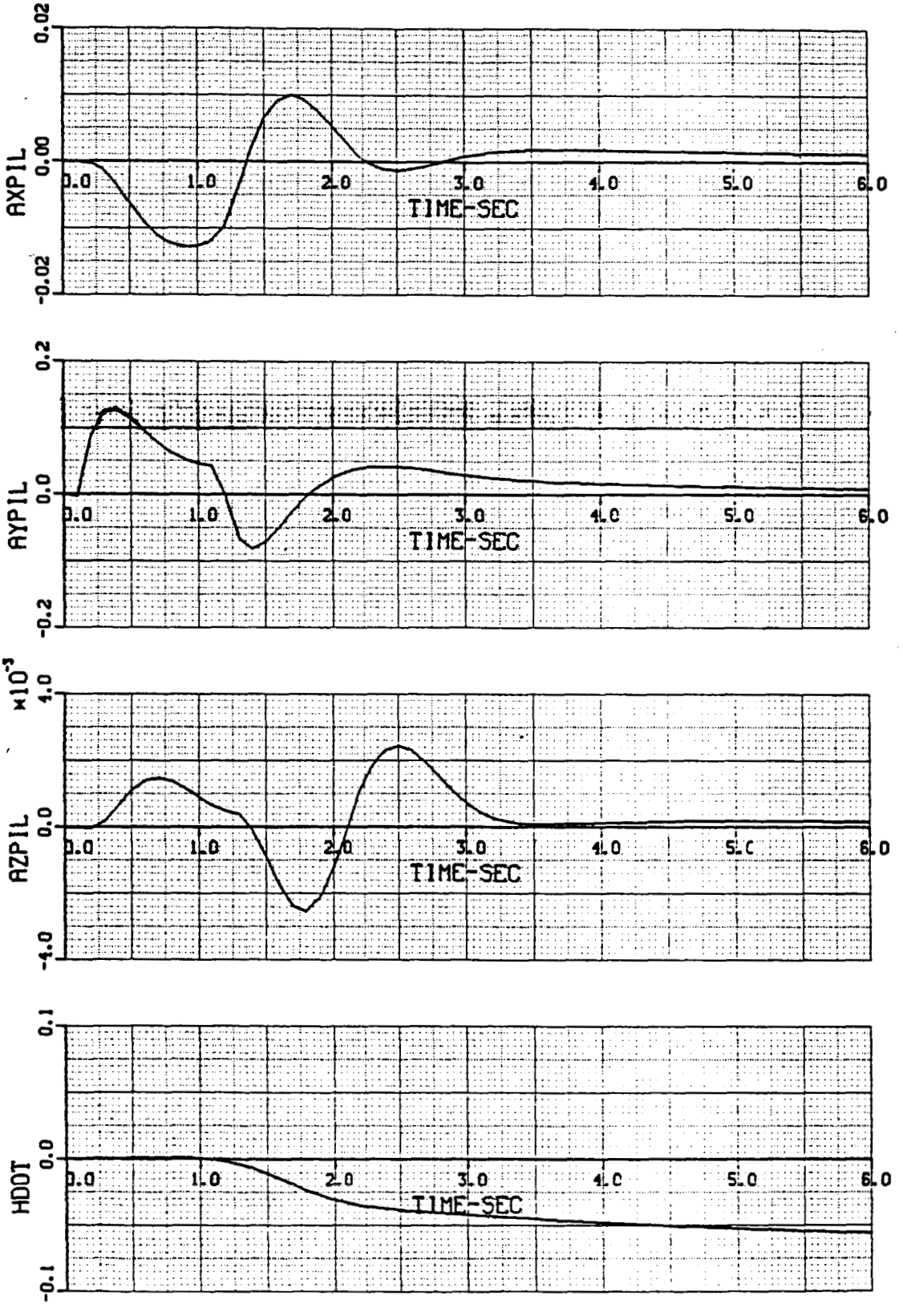

Figure A2.- Continued.

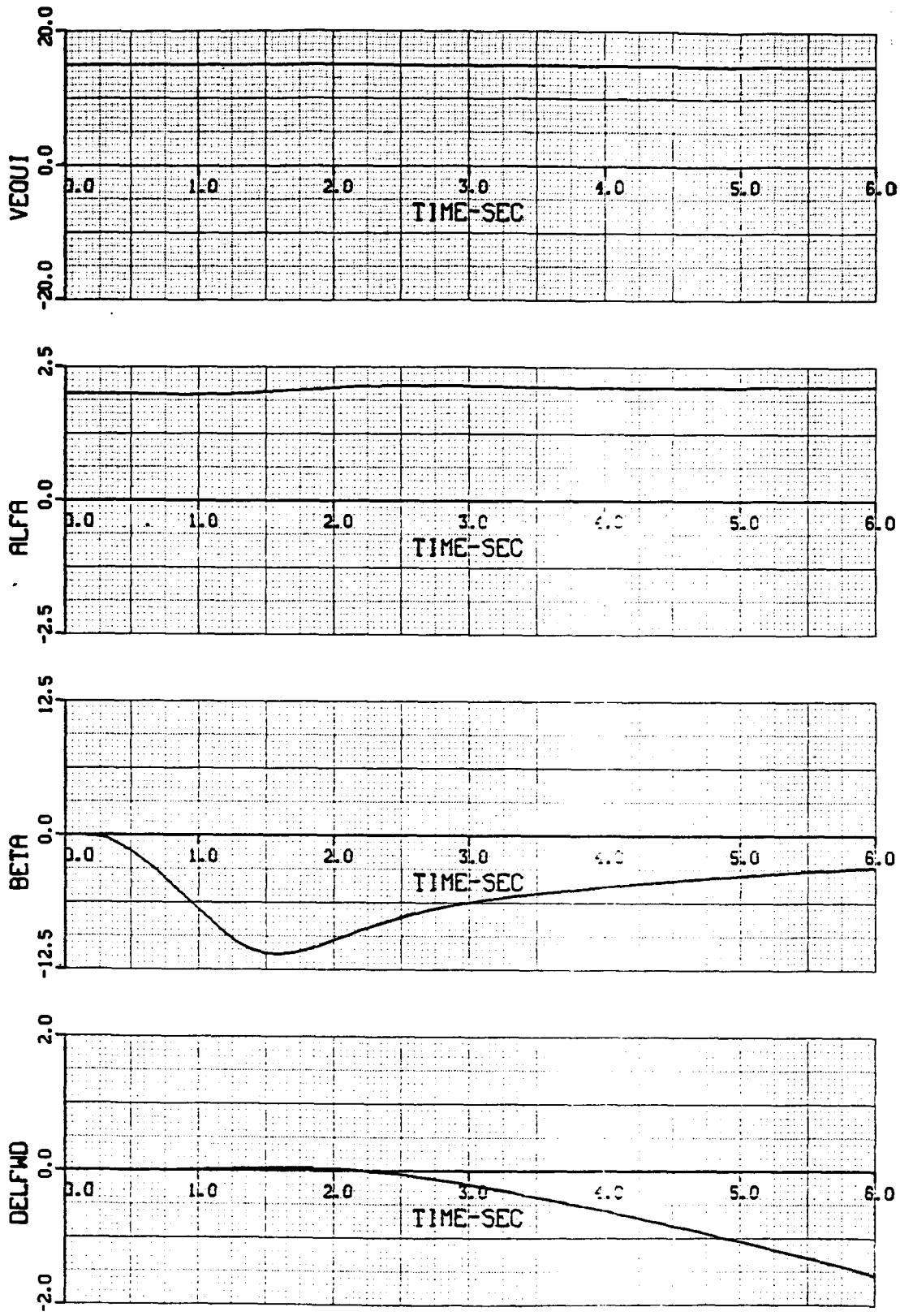

Figure A2.- Continued.

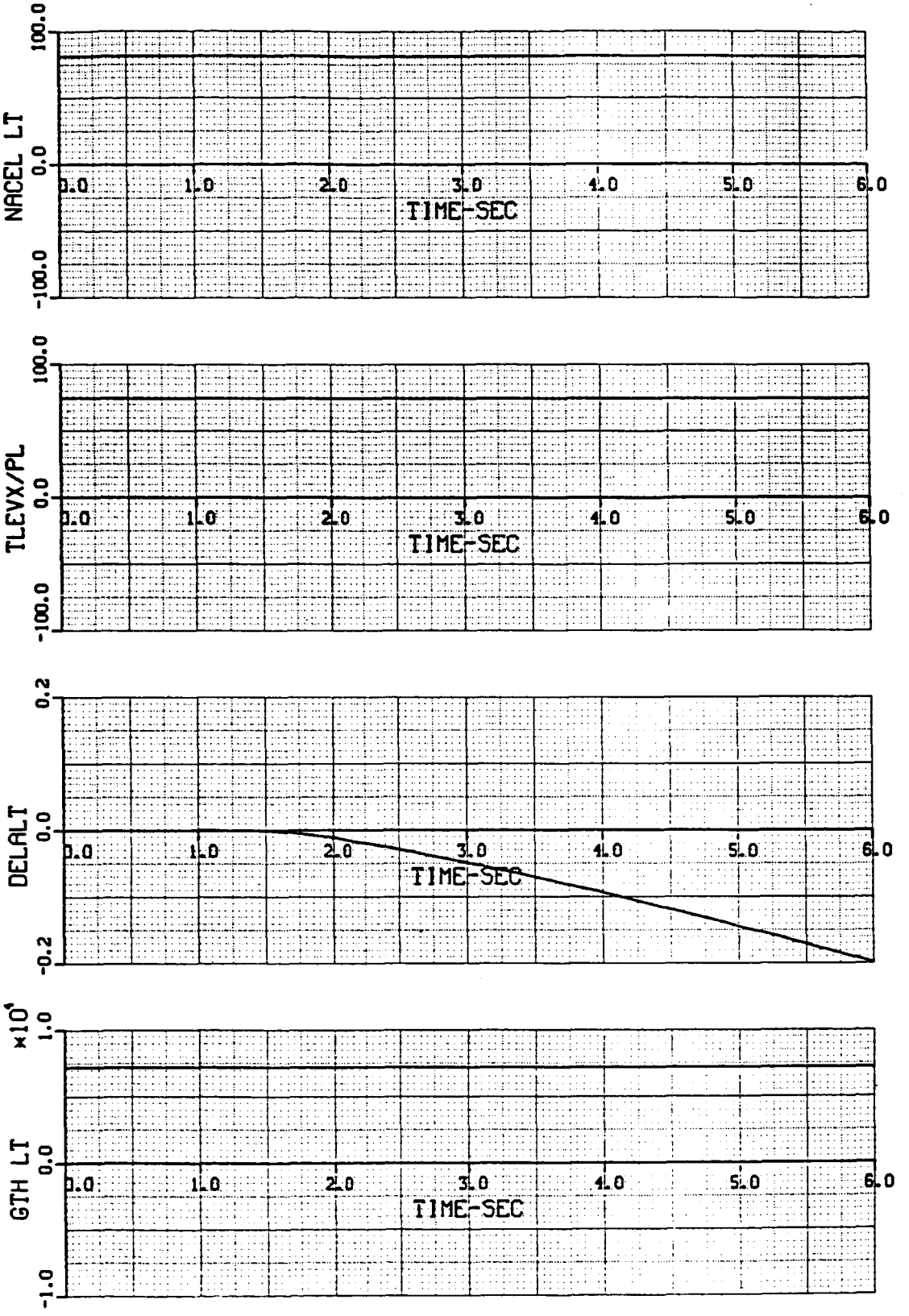

Figure A2.- Concluded.

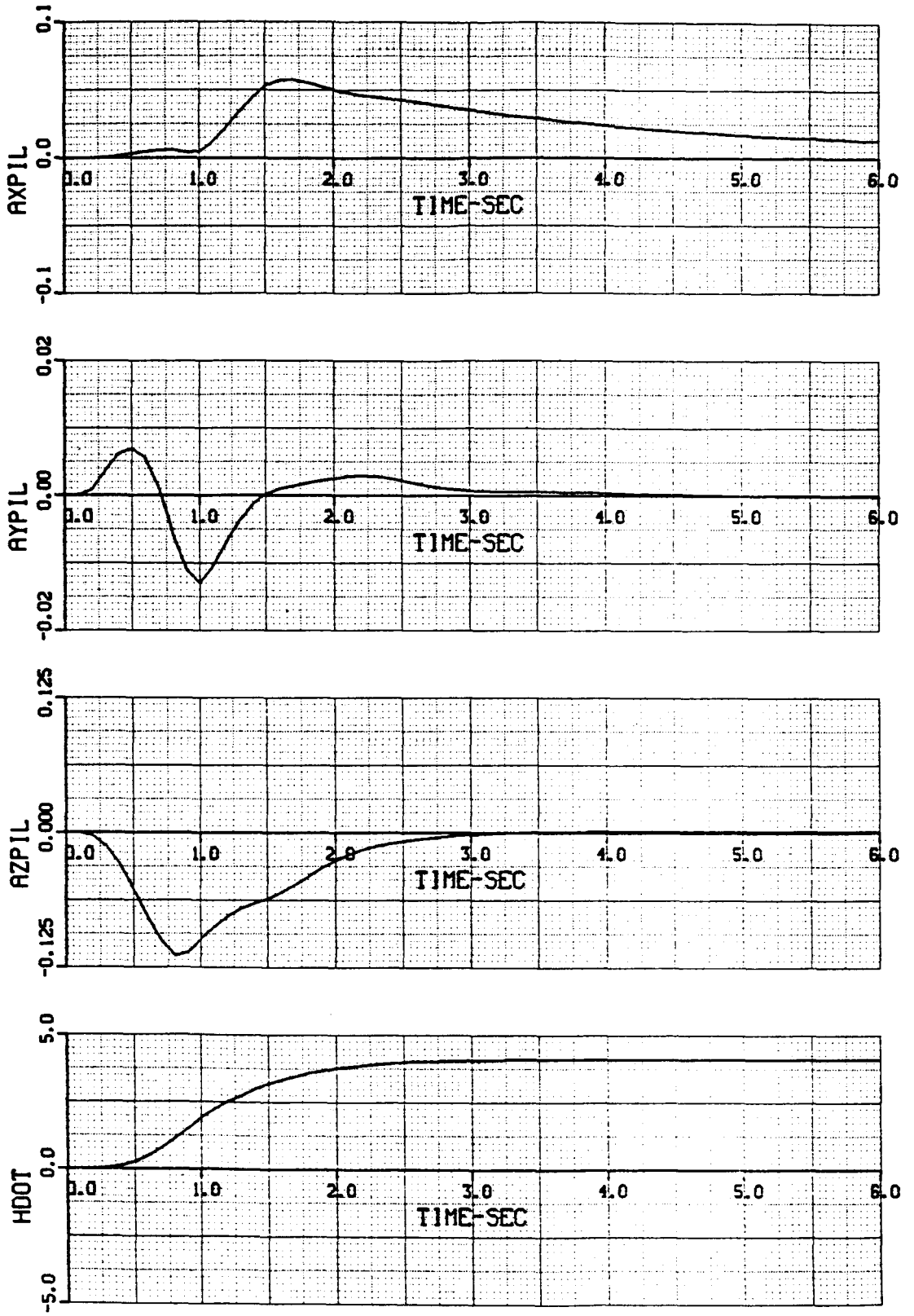

Figure A3.- Flightpath lever input.

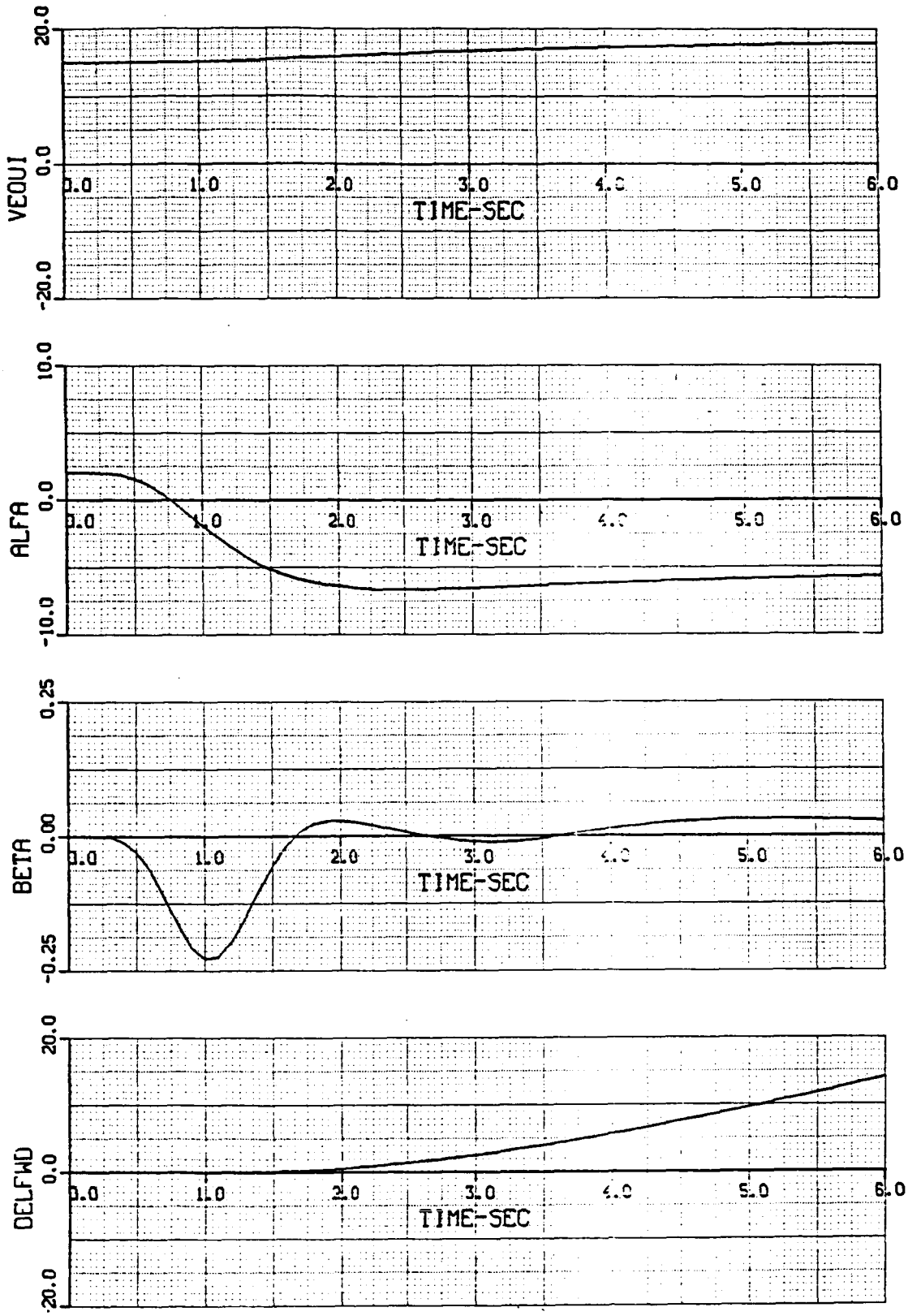

Figure A3.- Continued.

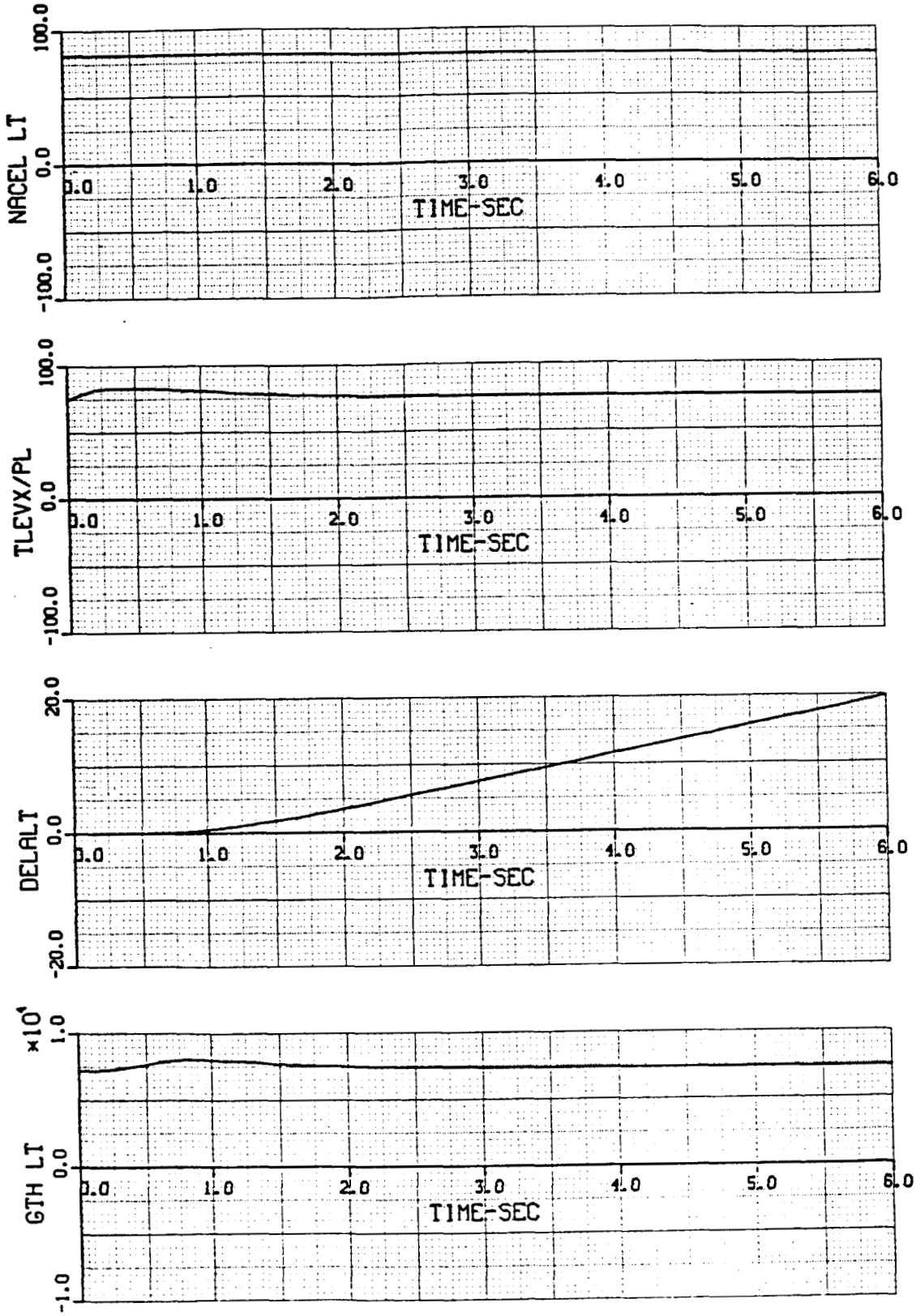

Figure A3.- Continued.

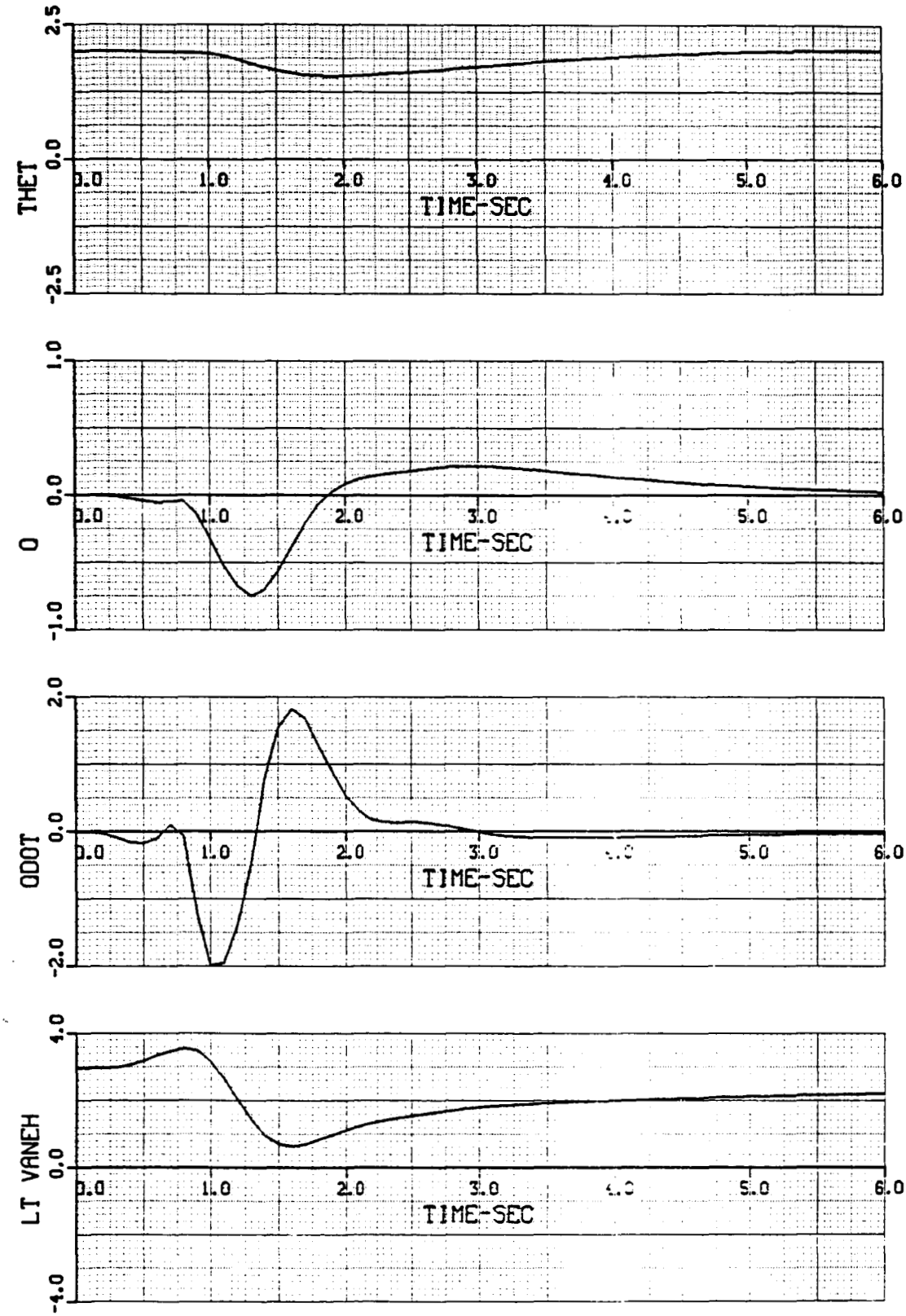

Figure A3.- Continued.

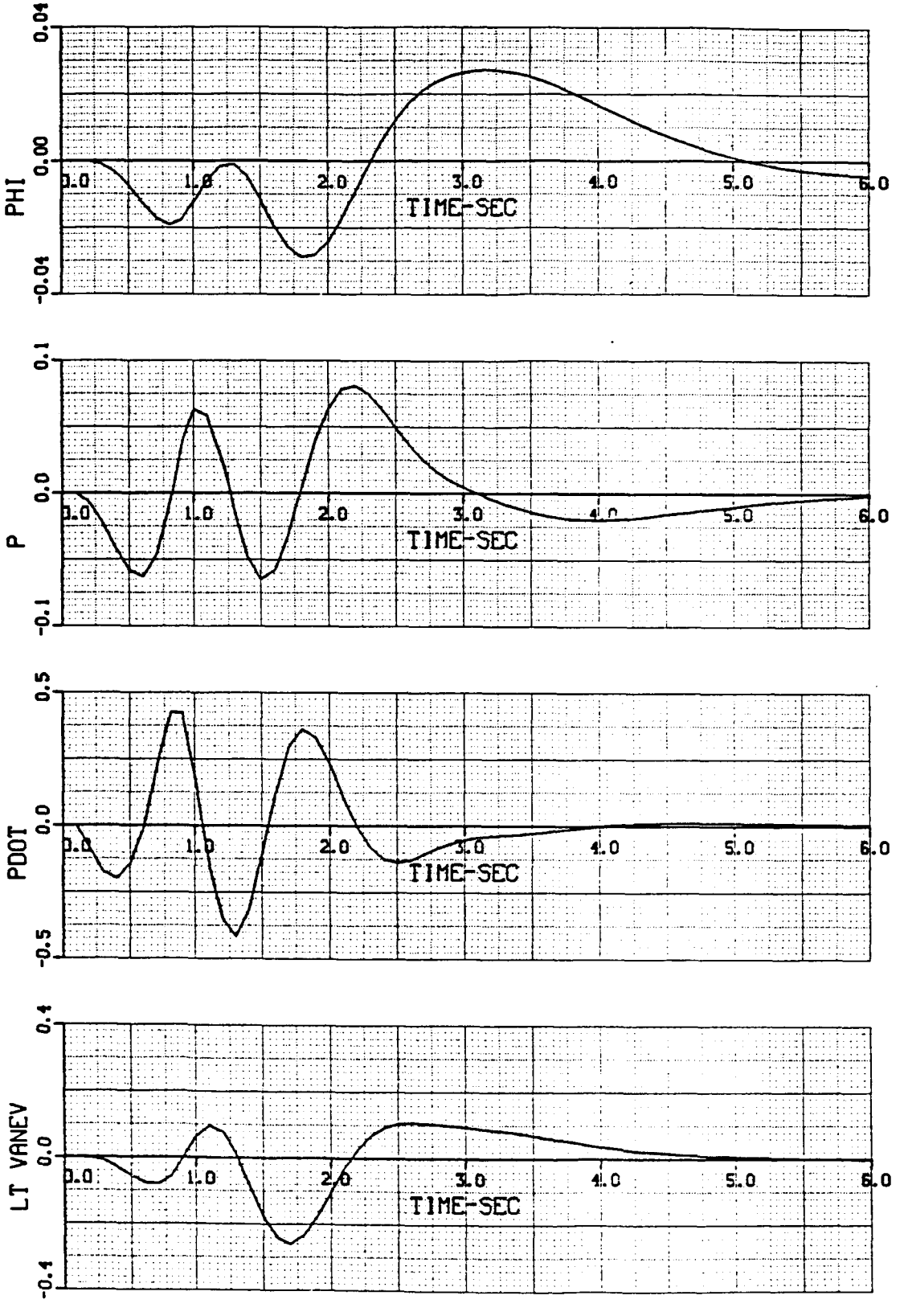

Figure A3.- Continued.

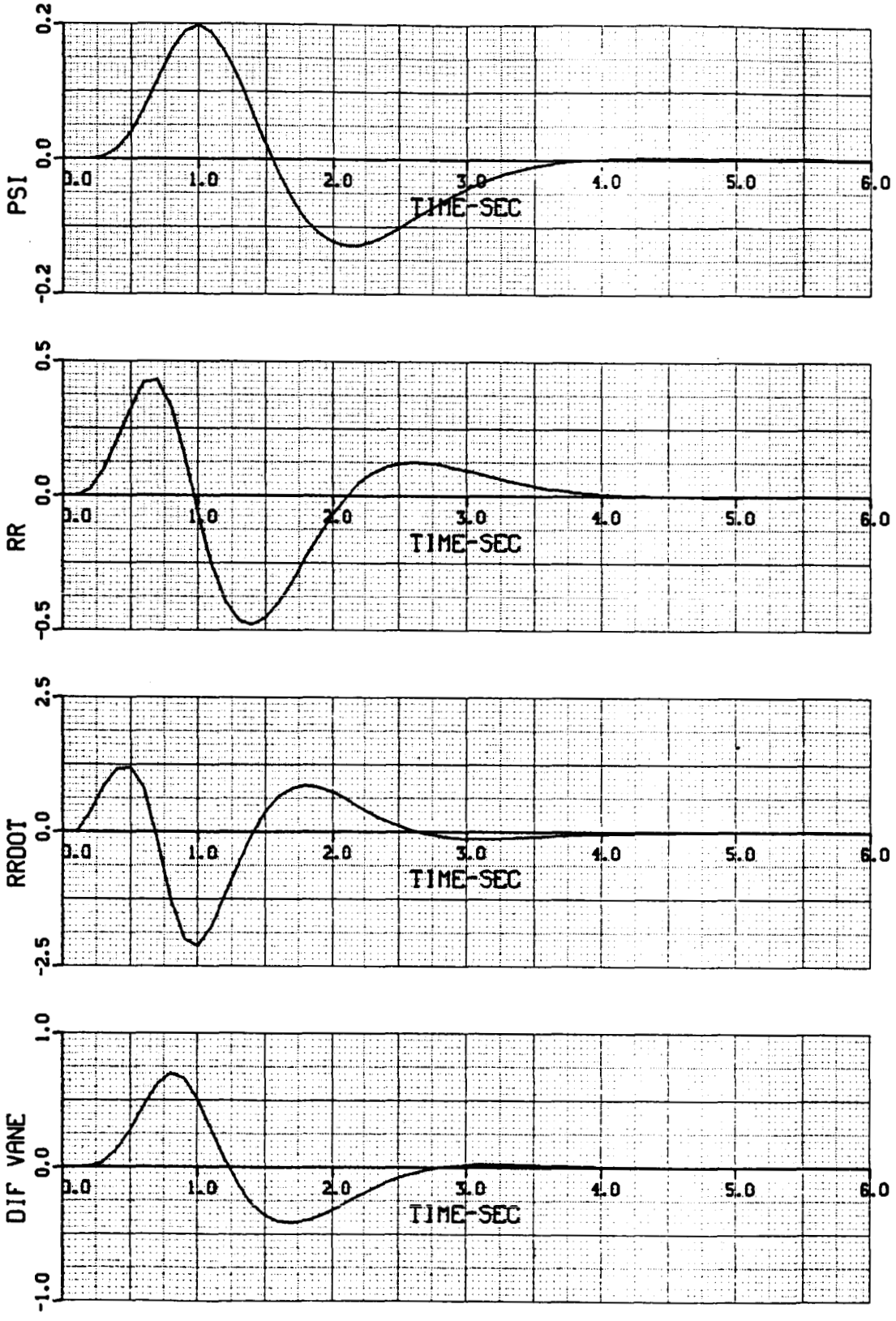

Figure A3.- Concluded.

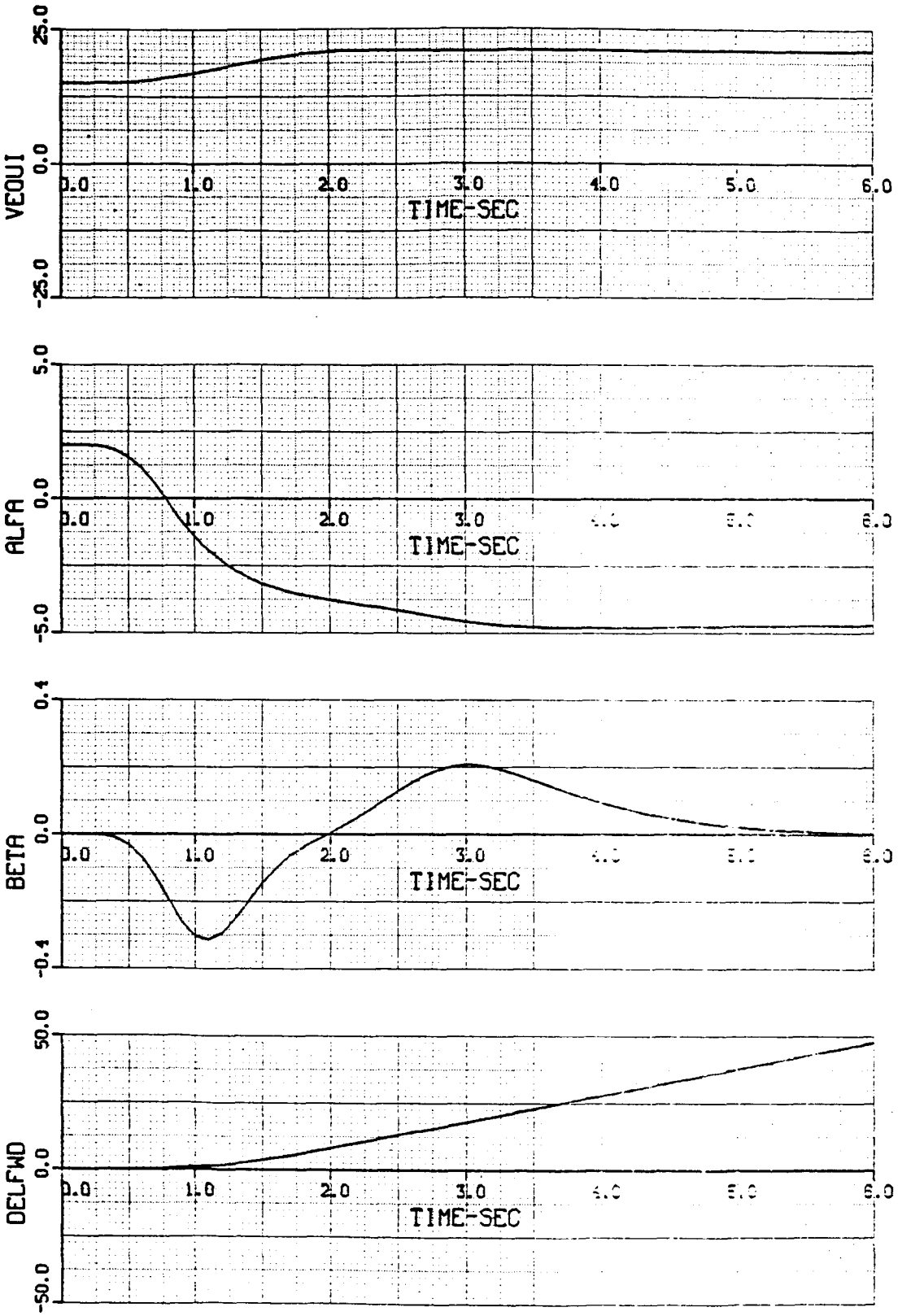

Figure A4.- Surge input.

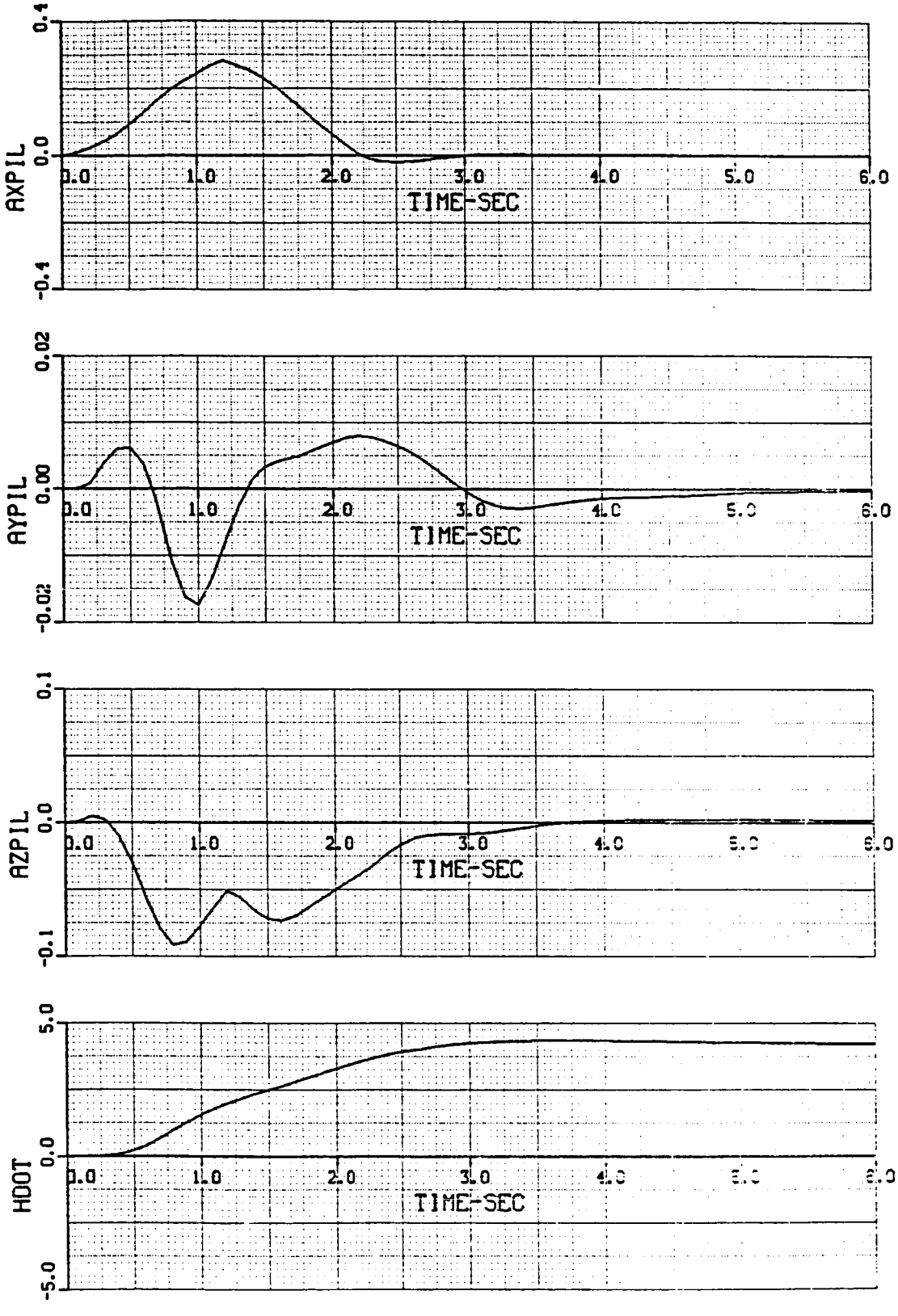

Figure A4.- Continued.

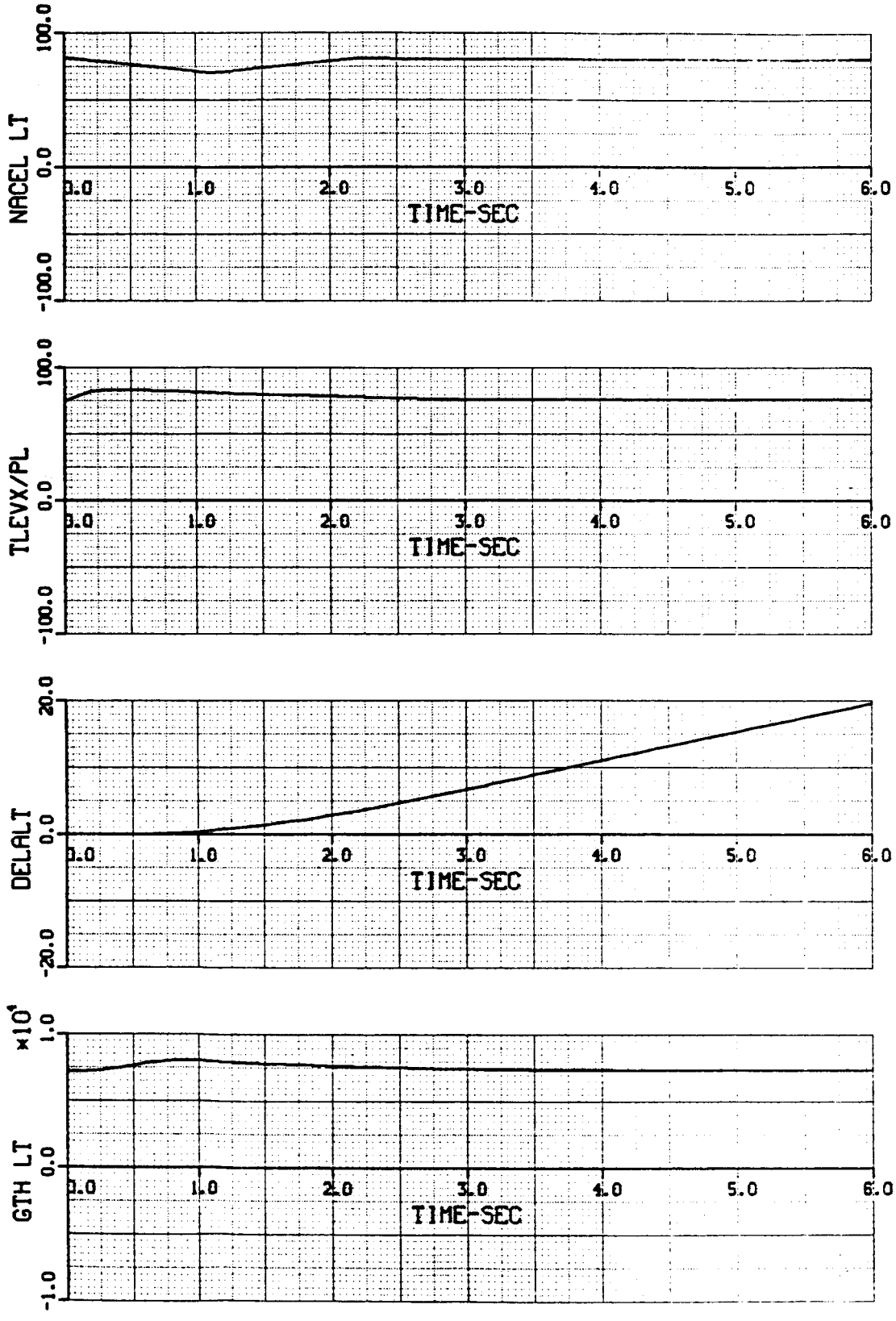

Figure A4.- Continued.

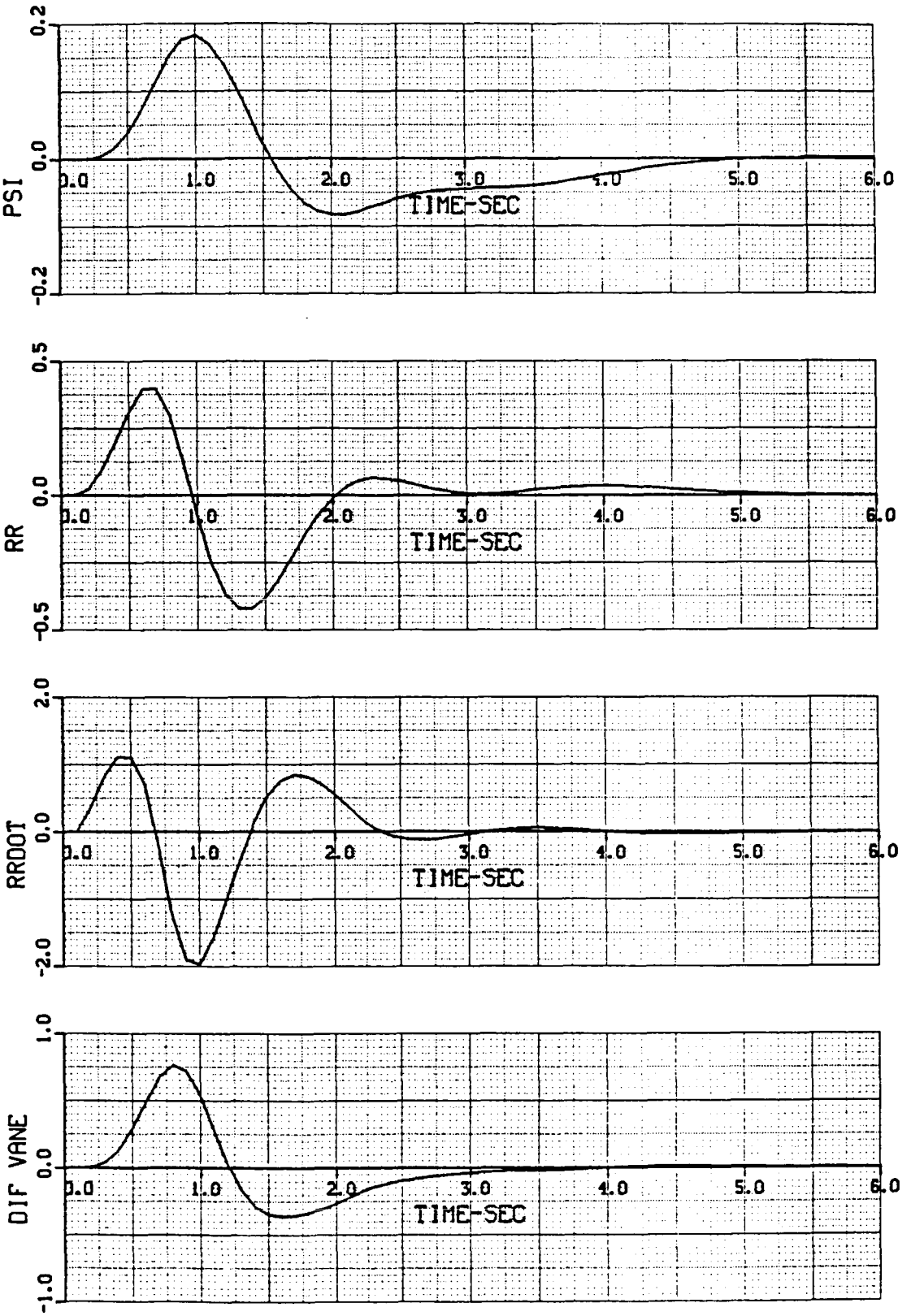

Figure A4.- Continued.

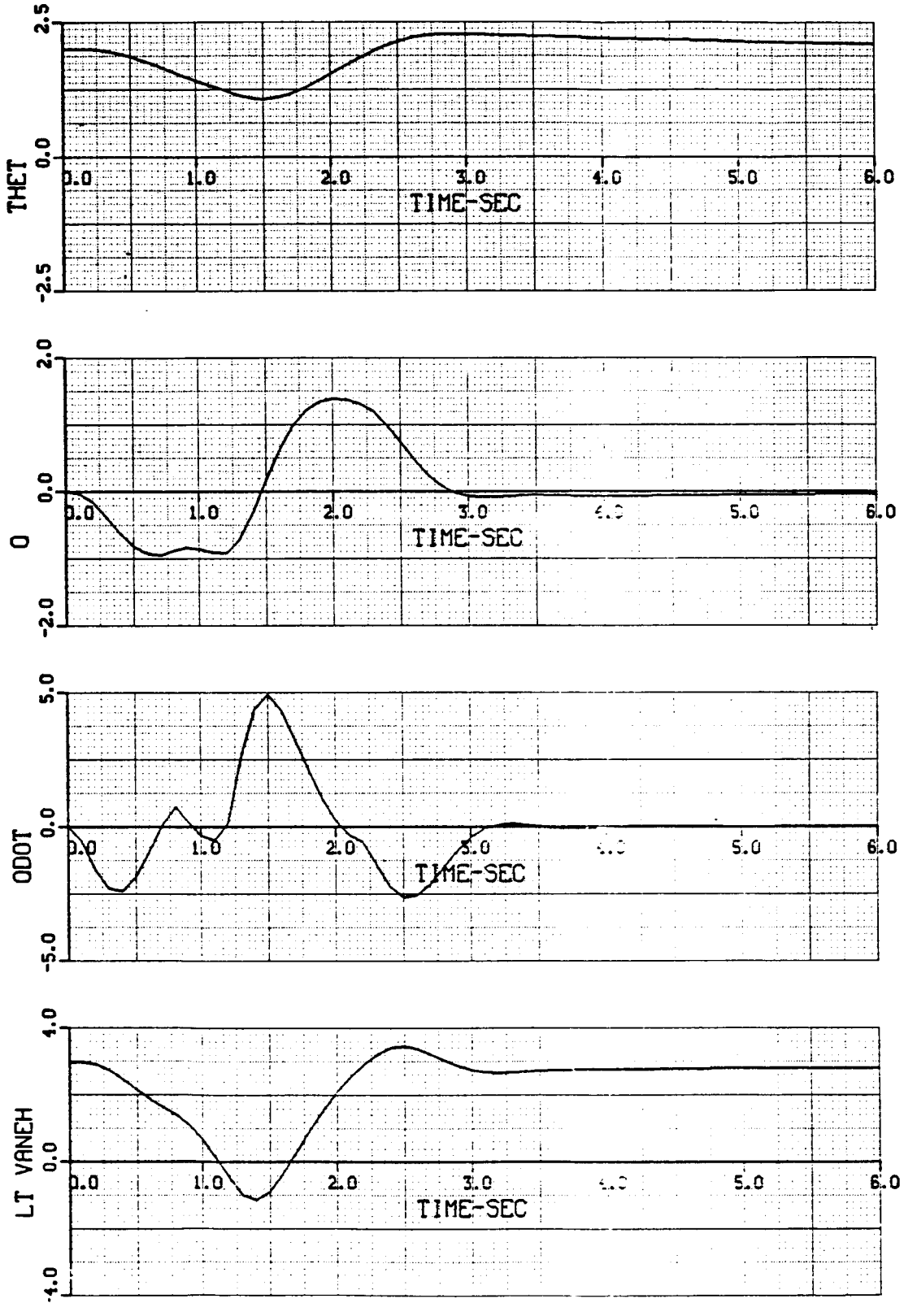

Figure A4.- Continued.

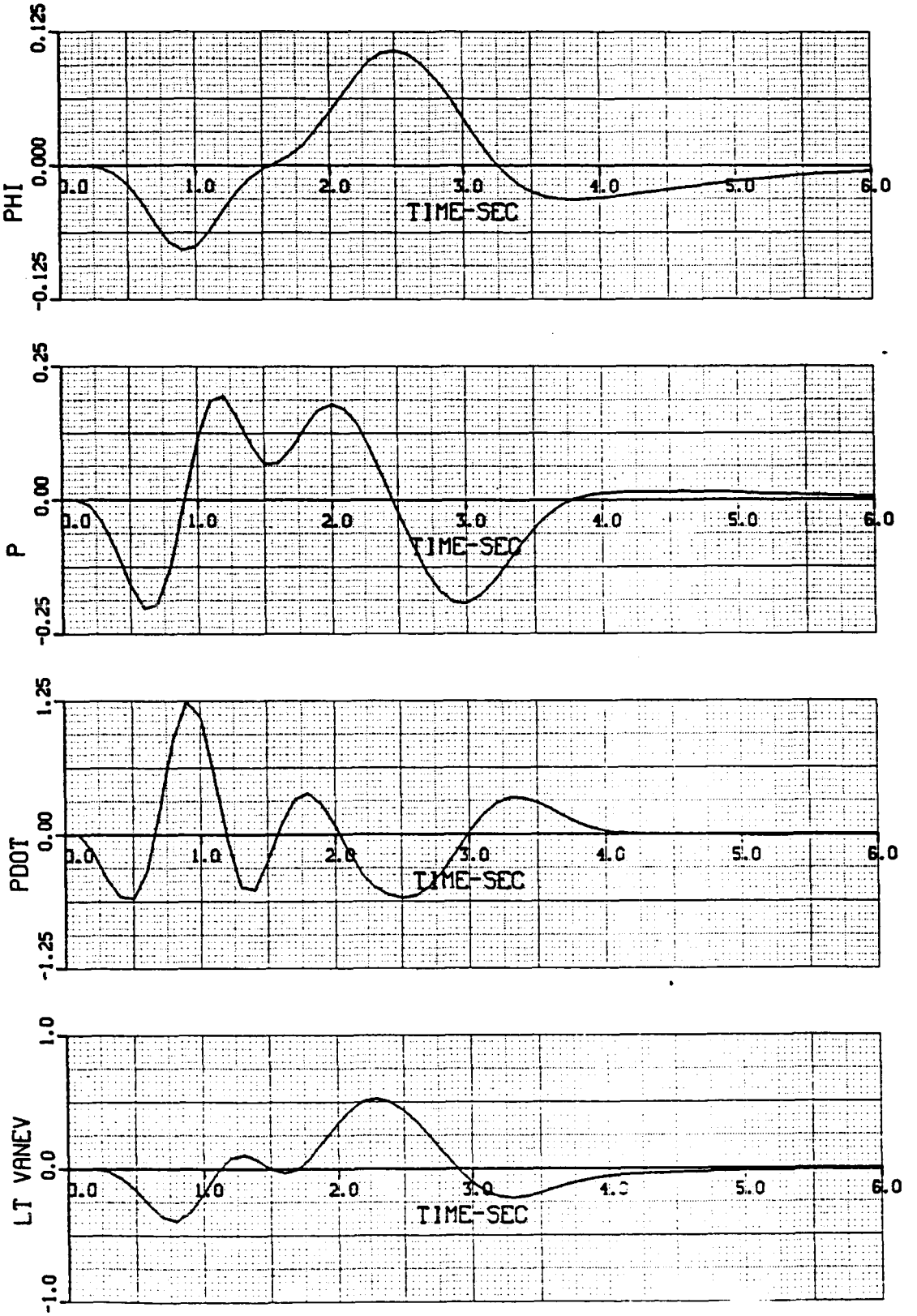

Figure A4.- Concluded.

APPENDIX B

FUNDAMENTAL TIME HISTORIES

The figures in Appendix B demonstrate fundamental time histories of the aircraft in Phase III for various hover control configurations for 1.0 in. of input deflection. These figures were generated by the Grumman 6DOF digital program and have been compared with the NASA Ames VMS responses.

ANACT	nacelle deflection, deg
DIF TRST	differential thrust between the left and right engines, lb/100
DIF VANE	differential thrust between the left and right horizontal vanes, deg
GVANEL	left guide vane deflection, deg
VXI	velocity of the aircraft in the inertial axis, x direction, ft/s
VYI	velocity of the aircraft in the inertial axis, y direction, ft/s
YAI	position change of the aircraft in the inertial axis

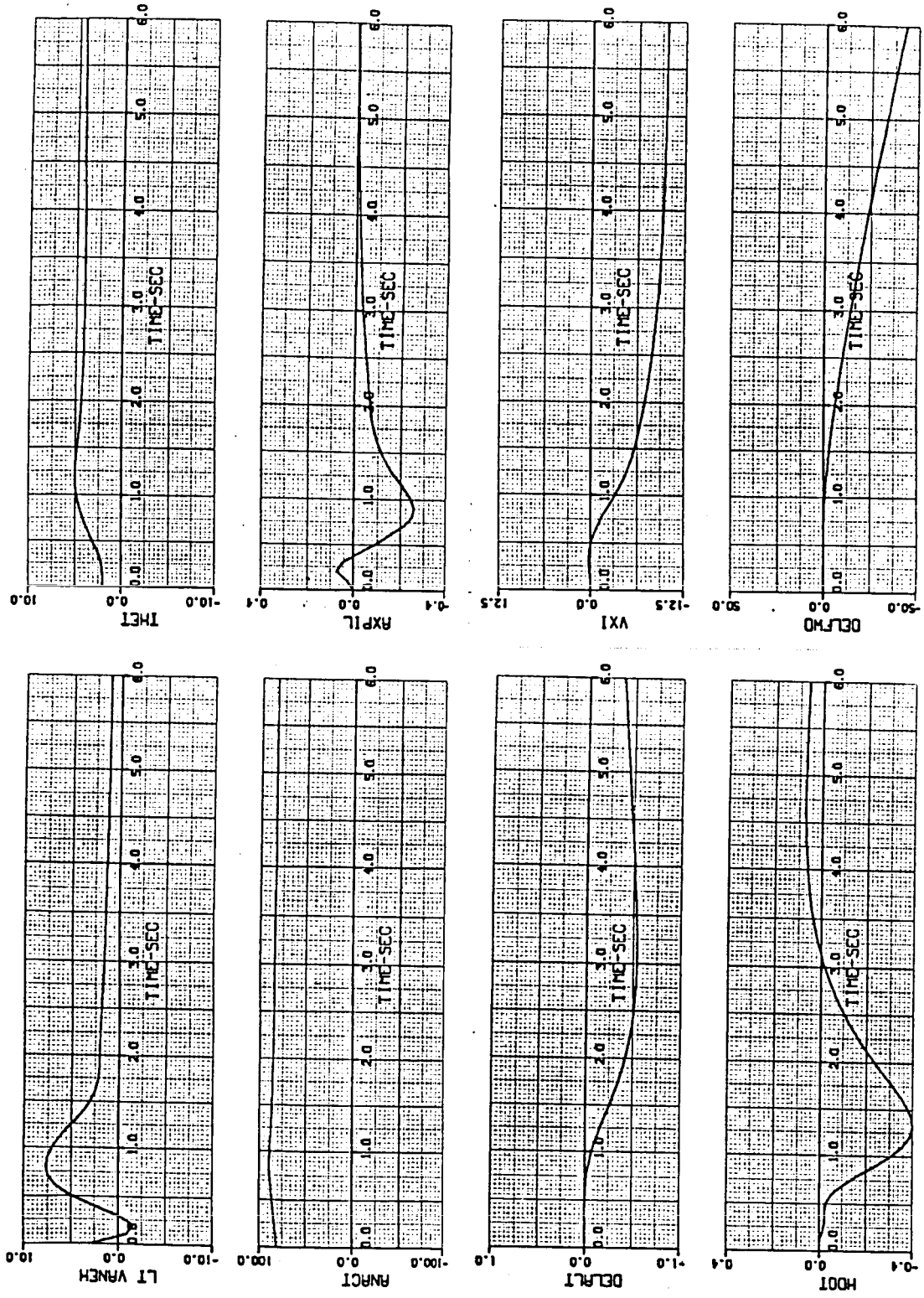

Figure B1.- 698 Longitudinal dynamic response. Final response characteristics--Phase III: 1-in. step-longitudinal stick input from trim hover in no-wind with flightpath augmentation on.

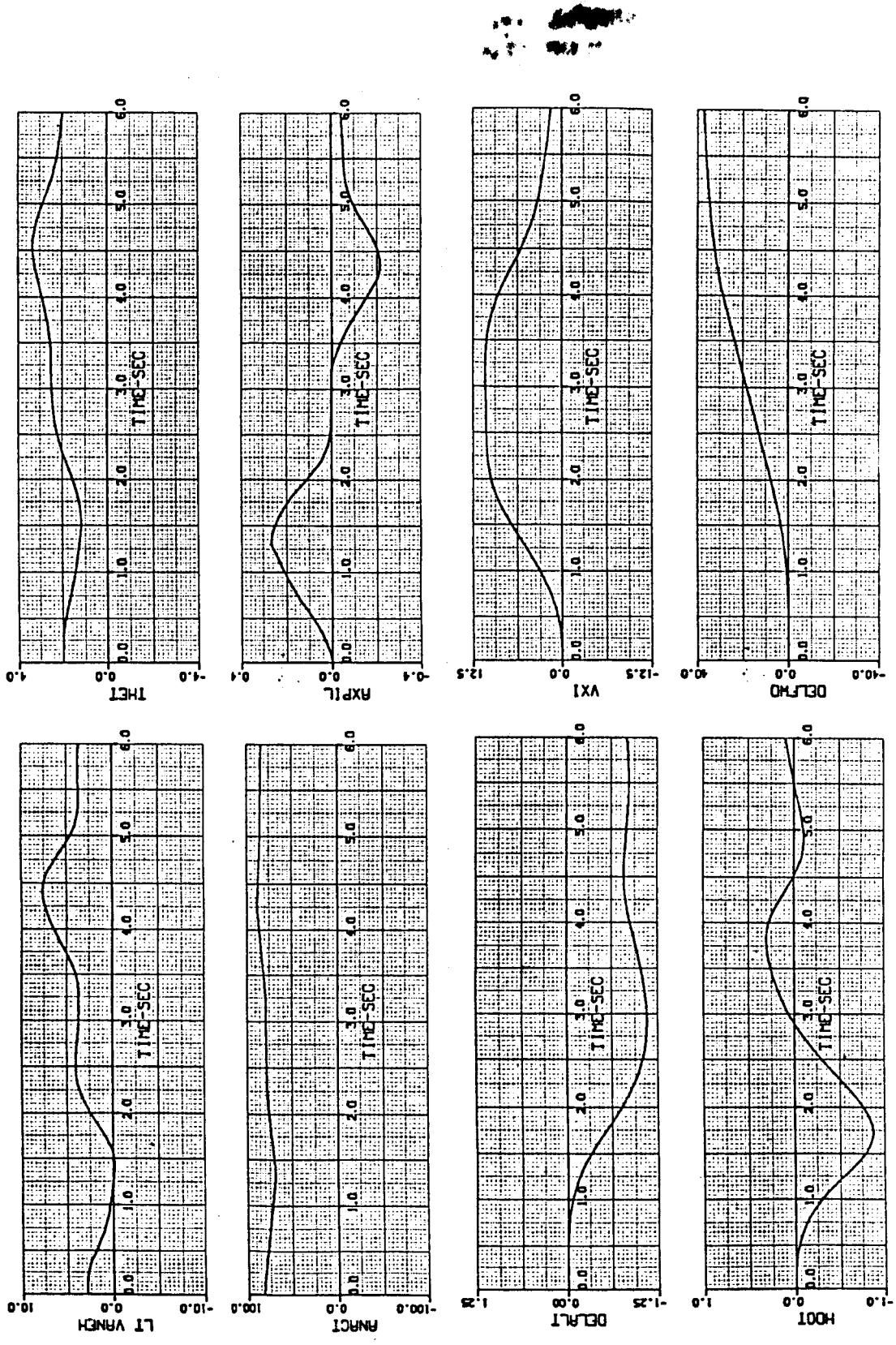

Figure B2.- 698 Longitudinal dynamic response. Final response characteristics--
Phase III: Full longitudinal tophat input from trim hover in no-wind with
flightpath augmentation on.

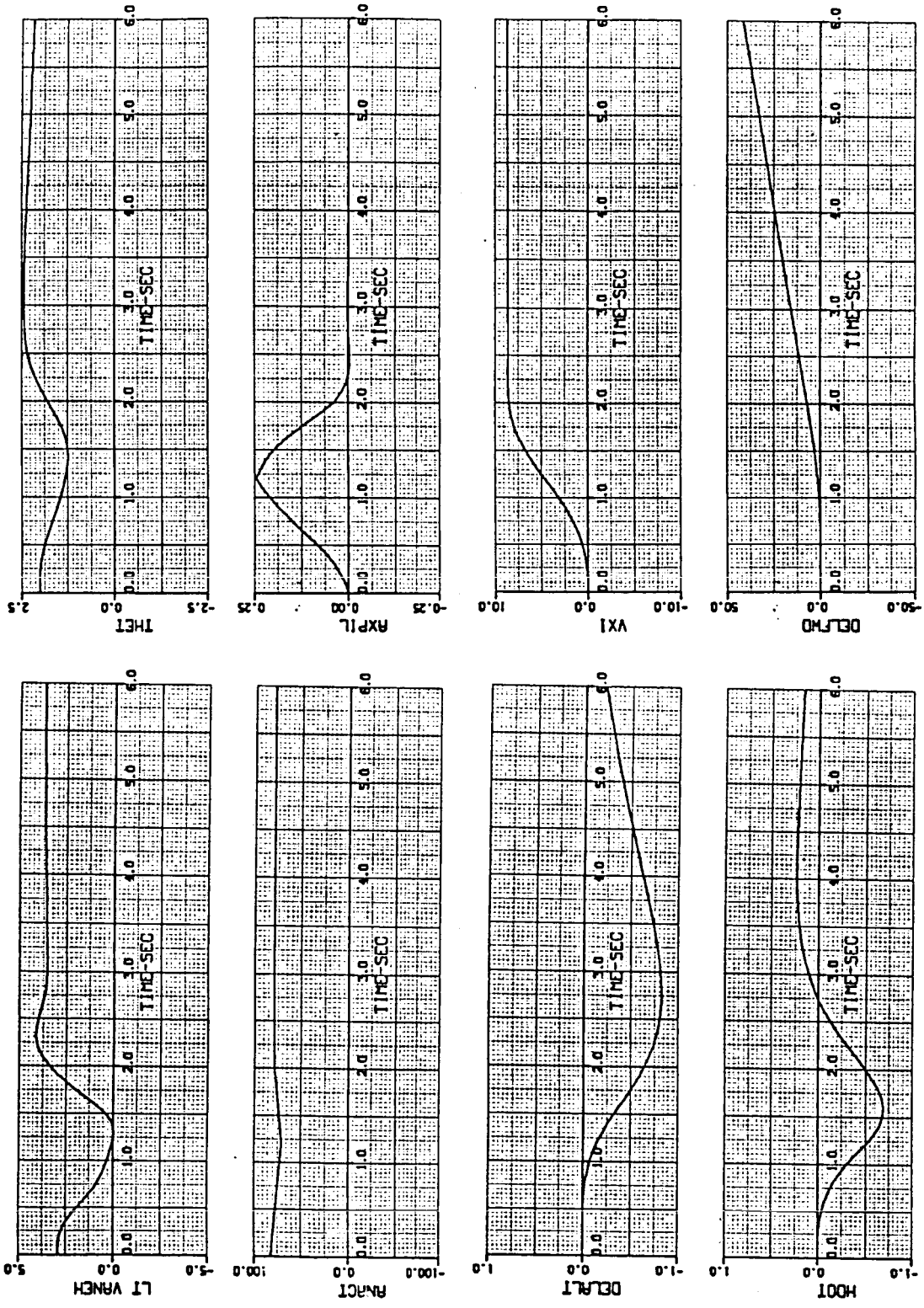

Figure B3.- 698 Longitudinal dynamic response. Final response characteristics--
Phase III: Full longitudinal surge-wheel input from trim hover in no-wind with
flightpath augmentation on.

CONTROL MODE
1 AND 2

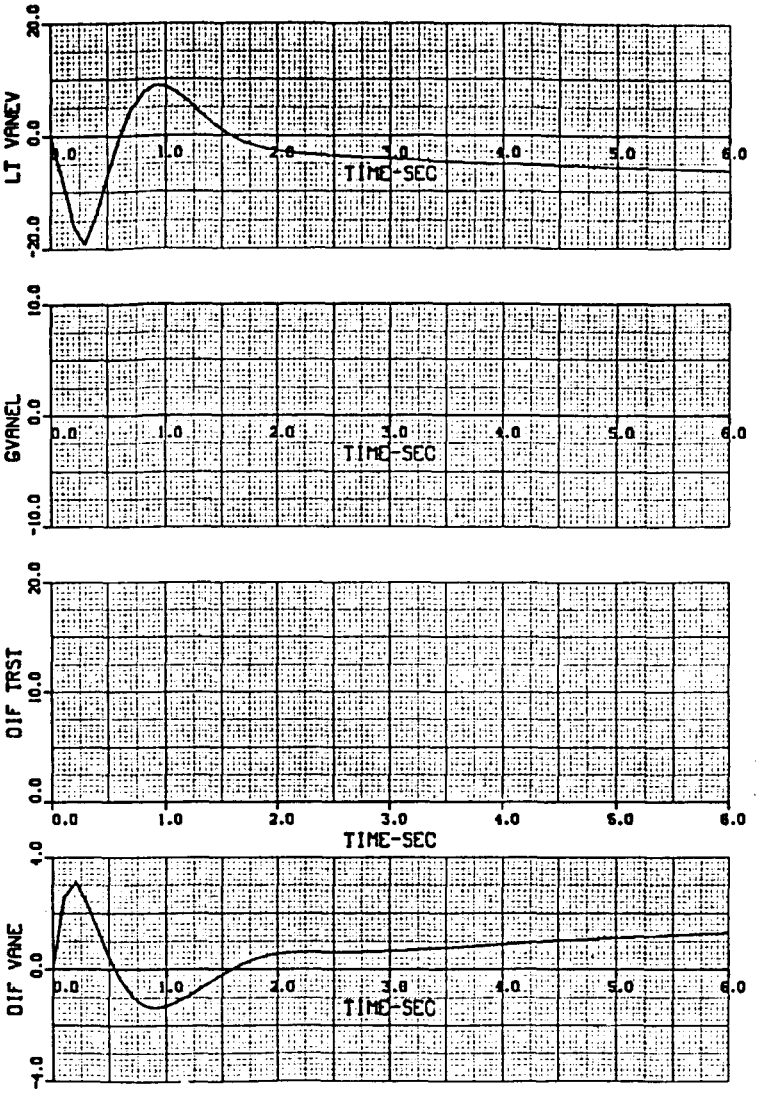

Figure B4.- 698 Lateral dynamic response. Final response characteristics--
Phase III: 1 in.-step lateral-stick input from trim hover in no-wind conditions
with flightpath augmentation on.

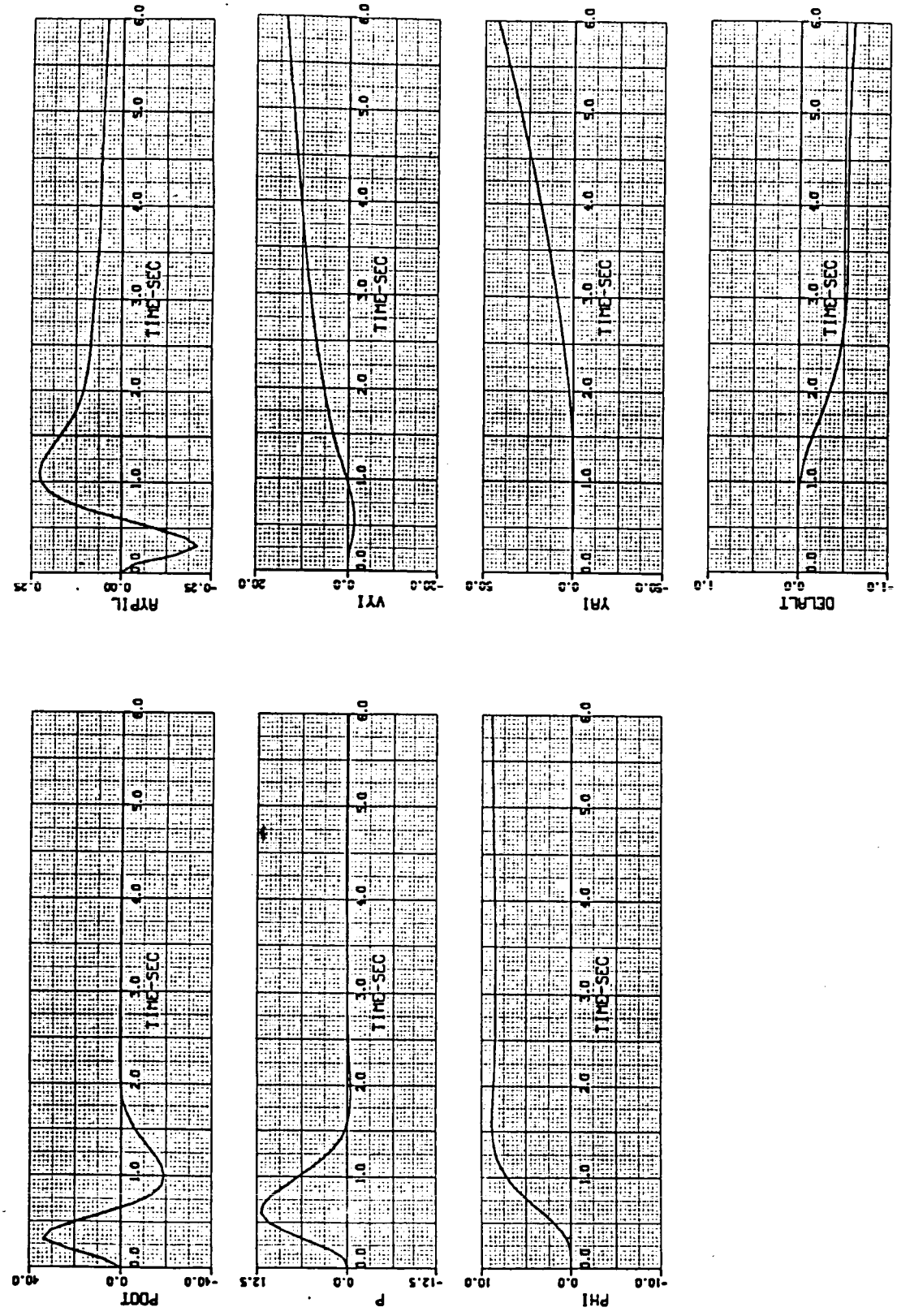

Figure B4.- Concluded.

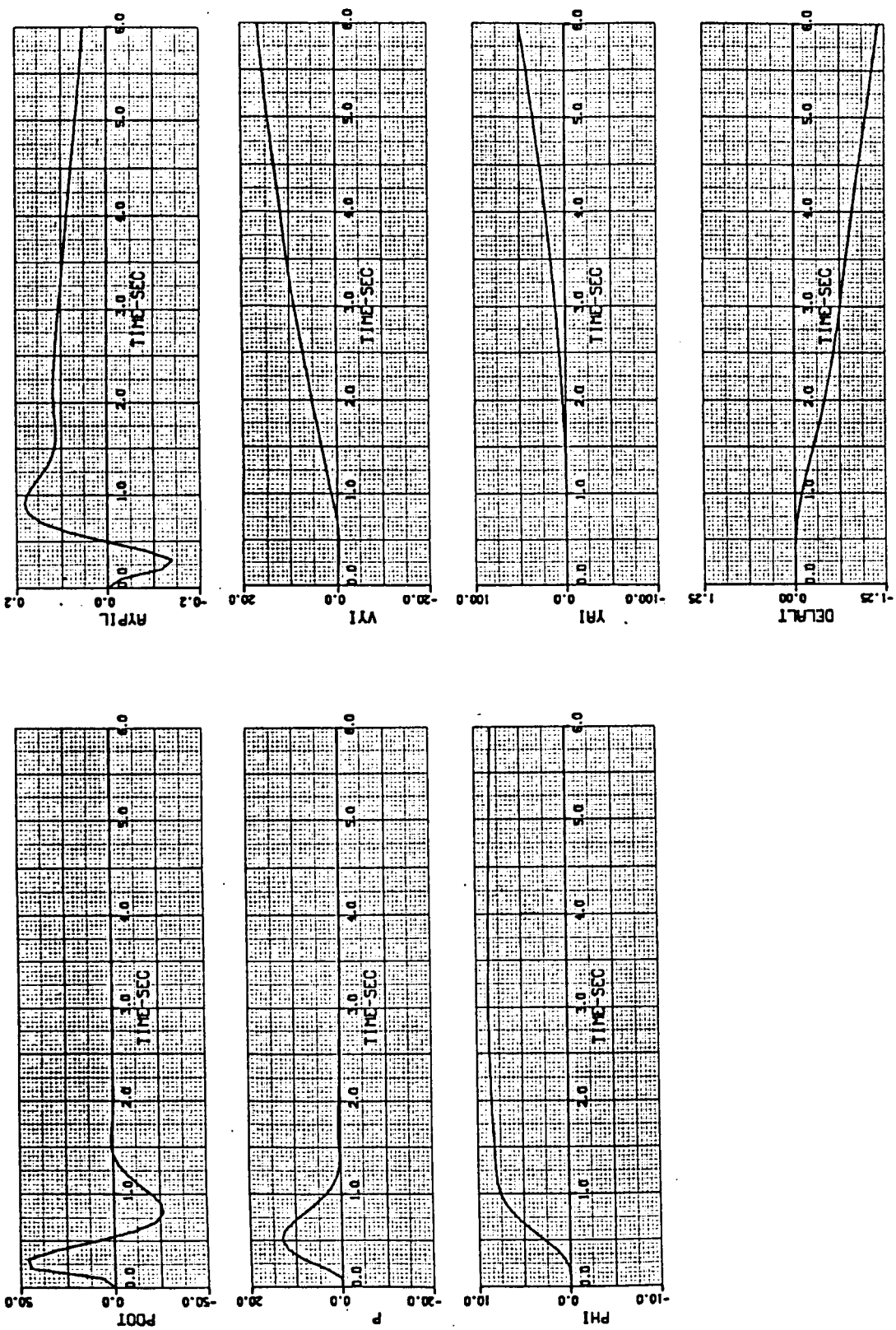

Figure B5.- 698 Lateral dynamic response. Final response characteristics--
Phase III: 1 in.-step lateral-stick input from trim hover in no wind with
flightpath augmentation on.

CONTROL MODE
1P

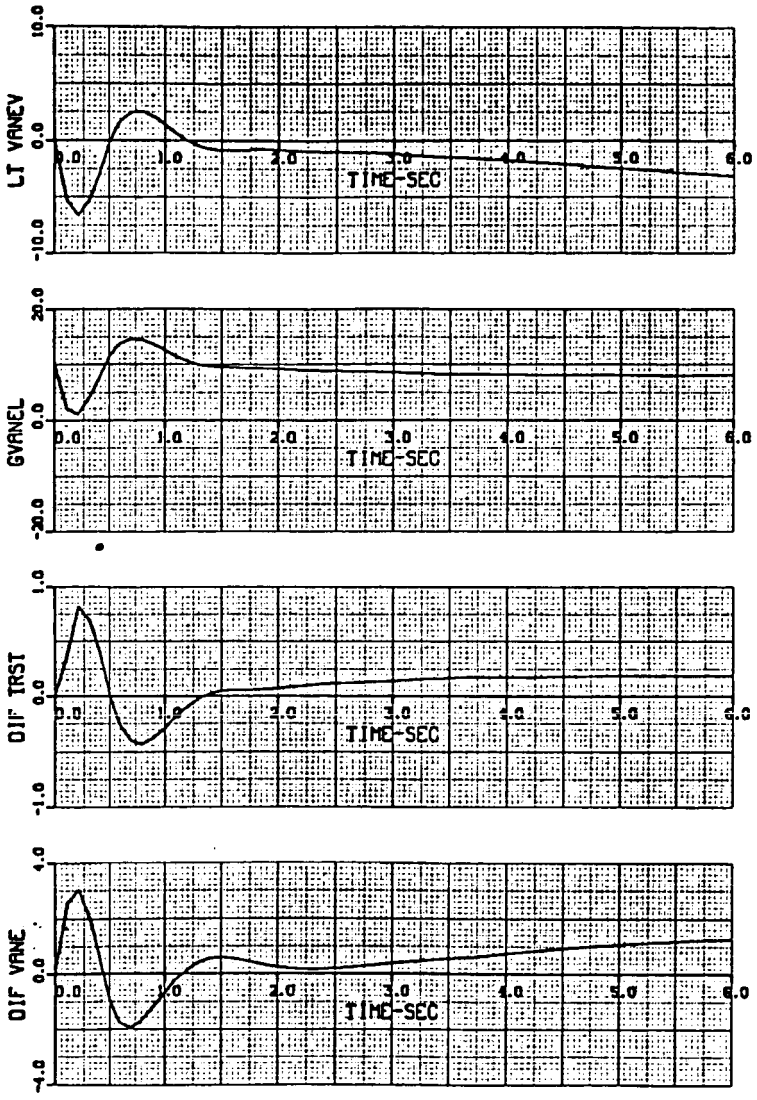

Figure B5.- Concluded.

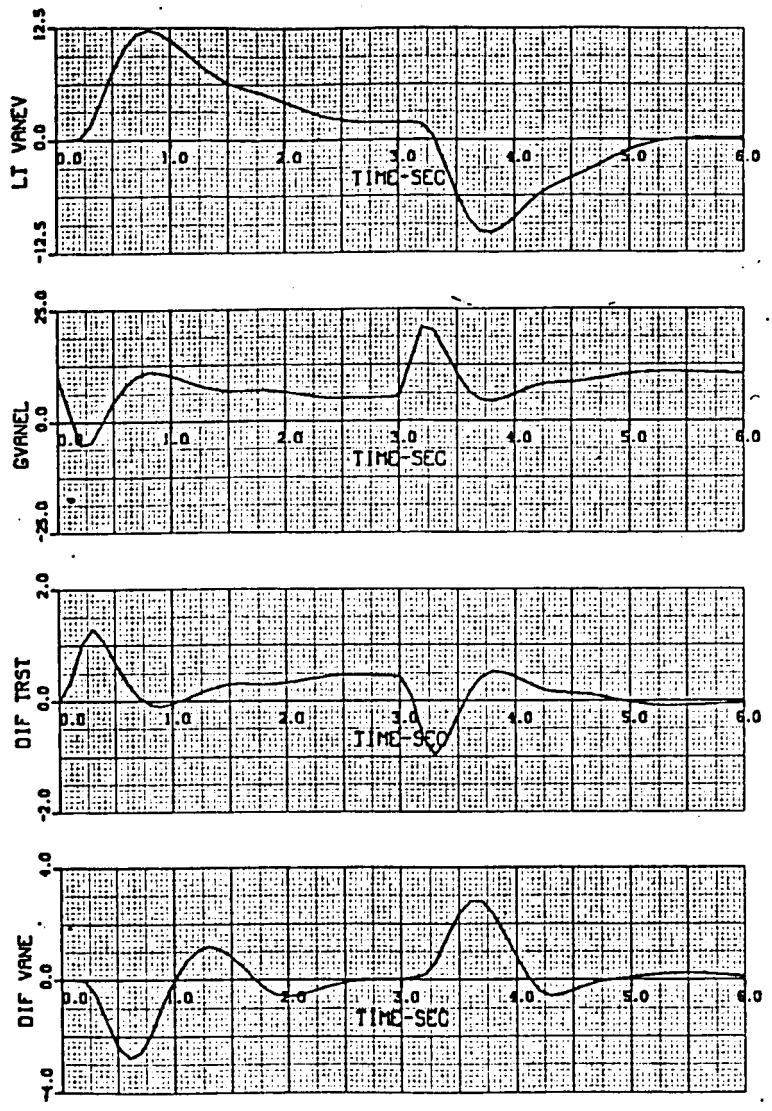

CONTROL MODE
1P

Figure B6.- 698 Lateral dynamic response. Final response characteristics--
Phase III: Full lateral tophat input from trim hover in no-wind with flightpath augmentation on.

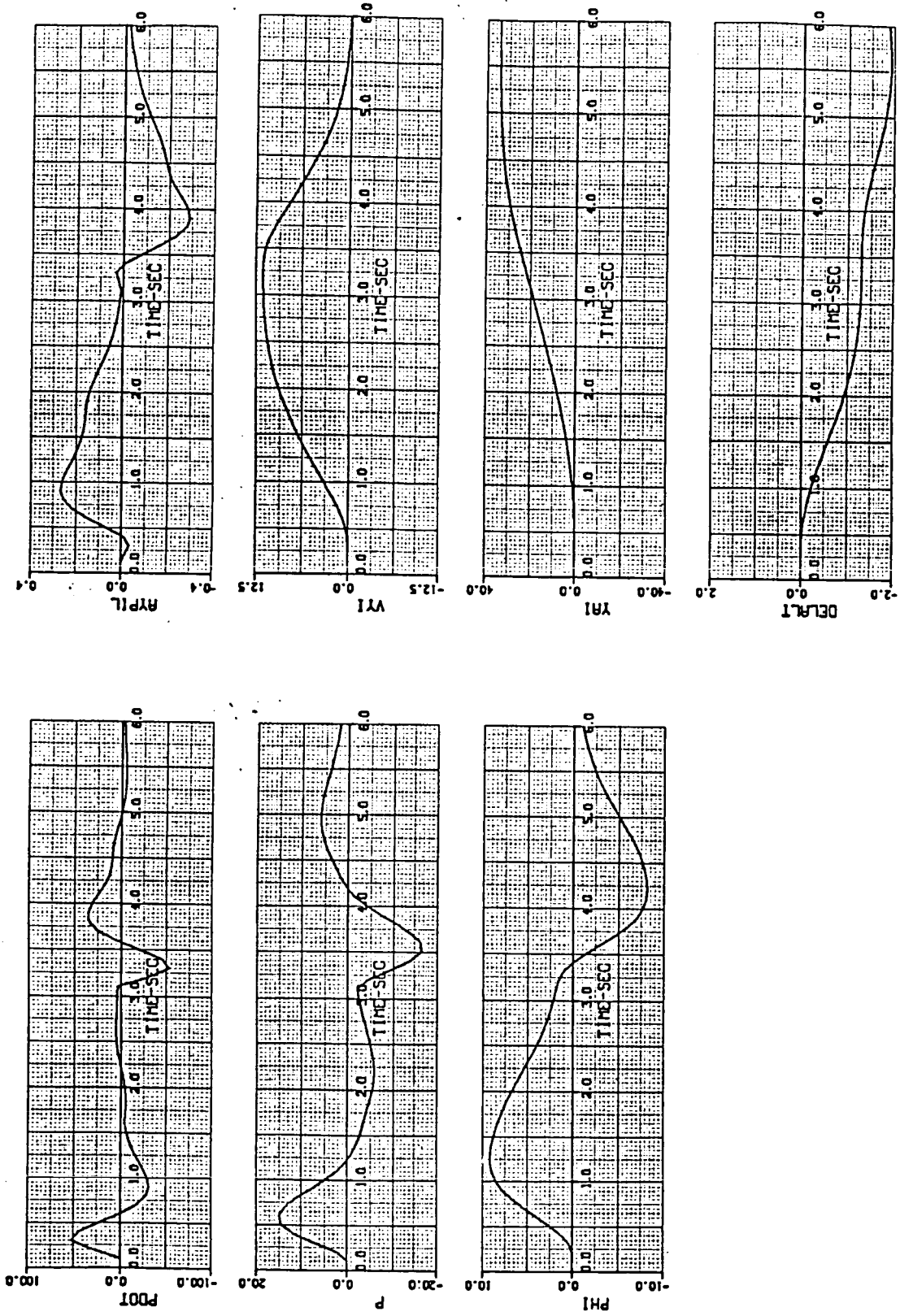

Figure B6.- Concluded.

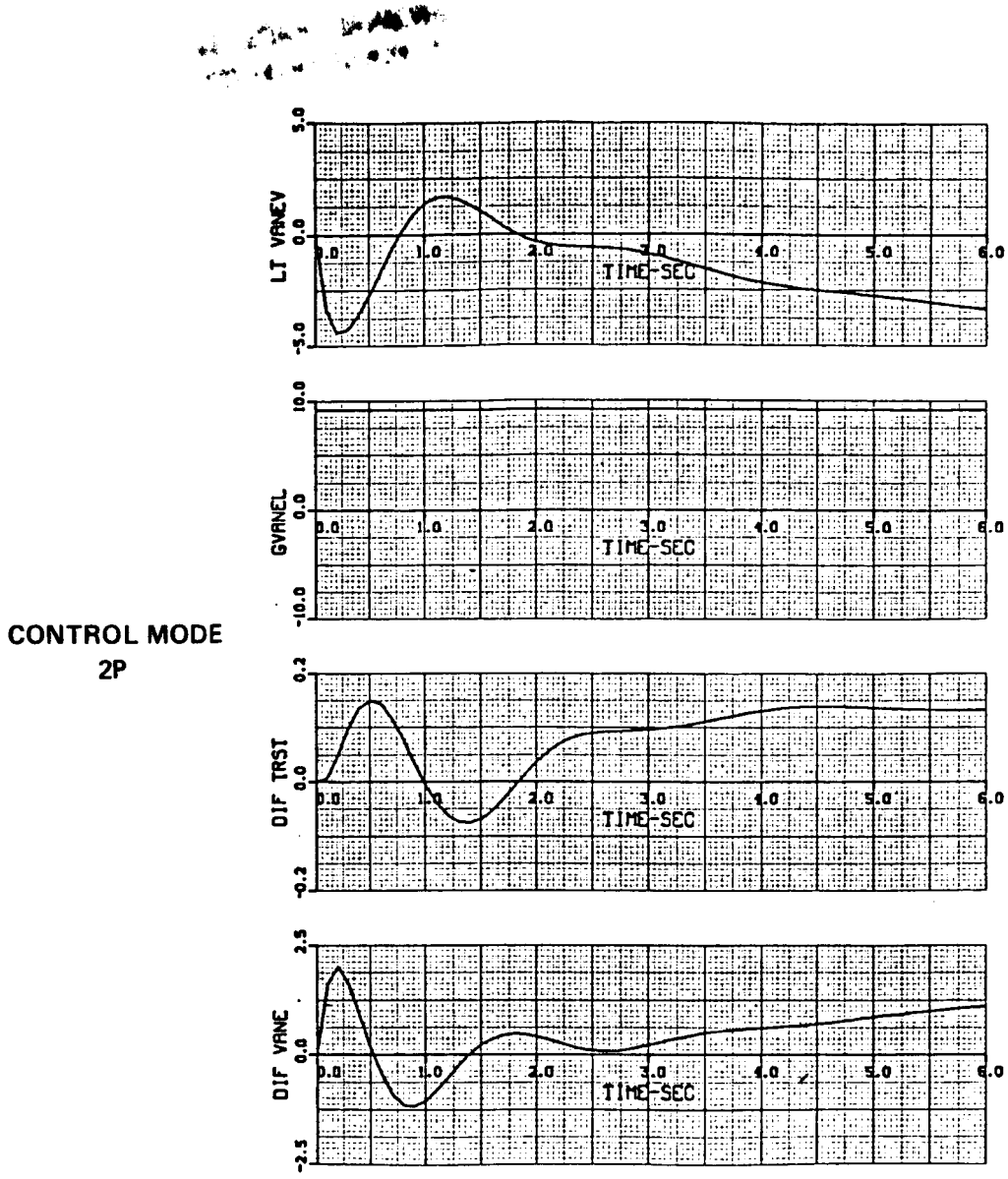

Figure B7.- 698 Lateral dynamic response. Final response characteristics--
Phase III: 1 in.-step lateral-stick input from trim hover in no wind with
flightpath augmentation on.

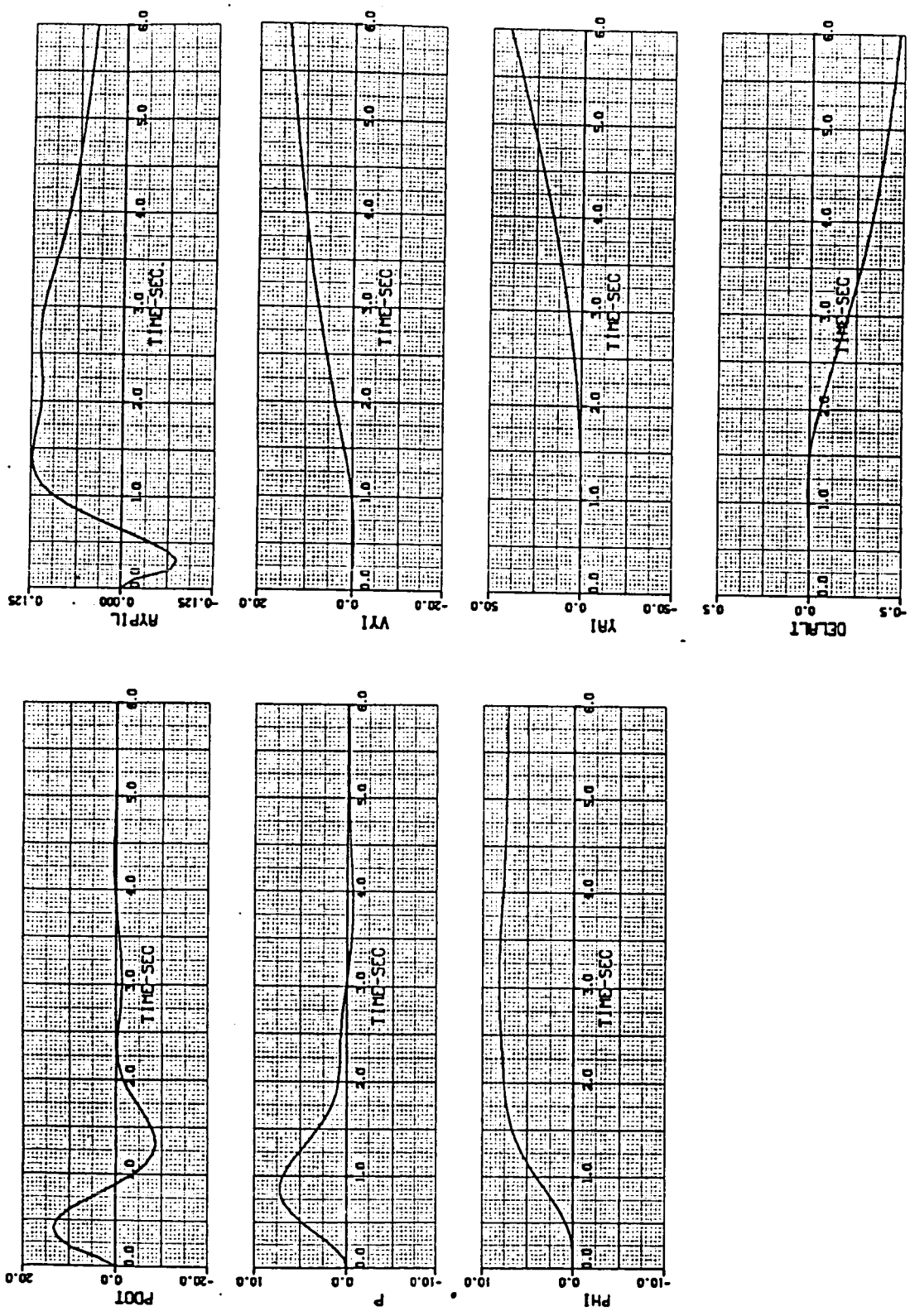

Figure B7.- Concluded.

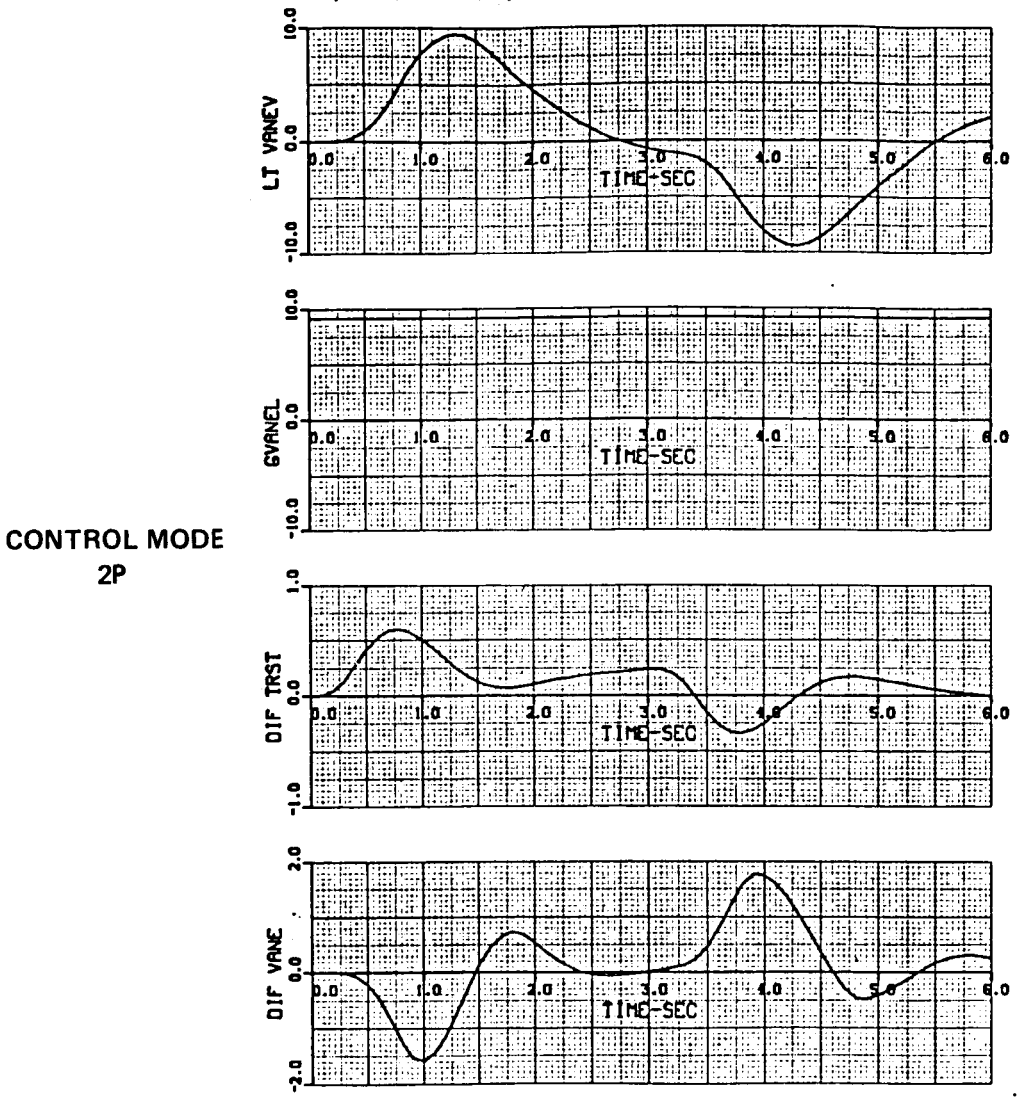

Figure B8.- 698 Lateral dynamic response. Final response characteristics--
Phase III: Full lateral tophat input from trim hover in no-wind with flightpath augmentation on.

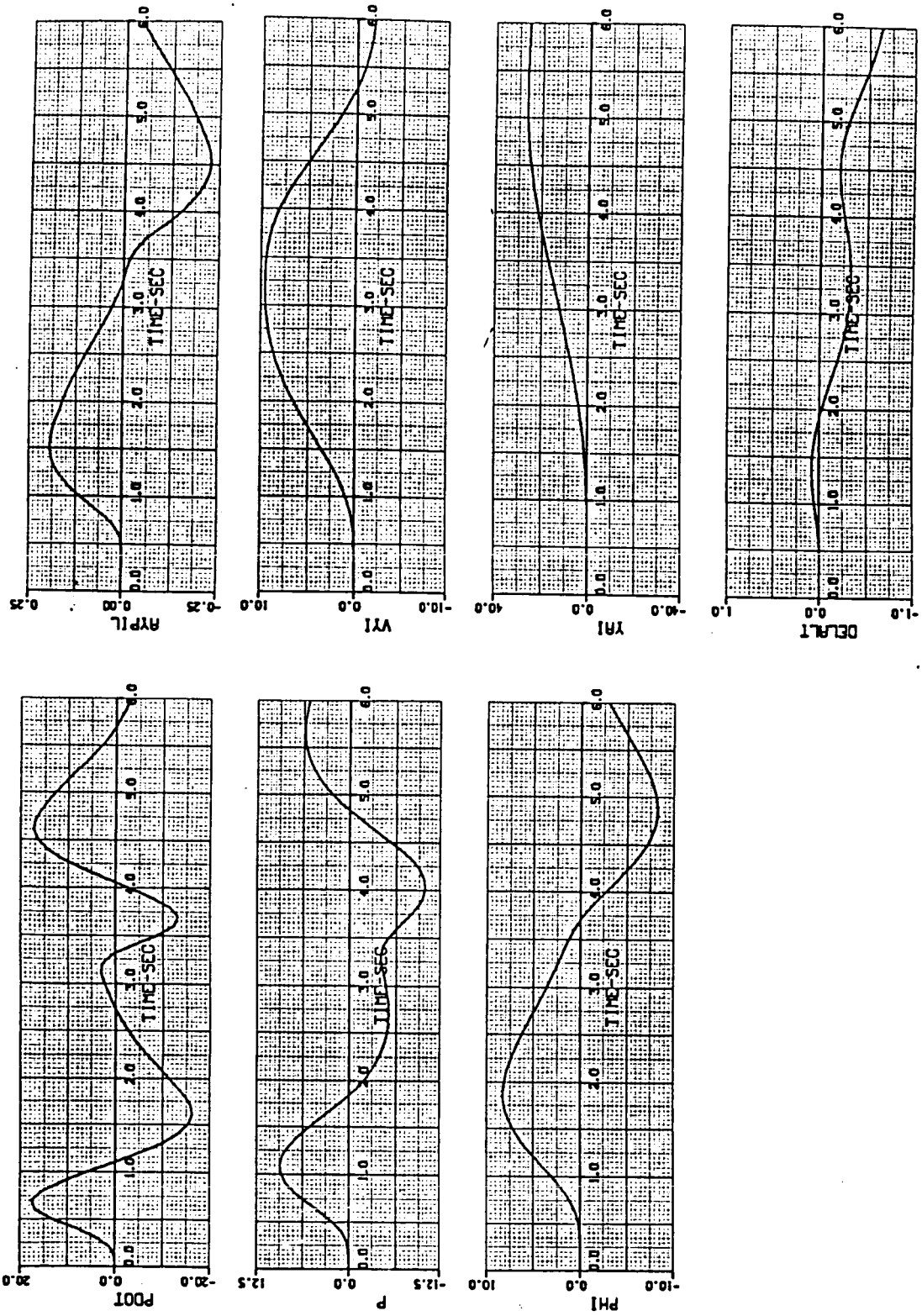

Figure B8.- Concluded.

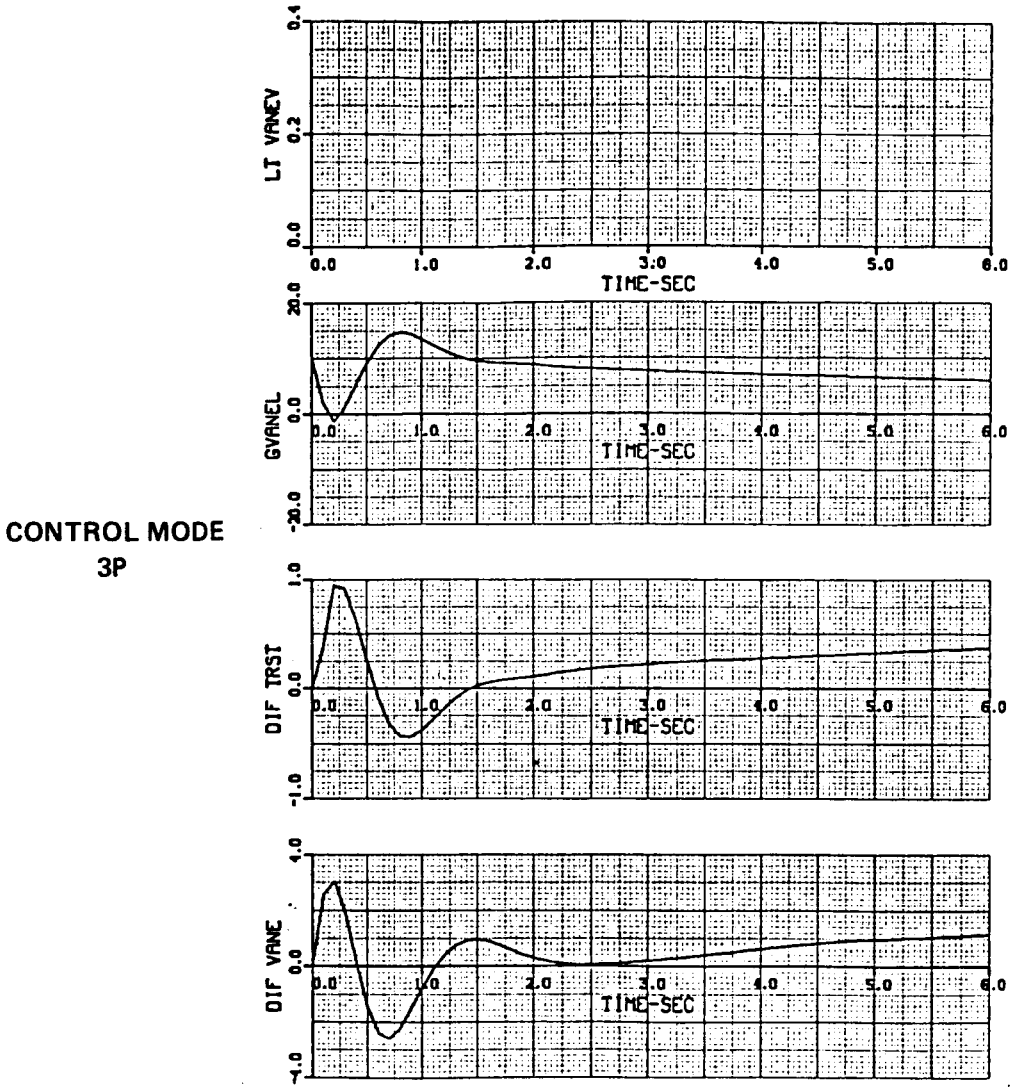

Figure B9.- 698 Lateral dynamic response. Final response characteristics--Phase III: 1 in.-step lateral stick input from trim hover in no-wind with flightpath augmentation on.

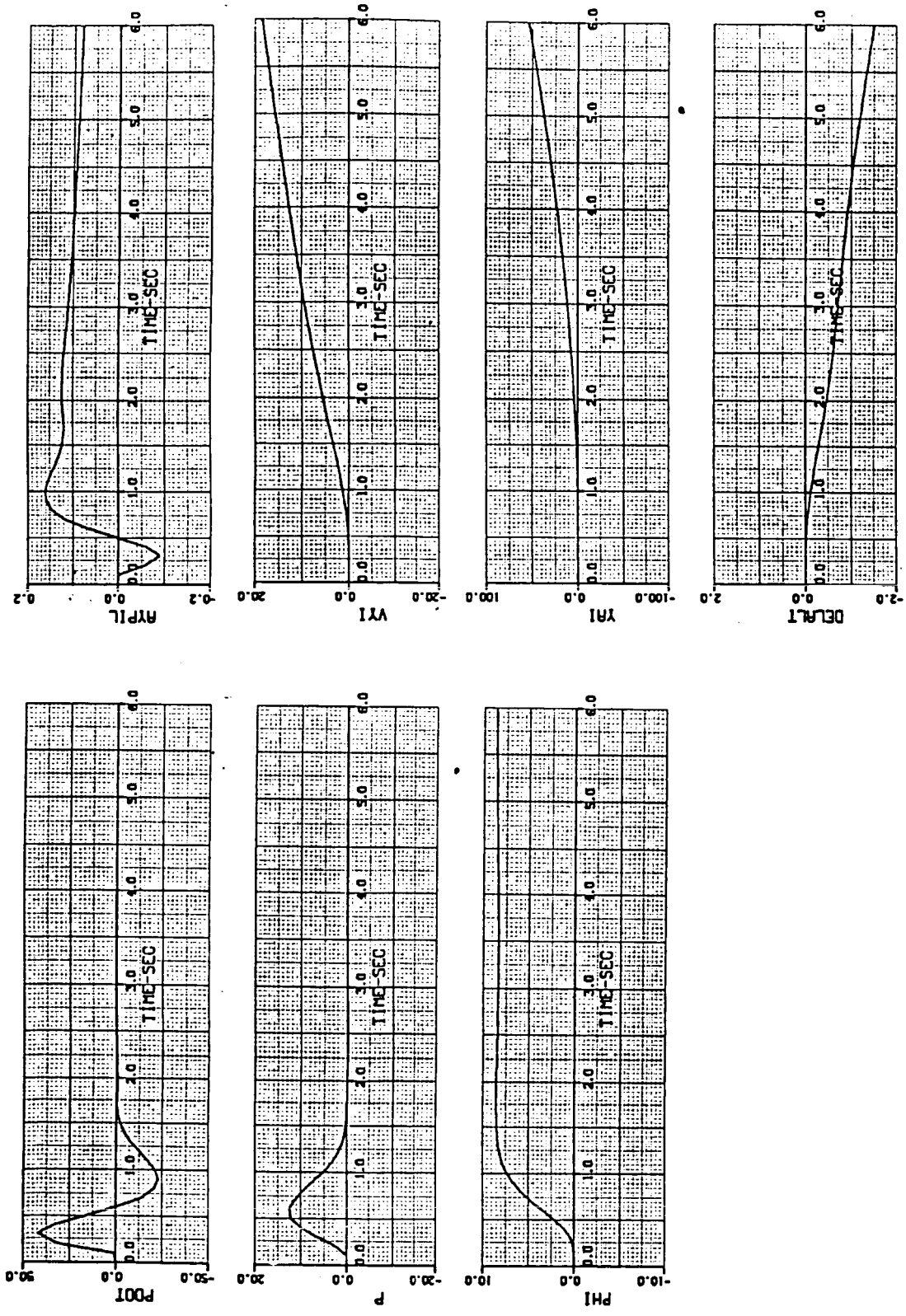

Figure B9.- Concluded.

CONTROL MODE
4

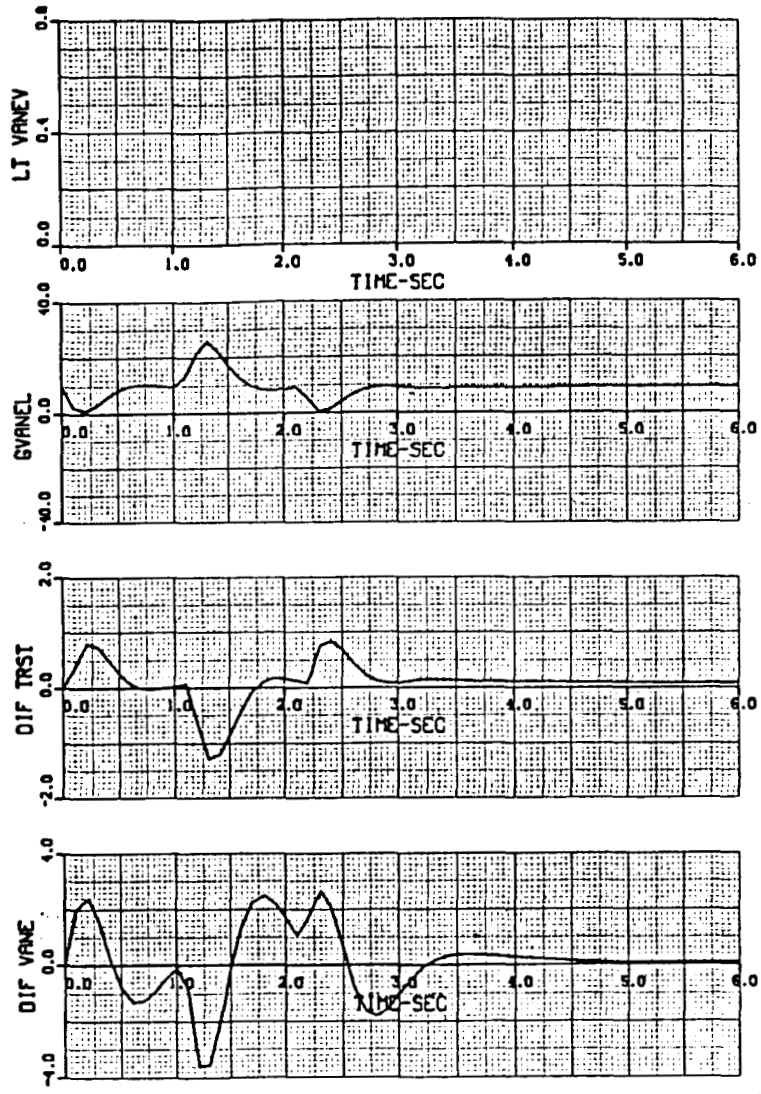

Figure B10.- 698 Lateral dynamic response. Final response characteristics--Phase III: 1 in.-step lateral-stick input from trim hover in no-wind with flightpath augmentation on.

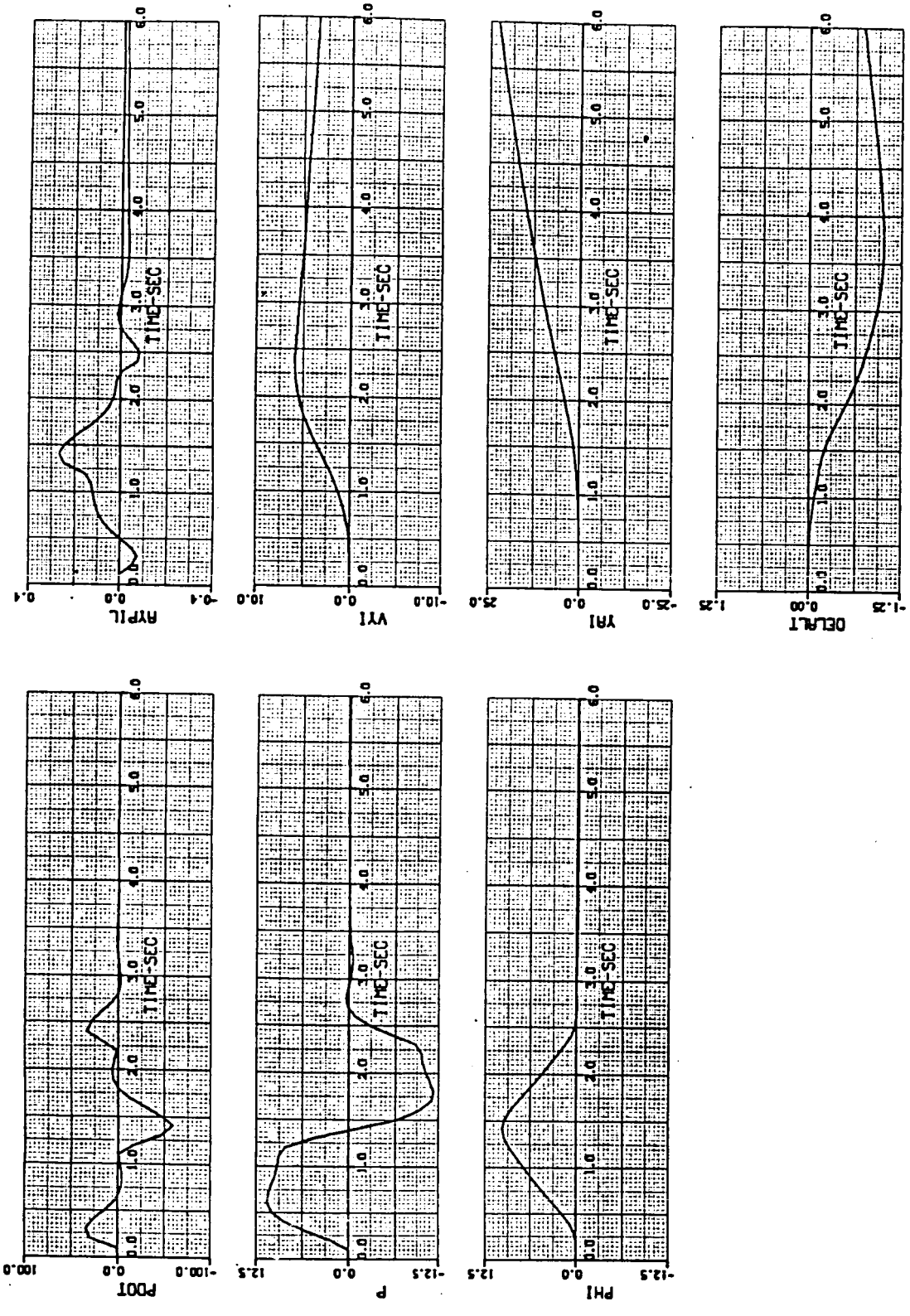

Figure B10.- Concluded.

REFERENCES

1. Kress, R. W.: An Affordable Means of Increasing Sea-Based Air Power. SAE Paper 801241, Oct. 1980.

2. Wilson, S. B.; Bowles, J. V.; and Foster, J. D.: Analysis of Selected VTOL Concepts for a Civil Transportation Mission. AIAA Paper 81-2655, Dec. 1981.

3. Ciminera, M. V.: The Development of a Twin-Turbofan V/STOL Aircraft. Presented at the 36 Annual Forum of the American Helicopter Society, May 1980.

4. Grumman Aerospace Corporation: Full-Scale Tests of Grumman Design 698-411 Tilt Nacelle V/STOL Model at the NASA-Ames Research Center. NAVAIR Report N00019-80-C-0115, Dec. 1981.

5. Jones, A. D.: Operations Manual: Vertical Motion Simulator (VMS) S.08. NASA TM-81180, May 1980.

6. Stapleford, R. L.; Clement, W. F.; Heffley, R. K; Booth, G. C.; and Fortenbaugh, R. L.: Flight Control/Flying Qualities Investigation for Lift/Cruise Fan V/STOL. Naval Air Development Center Report 777143-30, vol. I, II, III, Aug. 1979.

7. Merrick, V. K.: Simulation Study of Two VTOL Control/Display Systems in IMC Approach and Landing. NASA TM-81295, Aug. 1981.

8. Merrick, V. K.: A Translational Velocity Command System for VTOL Low-Speed Flight. NASA TM-34215, March 1982.

9. Merrick, V. K.: Study of the Application of an Implicit Model Following Flight Controller to Lift-Fan VTOL Aircraft. NASA TP-1040, Nov. 1977.

10. Greif, R. K.,; Fry, E. B.; Gerdes, R. M.: and Gossett, T. D.: Stabilization on VTOL Aircraft in Hovering Flight. NASA TN D-6900, Aug. 1972.

11. Valckenaere, W.: Tilt Nacelle V/STOL Aircraft Grumman Design 698-411 Flight Simulation Study Results (Phase I) Feb. 1984.

12. Cooper, G. E.; and Harper, R. P.: The Use of Pilot Rating in the Evaluation of Aircraft Handling Qualities. NASA TN D-5153, Apr. 1969.

13. Johns, J. B.; Clark, J. W., Jr.; and Donley, S. T.: Results of the Grumman Design 698-411, Phase II, Piloted Simulation. Naval Air Development Center 6053/6012 memorandum to memorandum 6051, Dec. 1983.

14. Donley, S. T.: Evaluation of Several Control/Display Control for V/STOL Shipboard Landing. Transactions of SAE, 1980.

15. Johns, J. B.; Clark, J. W., Jr.; and Donley, S. T.: Results of the Grumman Design 698: Phase III Piloted Simulation. Naval Air Development Center 6053/6012 memorandum to memorandum 6051, Sept. 1984.

16. Falarski, M. D.; Dudley, M. R.; Buckman, W.; and Pisano, A.: Aerodynamic Characteristics of a Large-Scale Twin Tilt-Nacelle V/STOL Model. AIAA Paper 81-0150, Jan. 1981.

17. Johns, J. B.; Donley, S. T.; and Clark, J. W., Jr.: Results of JVX Test #1 Piloted Simulation. Naval Air Development Center 6053/6012 memorandum to memorandum 609J, June 1984.

TABLE 1.- CLASSICAL CONTROL SYSTEM--PHASE I

CRUISE

BASIC UNAGUMENTED, STABLE AIRCRAFT
SAS[a] SELECTION PROVIDES
RATE DAMPING IN PITCH
RATE COMMAND/ATTITUDE HOLD IN ROLL
TURN COORDINATION IN YAW
PILOT RELIEF MODES
ALTITUDE HOLD
HEADING HOLD

CONVERSION

ATTITUDE COMMAND/ATTITUDE HOLD – PITCH
RATE COMMAND/ATTITUDE HOLD – ROLL
TURN COORDINATION IN YAW

TRANSITION

ATTITUDE COMMAND/ATTITUDE HOLD – PITCH
RATE COMMAND/ATTITUDE HOLD BECOMES ATTITUDE COMMAND/ATTITUDE HOLD AT 40 knot – ROLL
TURN COORDINATION BECOMES RATE COMMAND/ATTITUDE HOLD AT 60 knot – YAW
MANUAL OPERATION OF THROTTLE/NACELLE ON THRUST LEVER
FLIGHTPATH CONTROL ($\dot{h}$, $\ddot{x}$) AVAILABLE ON SEPARATE VELOCITY LEVER
ALTITUDE HOLD AVAILABLE WHILE ON APPROACH TO LANDING SITE

HOVER AND LANDING

MAY BE ATTEMPTED WITH ABOVE SYSTEM

[a]SAS: STABILITY-AUGMENTATION SYSTEM.

TABLE 4.- CLASSICAL CONTROL SYSTEM--PHASE II

- ABOVE 160 knots (PRIOR TO NACELLE UNLOCK)

LONGITUDINAL:	PITCH RC
LATERAL/DIRECTIONAL:	ROLL RC/AH TURN COORDINATION HEADING HOLD AVAILABLE
VERTICAL:	MANUAL THROTTLE ALTITUDE HOLD AVAILABLE

- BETWEEN 160 knots AND 50 knots (CONVERSION/TRANSITION)

LONGITUDINAL/VERTICAL:	PITCH RC/AH OPTIONS: (1) MANUAL THROTTLE AND NACELLE TILT (2) FLIGHTPATH AUGMENTATION: $\dot{h}$, $\ddot{x}$ COMMAND/h, $\dot{x}$ HOLD
LATERAL/DIRECTIONAL:	ROLL RC/AH TURN COORDINATION

- AT 50 knots AND BELOW:

LONGITUDINAL/VERTICAL:	OPTIONS: (1) STANDARD MODE: PITCH AC/AH VIA STICK (2) PRECISION MODE: $\dot{x}$ COMMAND/$\dot{x}$ HOLD VIA STICK $\dot{x}$ COMMAND/$\dot{x}$ HOLD/AH VIA TRC BUTTON OPTIONS: (1) MANUAL THROTTLE AND NACELLE TILT (2) FLIGHT PATH AUGMENTATION: $\dot{h}$, $\ddot{x}$ COMMAND/h, $\dot{x}$ HOLD
LATERAL/DIRECTIONAL:	OPTIONS: (1) STANDARD MODE: ROLL AC/AH VIA STICK (2) PRECISION MODE: $\dot{y}$ COMMAND/$\dot{y}$ HOLD VIA STICK $\dot{y}$ COMMAND/$\dot{y}$ HOLD/AH VIA TRC BUTTON YAW RC/HEADING HOLD

RC – RATE COMMAND
AH – ATTITUDE HOLD
AC – ATTITUDE COMMAND

$\dot{h}$ – ALTITUDE RATE
$\ddot{x}$ – LONGITUDINAL ACCELERATION
$\dot{x}$ – LONGITUDINAL VELOCITY
$\dot{y}$ – LATERAL VELOCITY

TABLE 5.- DESIGN 698 TEST MATRIX--PHASE II

TASK NO.	TASK	RATING SEGMENT	FLIGHT CONTROL			ENVIRONMENT			INITIAL CONDITIONS
1	INBOUND TRANSITION TO AN LPH	INITIAL CONVERSION DECEL TO ~ 110 knots	A	MANUAL THROTTLE		1	10 knot WOD AT 0° LT/MOD TURB		ALTITUDE = 1200 ft RANGE = 8 n. mi. AIRSPEED = 200 knots $\gamma = 0°$ CLEAN CONFIG.
		INTERCEPT AND TRACK GS DECEL TO H/LS	—						
		STATION KEEPING	B	FLIGHT PATH AUG					
2	OUTBOUND TRANSITION FROM AN LPH	LATERAL TRANSLATION	A	MANUAL THROTTLE		1	10 knot WOD AT 0° LT/MOD TURB		HOVER OVER TD SPOT ALTITUDE ~ 50 ft GEAR DOWN
		ACCEL TO ~ 160 knots UP TO NACELLE LOCK	—						
		ACCEL TO CLEAN FLIGHT INCL. NACELLE LOCK	B	FLIGHT PATH AUG					
3	APPROACH TO AND LANDING ON AN LPH	LATERAL TRANSLATION	A	STANDARD	FPA	1	15 knot WOD AT 0° LT/MOD TURB	SS 3	ALTITUDE = 1200 ft RANGE = 5 n. mi. AIRSPEED = 110 knots $\gamma = 0°$ GEAR DOWN
		HOVER OVER TD SPOT	B	PRECISION NON-X-SHAFT		2	15 knot WOD AT 0° MOD TURB		
		DESCEND AND LAND	C	PRECISION X-SHAFT		3	25 knot WOD AT 0° MOD TURB		
4	INBOUND TRANSITION TO A DD-963	TRANSLATION TO HOVER OVER DECK	A	STANDARD	FPA	1	25 knot WOD AT - 60° AIRWAKE TURB	SS 3	1000 ft AFT OF DECK ON A 30° RADIAL ALTITUDE = 90 ft $\gamma = 0°$ 10 knot CLOSURE RATE
		HOVER OVER TD SPOT	B	PRECISION NON-X-SHAFT					
		DESCEND AND LAND	C	PRECISION X-SHAFT		2	35 knot WOD AT -60° AIRWAKE TURB	SS 5	
5	SPOT TURN OVER A VTOL PAD		A	STANDARD	MAN	1	15 knot WIND LT/MOD TURB		OUT-OF-GROUND-EFFECT
			B	STANDARD	FPA				
			C	PRECISION		2	25 knot WIND LT/MOD TURB		

GS - GLIDESLOPE
H/LS - HOVER/LOW-SPEED
SS - SEA STATE
WOD - WIND OVER DECK
TD - TOUCHDOWN
MAN - MANUAL THROTTLE
FPA - FLIGHT PATH AUGMENTATION
X-SHAFT - VIGV CONTROL OF DIFF. THRUST
NON-X-SHAFT - Δ RPM CONTROL OF DIFF. THRUST

TABLE 6.- CLASSICAL CONTROL SYSTEM--PHASE III

LONGITUDINAL/VERTICAL:

RESPONSE TYPE	CONTROL EFFECTORS
ATTITUDE, $\dot{x}$ COMMAND /ATTITUDE, $\dot{x}$ HOLD VIA STICK	HORIZONTAL VANE, NACELLE TILT
$\dot{x}$ COMMAND /$\dot{x}$, ATTITUDE HOLD VIA TOP HAT	NACELLE TILT, HORIZONTAL VANE
$\ddot{x}$ COMMAND/$\dot{x}$, ATTITUDE HOLD	NACELLE TILT, HORIZONTAL VANE

LATERAL:

RESPONSE TYPE	CONTROL EFFECTORS
MODE 1 AND 2 AC/AH VIA STICK	VERTICAL VANE
MODE 1P (X-SHAFTED) AC/AH VIA STICK	VERTICAL VANE DIFFERENTIAL GUIDE VANE (DIFFERENTIAL THRUST)
$\dot{y}$ COMMAND/$\dot{y}$, HOLD VIA TOP HAT	DIFFERENTIAL GUIDE VANE (DIFFERENTIAL THRUST), VERTICAL VANE
MODE 2P (NON-X-SHAFTED) AC/AH VIA STICK	VERTICAL VANE, DIFFERENTIAL RPM (DIFFERENTIAL THRUST)
$\dot{y}$ COMMAND/$\dot{y}$ HOLD VIA TOP HAT	DIFFERENTIAL RPM (DIFFERENTIAL THRUST), VERTICAL VANE
MODE 3 (X-SHAFTED) AC/AH VIA STICK	DIFFERENTIAL GUIDE VANE (DIFFERENTIAL THRUST)
MODE 4 (X-SHAFTED) RC/AH VIA STICK	DIFFERENTIAL GUIDE VANE(DIFFERENTIAL THRUST)

TABLE 7.- DESIGN 698 CONTROL SYSTEM--PHASE III

TASK	ENVIRONMENT		INIT. COND	FLT. CONT. MODE		ENGINES
COMPLETE INBOUND TRANSITION	20 knot WOD AT 0° MODERATE TURB. DAY		ALT 1200 ft ASL RANGE 10 NM AIRSPEED 200 knots CLEAN	1		X-SHAFTED
				2		NON-X-SHAFTED
APPROACH TO AND LANDING ON AN LPH	20 knot WOD AT 0° MODERATE TURB. SS 3	DAY	ALT 80 ft ASL 100 ft AFT AND TO PORT STATION KEEPING	1		X-SHAFTED
				1P (TH, STK, AND BW)		
				2		NON-X-SHAFTED
				2P (TH, STK, AND BW)		
		NIGHT		3		X-SHAFTED
				4		
APPROACH TO AND LANDING ON A DD 963	26 knot WOD AT -30° MODERATE TURB. SHIP AIRWAKE SS 3 DAY		ALT 90 ft ASL 1000 ft AFT ON A 30° RADIAL 15 knot CLOSURE RATE	1P		X-SHAFTED
	35 knot WOD AT -30° MODERATE TURB. SHIP AIRWAKE SS 5 DAY			3		
SPOT TURN OVER A VTOL PAD	15 knot WOD MODERATE TURB. DAY		ALT 40 ft AGL CENTER OF THE PAD HOVER	1P	SURGE ON	X-SHAFTED
	25 knot WOD MODERATE TURB. DAY				SURGE OFF	

WOD = WIND OVER DECK
TURB = TURBULENCE
ALT = ALTITUDE
ASL = ABOVE SEA LEVEL
AGL = ABOVE GROUND LEVEL
TH = TOP HAT
STK = STICK
BW = BEST WAY

TABLE 8.- PILOT RATINGS FOR INBOUND TRANSITION AND LANDING ON LPH--PHASE I

TASK NO.	FLIGHT CONTROL	WIND OVER DECK	LEVEL LEG	LEVEL TRANS	GS & LOC TRACK	ARREST SINK & CLOSURE	DECEL TO STN KEEP	TRANS TO OGE HOVER	DESCENT & TD
1	ELEM	10 @ 0°	5	5	5	5	5	6	7
1	ELEM	10 @ 0°	5	7	5	7	5	4	7
1	ELEM	10 @ 0°	4	5	3	4	3	3	5
3-1-A	ELEM	15 @ 0°	—	3	4	5	5	?	7
3-1-A	ELEM	15 @ 0°	—	3	6	6	5	7	7
3-2-A	ELEM VVC	15 @ 0°	—	2	3	4	4	5	6
3-2-A	ELEM VVC	15 @ 0°	—	3	6	7	4	7	8
3-2-A	ELEM VVC	15 @ 0°	—	2-1/2	3	3-1/2	3	3	3
3-1-B	ELEM	25 @ 0°	—	4	5	5	5	5	7
3-1-B	ELEM	25 @ 0°	—	—	6	6	5	7	8
3-1-B	ELEM	25 @ 0°	3	3	3	3	3	4	5
3-1-B	ELEM	25 @ 0°	3	4	3	3	3	3	5
3-2-B	ELEM VVC	25 @ 0°	—	1	2	4	4	4	6
3-2-B	ELEM VVC	25 @ 0°	—	2	5	6	3	7	7
3-2-B	ELEM VVC	25 @ 0°	3	3	3	2	2	2	2
3-2-B	ELEM VVC	25 @ 0°	3	4	3	3	3	3	4
3-1-C	ELEM	25 @ -30°	—	4	4	5	6-8	6	7
3-1-C	ELEM	25 @ -30°	—	—	7	8	7	7	8
3-2-C	ELEM VVC	25 @ -30°	—	4	4	5	5-8	6	6
3-2-C	ELEM VVC	25 @ -30°	—	—	6	7	7	7	8
4-1-D	ELEM VVC	15 @ -30°	—	—	—	—	4	6	N/A
4-1-D	ELEM VVC	15 @ -30°	—	—	—	—	5	7	N/A
5-1-B	ELEM VVC	25 @ 0°	—	—	3	8	5-6	N/A	6
5-1-B	ELEM VVC	25 @ 0°	3	3	6	6	5	N/A	7

TABLE 9.- PILOT RATINGS FOR HOVER--PHASE I

MOTION / WIND	LONG POSITION	LAT POSITION	SIMU LAT & LONG	SPOT TURN	STEP	ROLL RECOV	PITCH RECOV	HEIGHT RECOV
NO 0 knot	4 ATT 3 ATT + TILT	4	4	3	(EASY)	EASY	EASY	(EASY)
NO 15 knot	—	—	4	7, (5)	—	—	—	—
NO 25 knot	—	—	4, (3)	10	—	—	—	—
YES 0 knot	3, (3) SM 5, (3) LG	5, (5) SM 7, (7) LG	—	1	5, (3)	2	2	5, (3)
YES 15 knot	—	—	—	7, (6)	5	—	—	—
YES 0 knot	3, (2) SM 5, (2) LG	3, (2) SM	3, (3) SM	2	4, (2)	—	—	—
YES 25 knot	—	—	—	8, (7)	—	—	—	—

NOTE: RATINGS WITHIN PARENTHESES ARE FOR VERTICAL VELOCITY COMMAND AND SURGE COMMAND ENGAGED: MANUAL THROTTLE AND NACELLE TILT OTHERWISE. SM - SMALL INPUTS; LG - LARGE INPUTS.

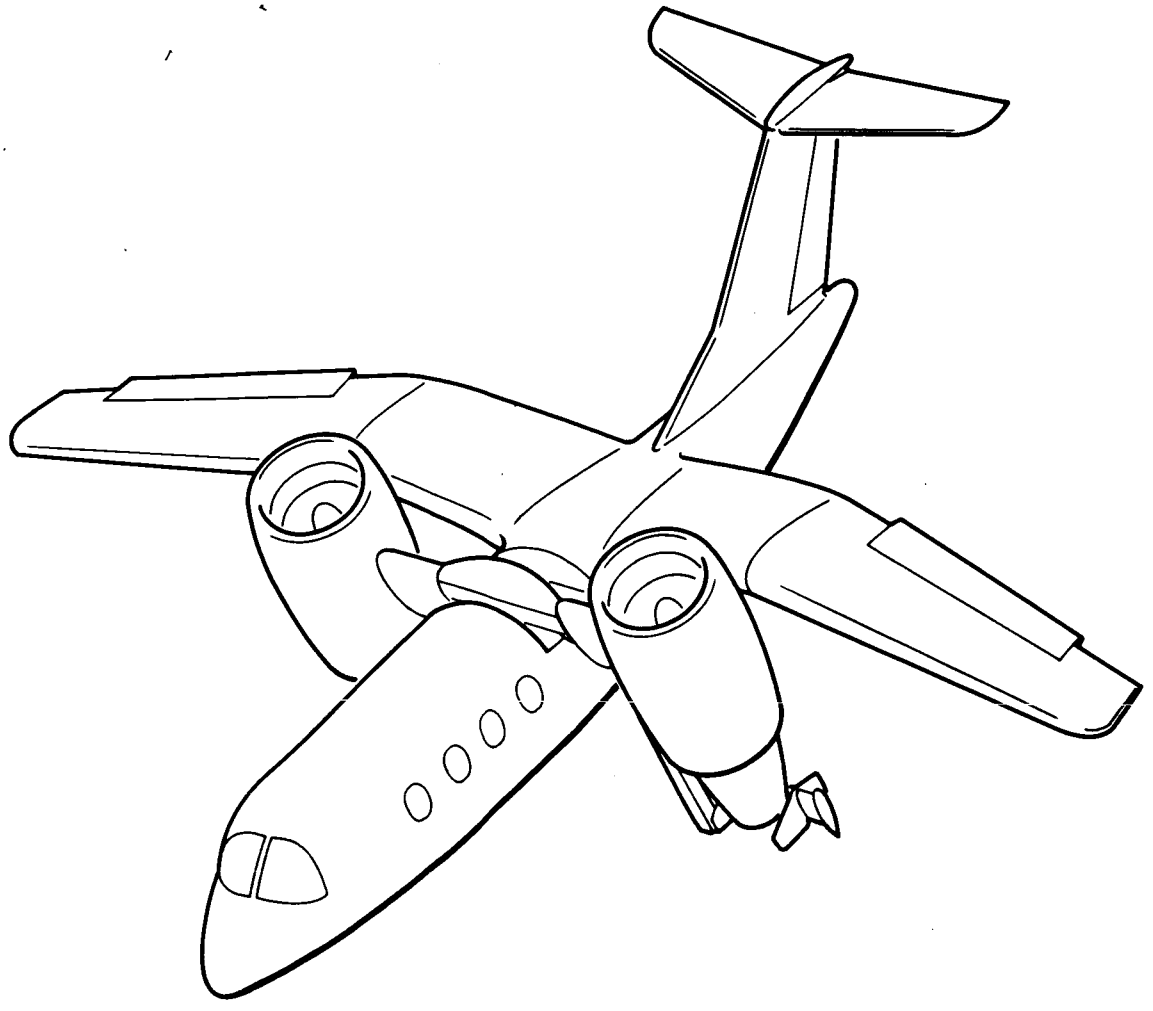

Figure 1.- Model 698 research aircraft.

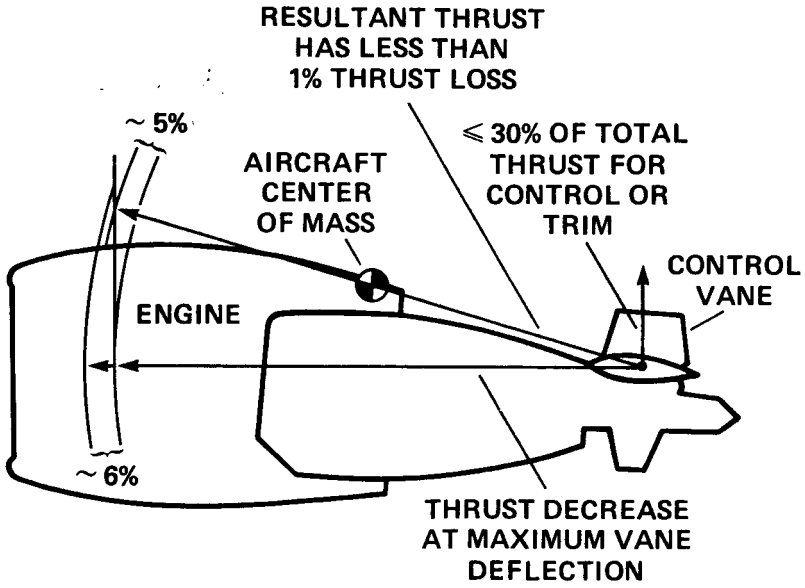

Figure 2.- Thrust vector diagram.

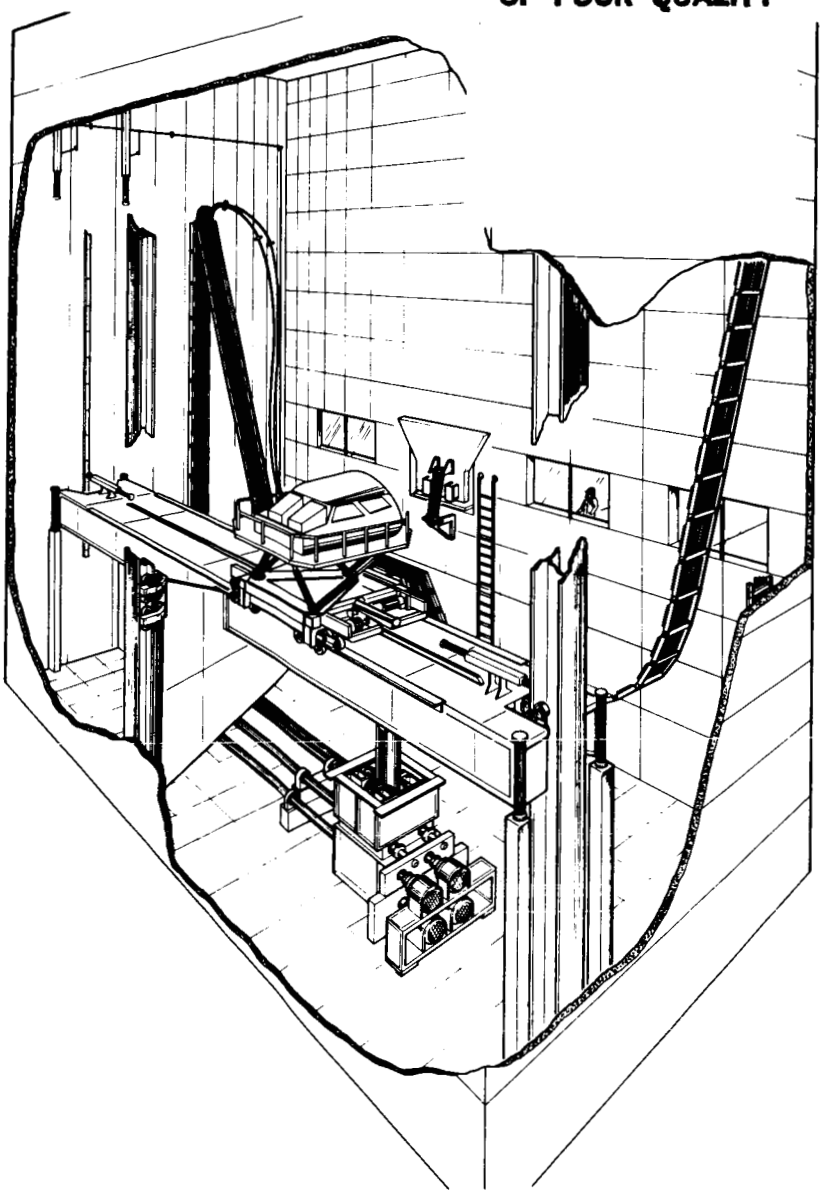

Figure 3.- Vertical motion simulator.

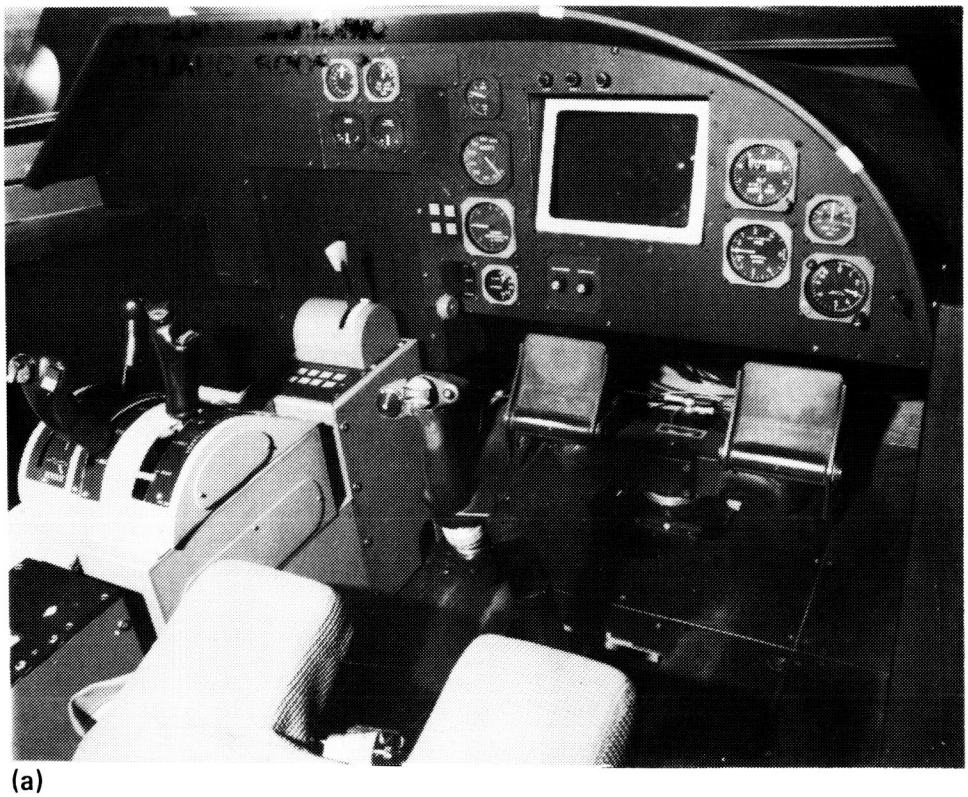

(a)

(b)

Figure 4.- Simulator cockpit. (a) Phase I. (b) Phases II and III.

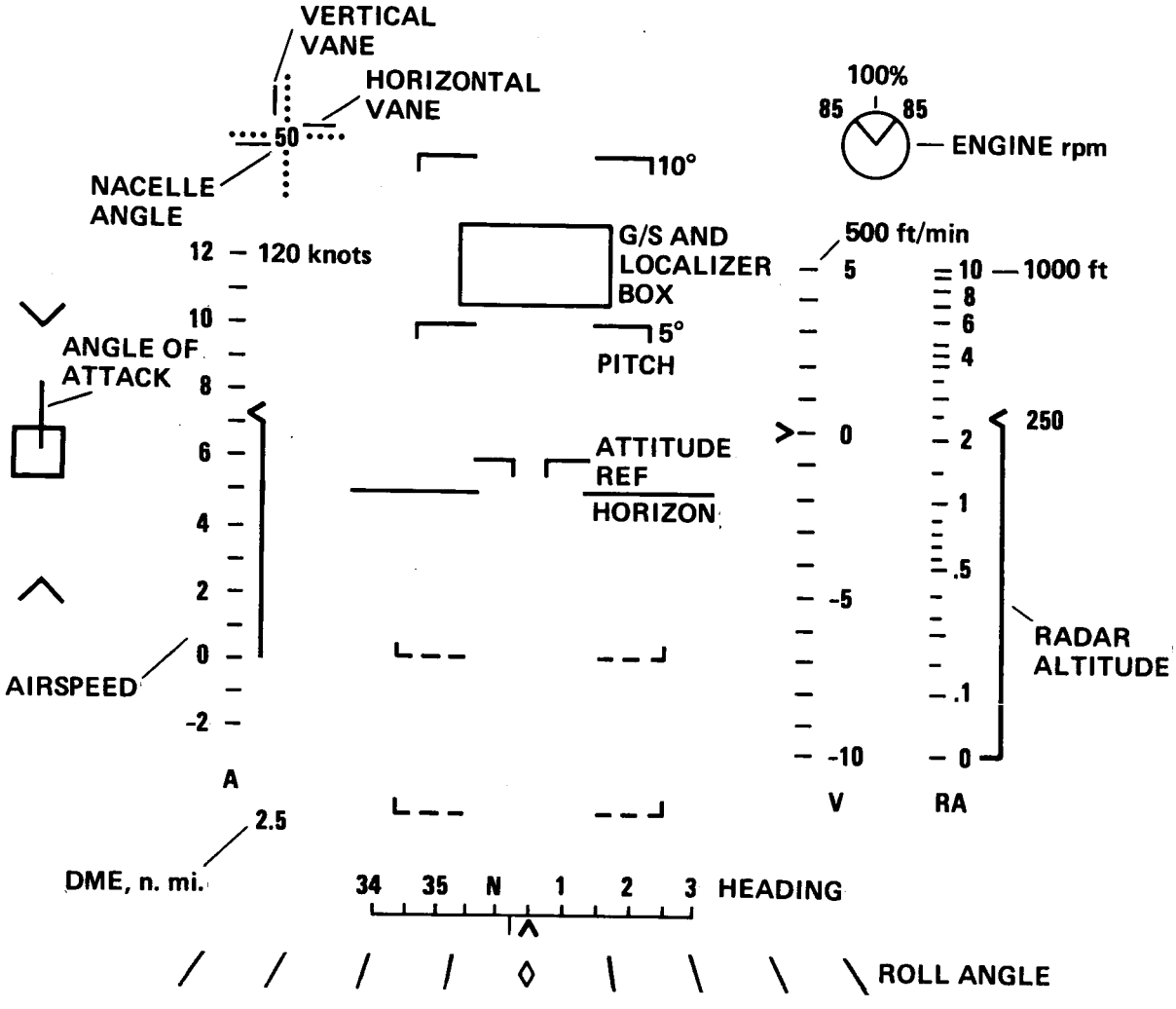

(a) Phase I.

Figure 5.- Design 698 V/STOL HUD format.

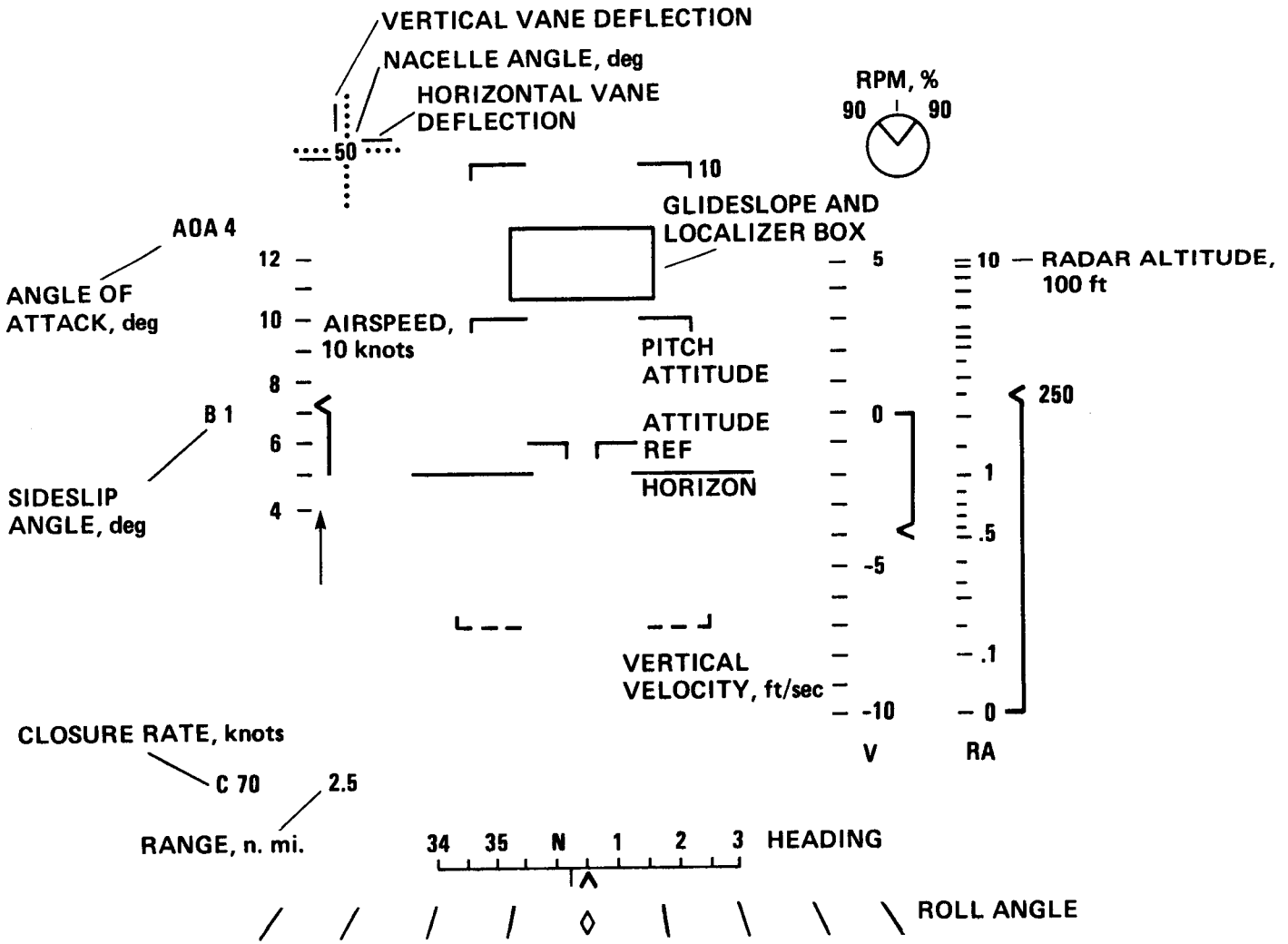

(b) Phases II and III--below 40 knots.

Figure 5.- Continued.

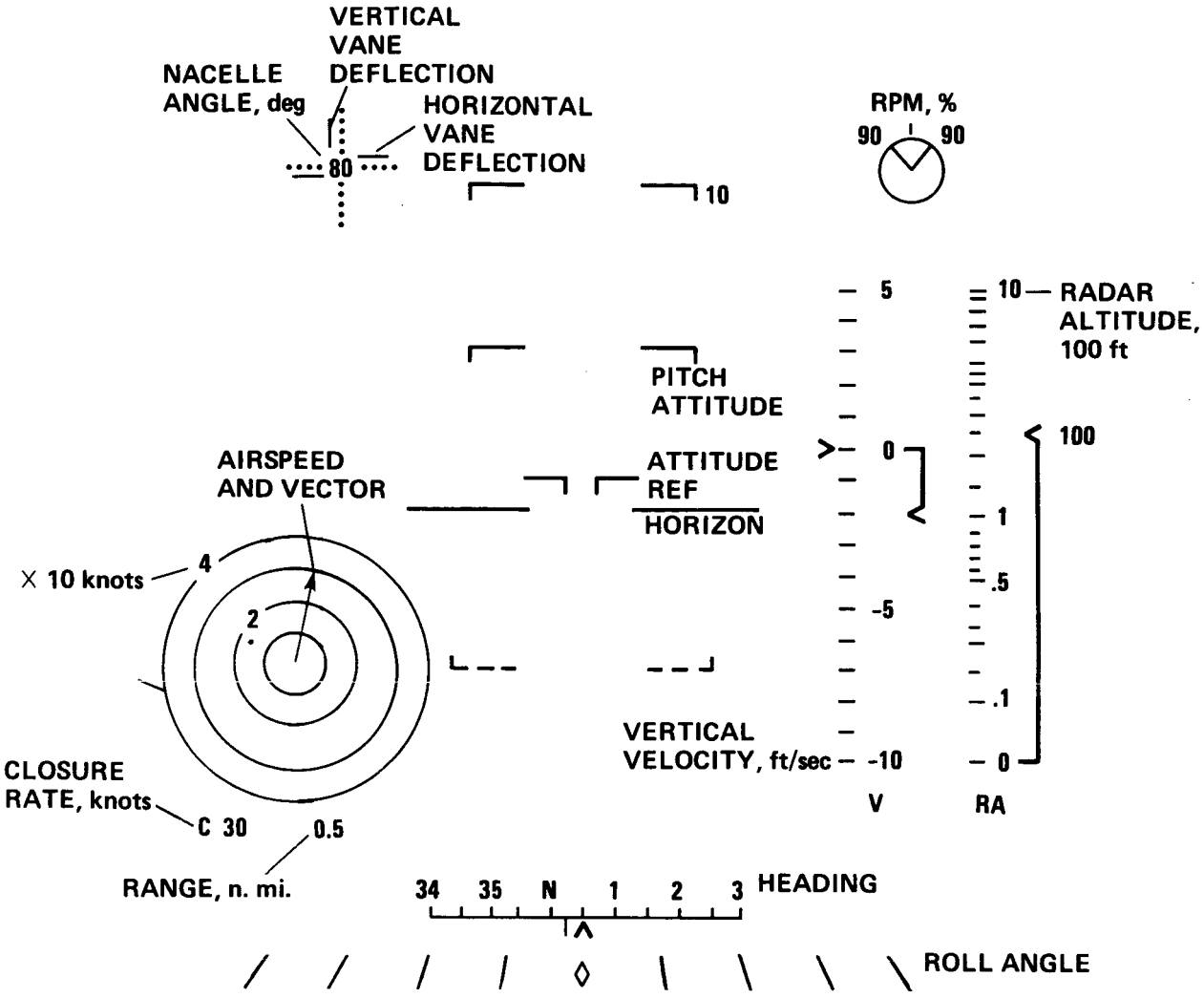

(c) Phases II and III--above 40 knots.

Figure 5.- Concluded.

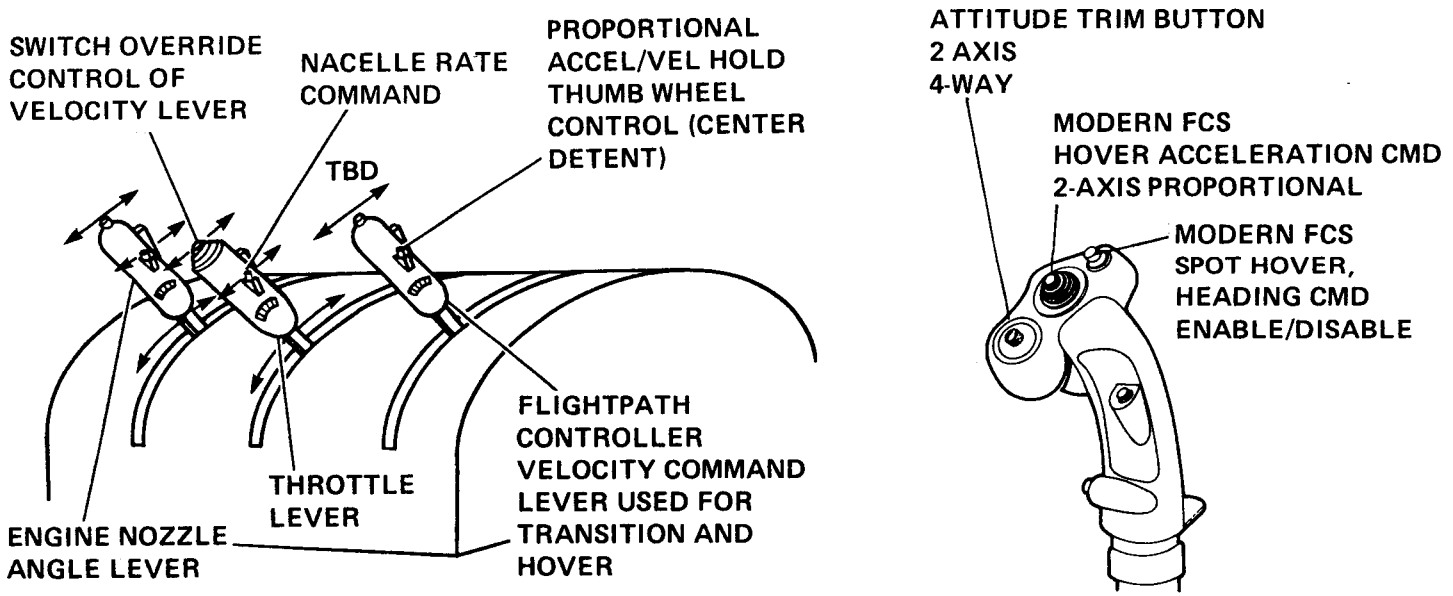

(a) Phase I.

Figure 6.- Power management quadrant.

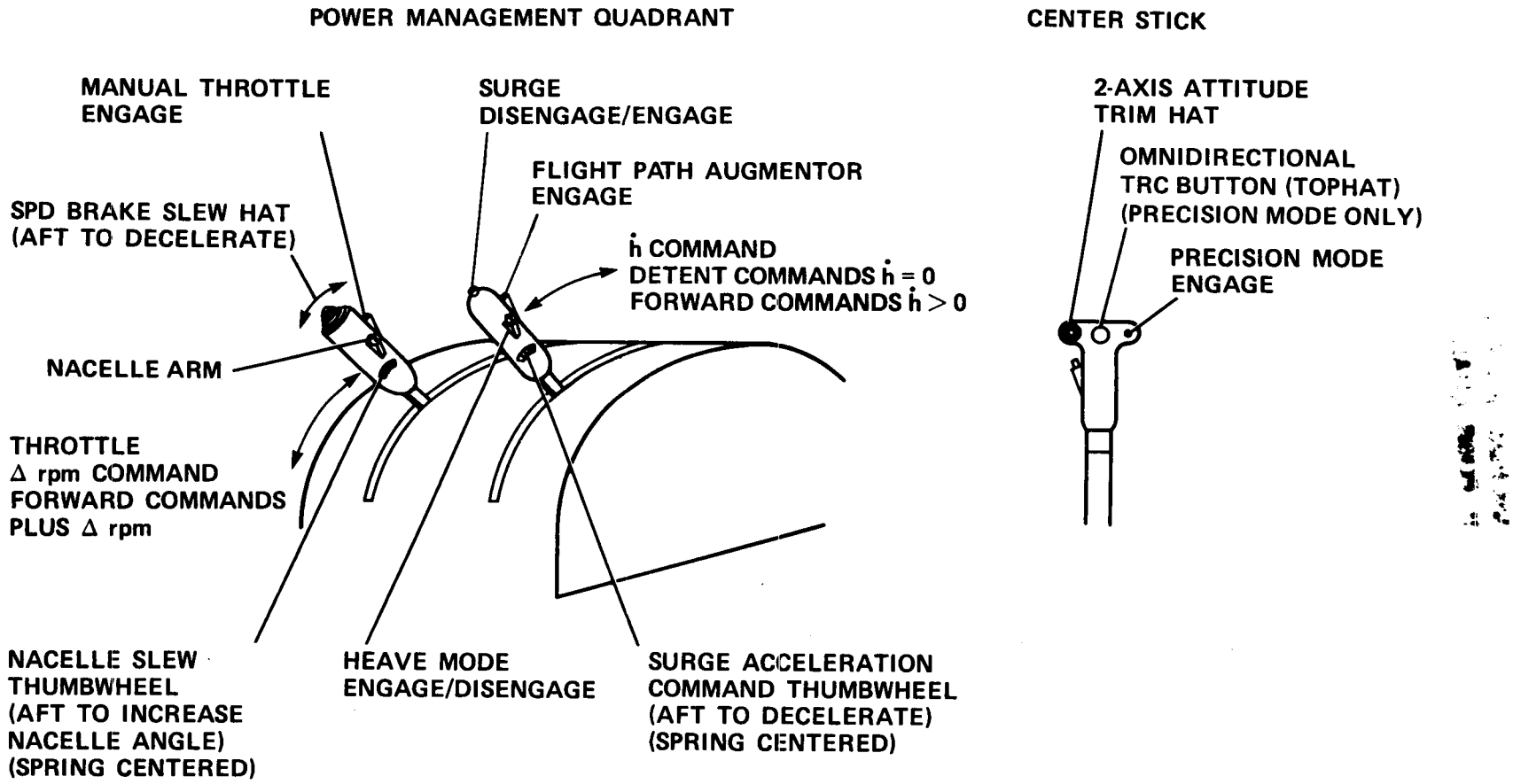

(b) Phases II and III.

Figure 6.- Concluded.

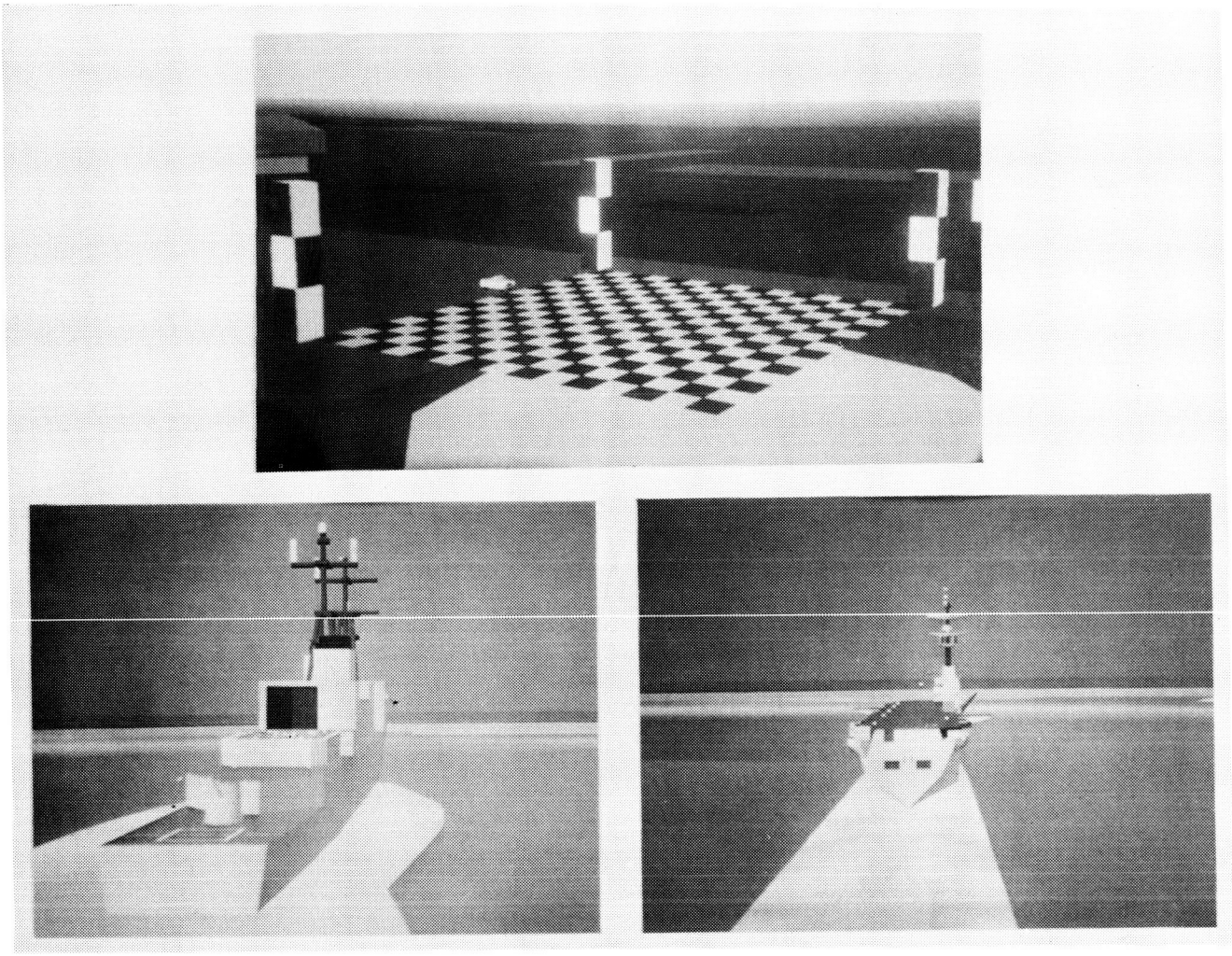

Figure 7.- 1980 Visual scene capability.

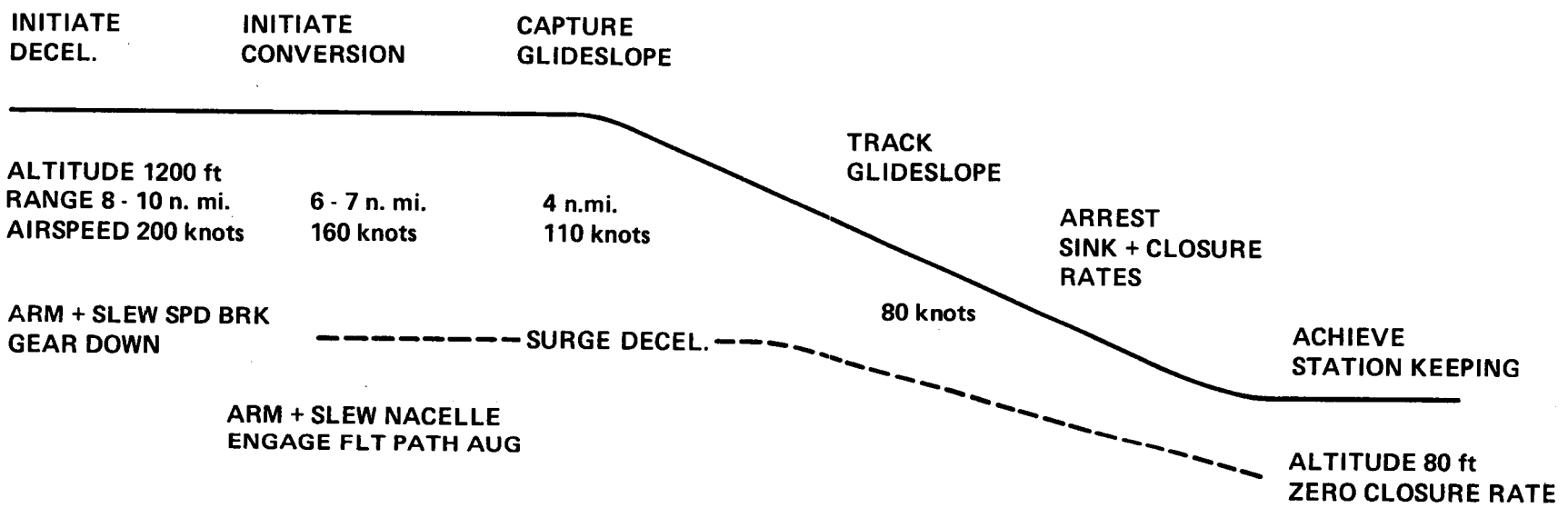

Figure 8.- Inbound transition profile.

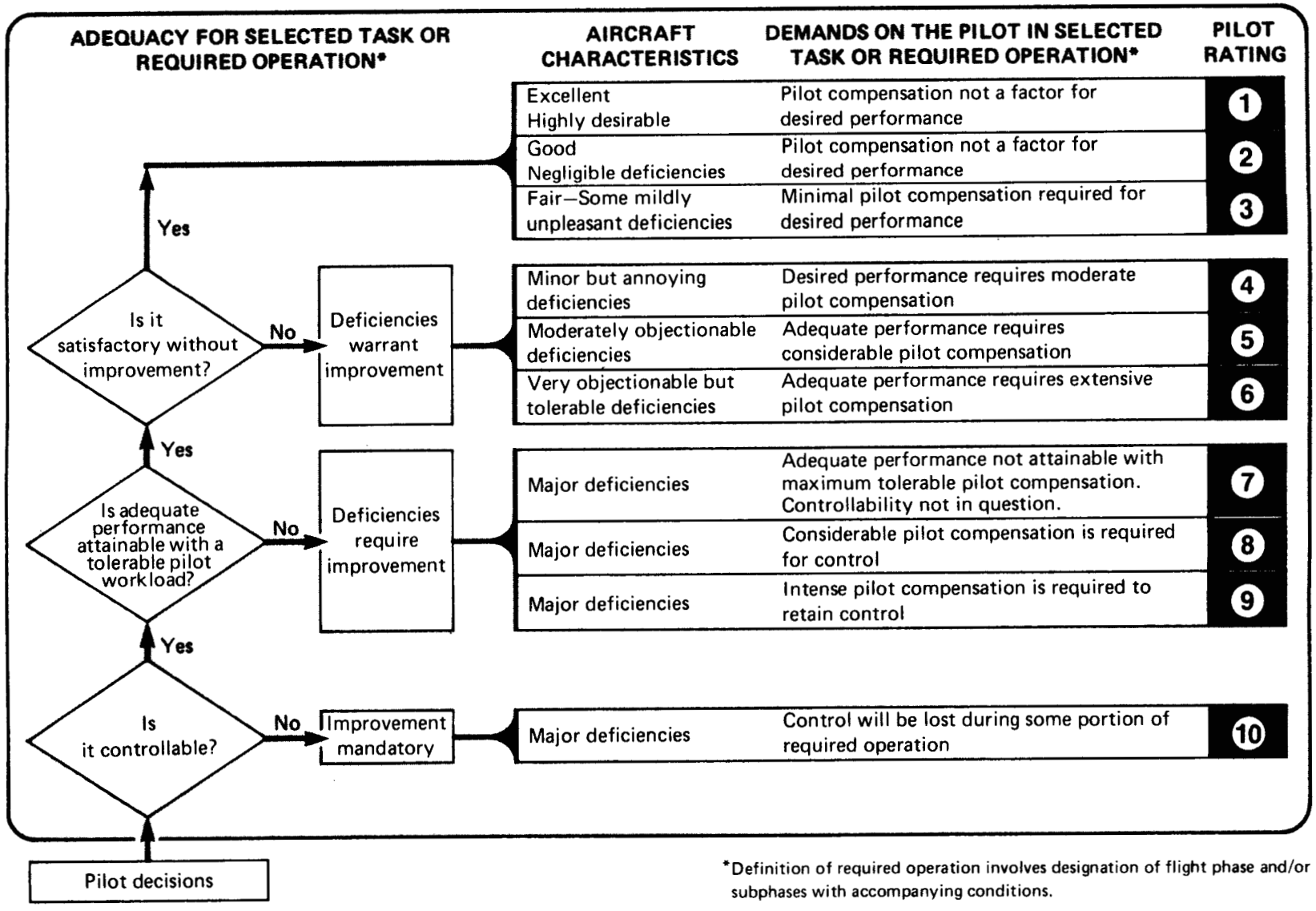

Figure 9.- Cooper-Harper handling qualities ratings scale (ref. 12).

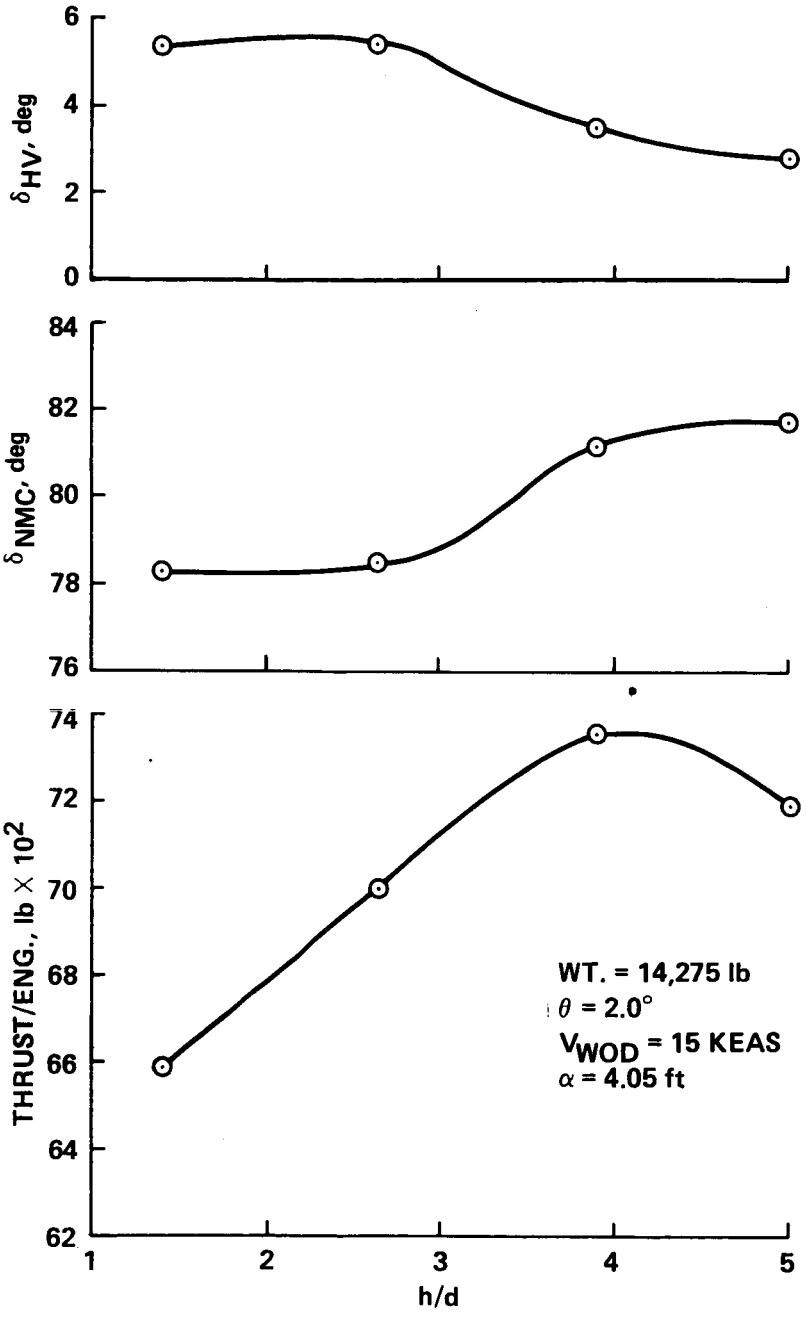

Figure 10.- Ground-effect trim requirements.

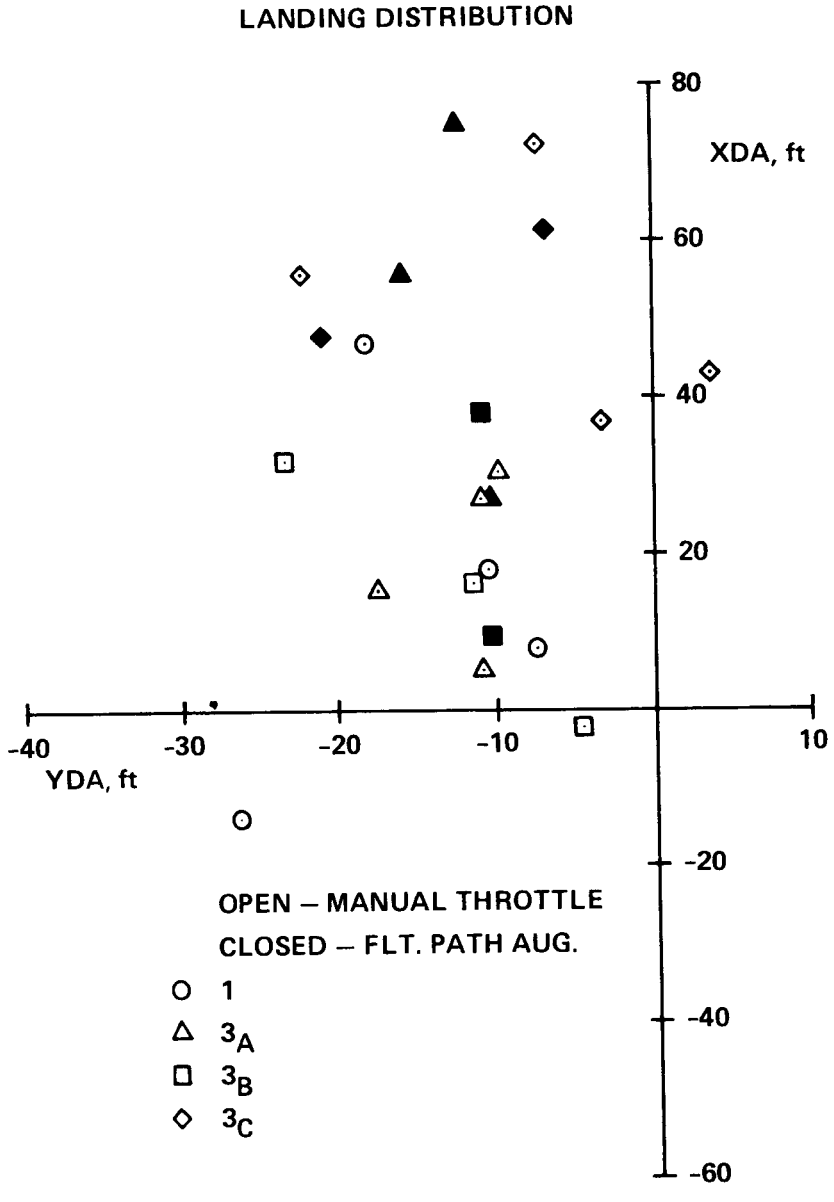

Figure 11.- Landing distribution on an LPH--phase I.

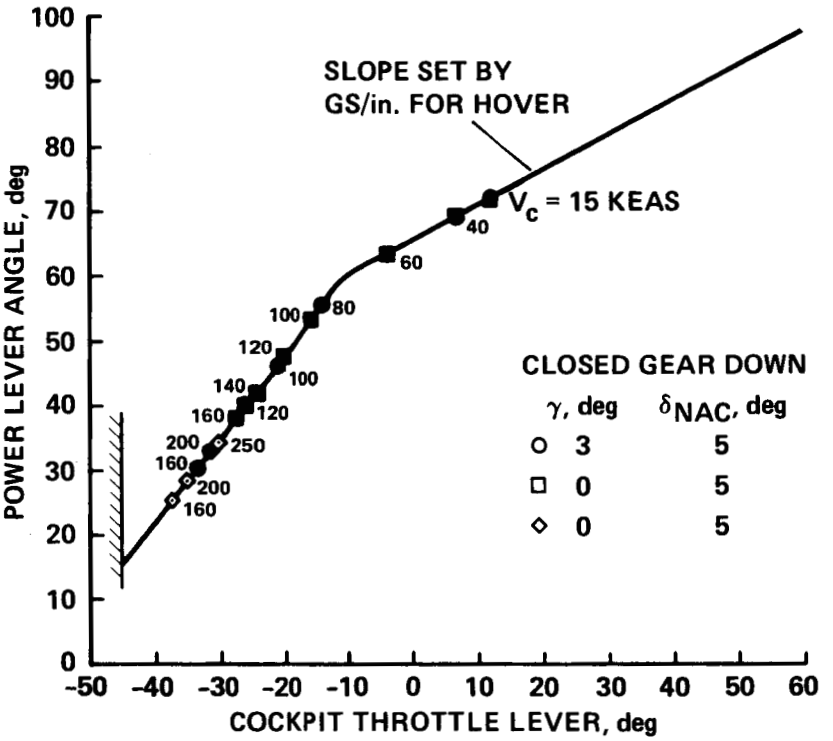

Figure 12.- Engine thrust-response characteristics--inbound transition profile.

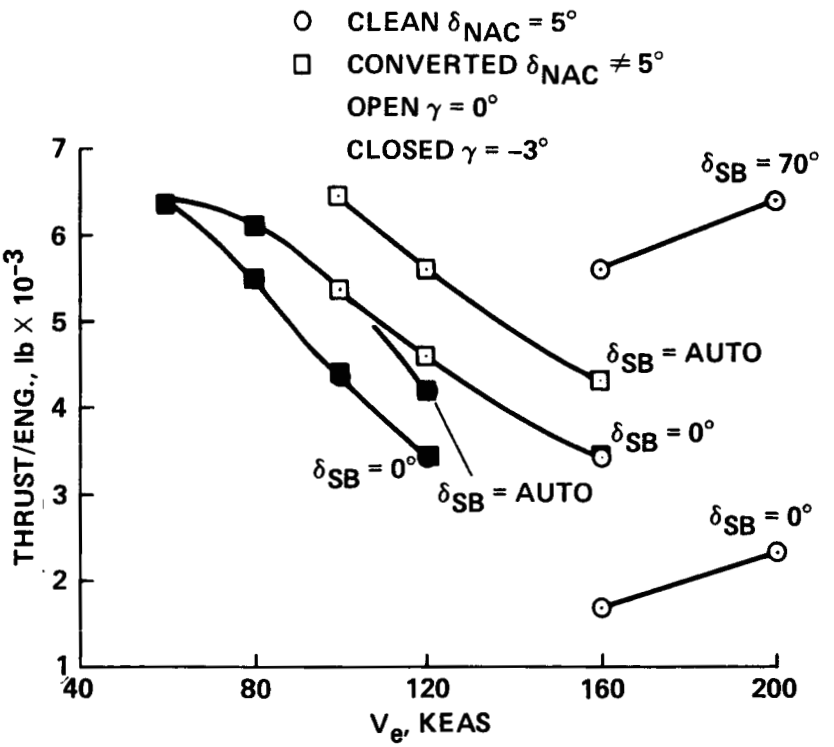

Figure 13.- Throttle lever vs. power lever--aircraft trim points.

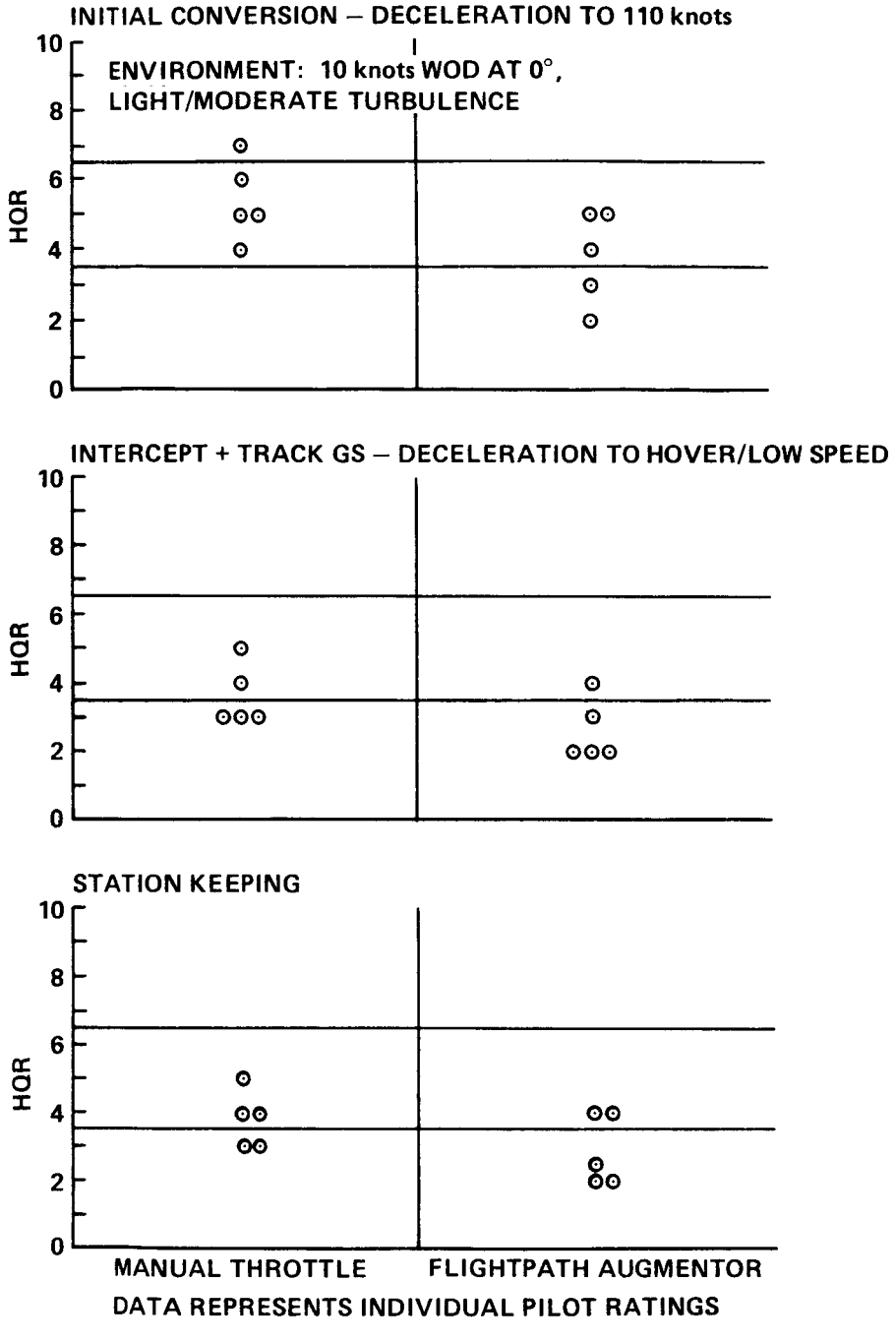

Figure 14.- Individual pilot ratings for inbound transition to an LPH: manual vs flightpath augmentor--phase II.

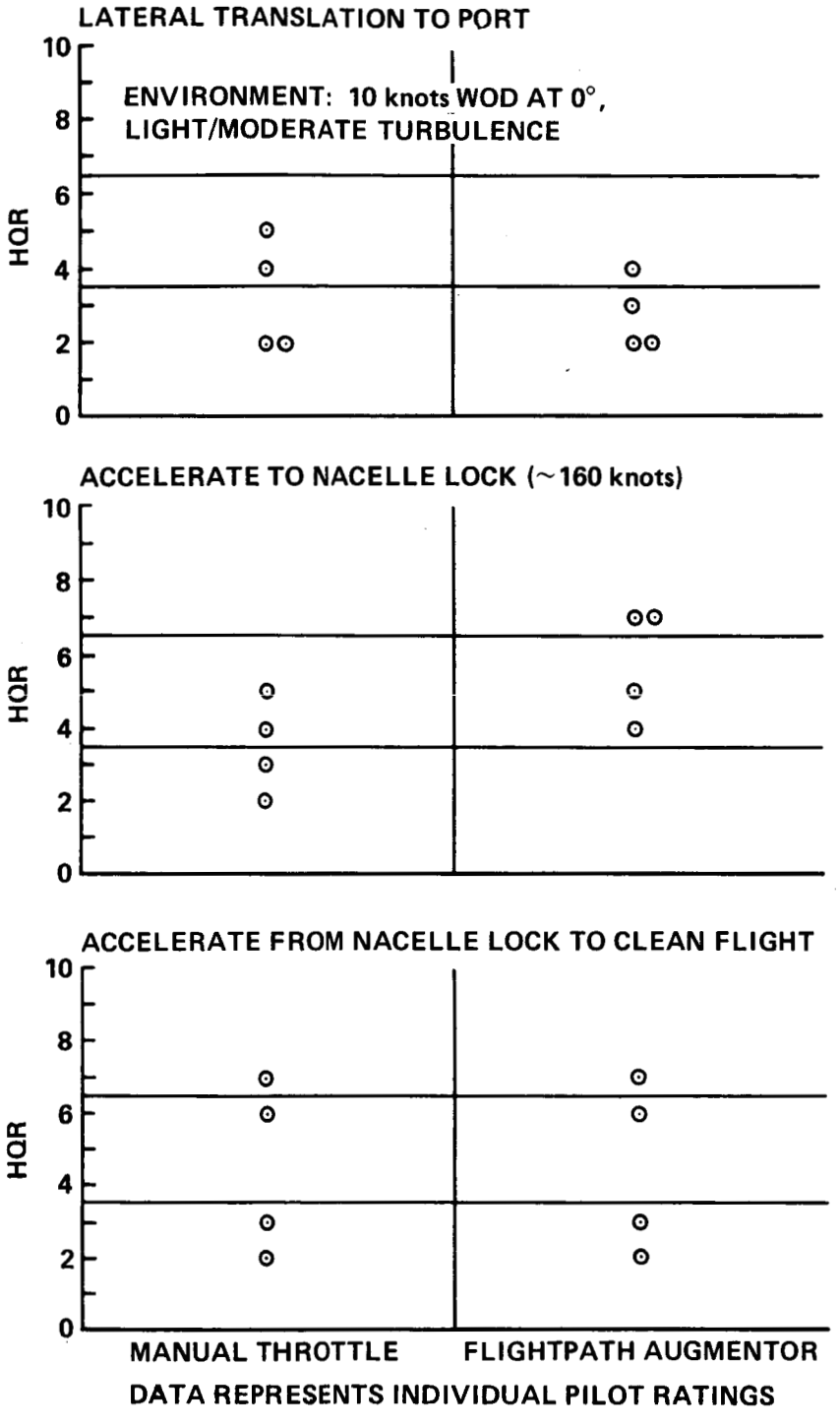

Figure 15.- Individual pilot ratings for outbound transition from an LPH: manual vs flightpath augmentor--phase II.

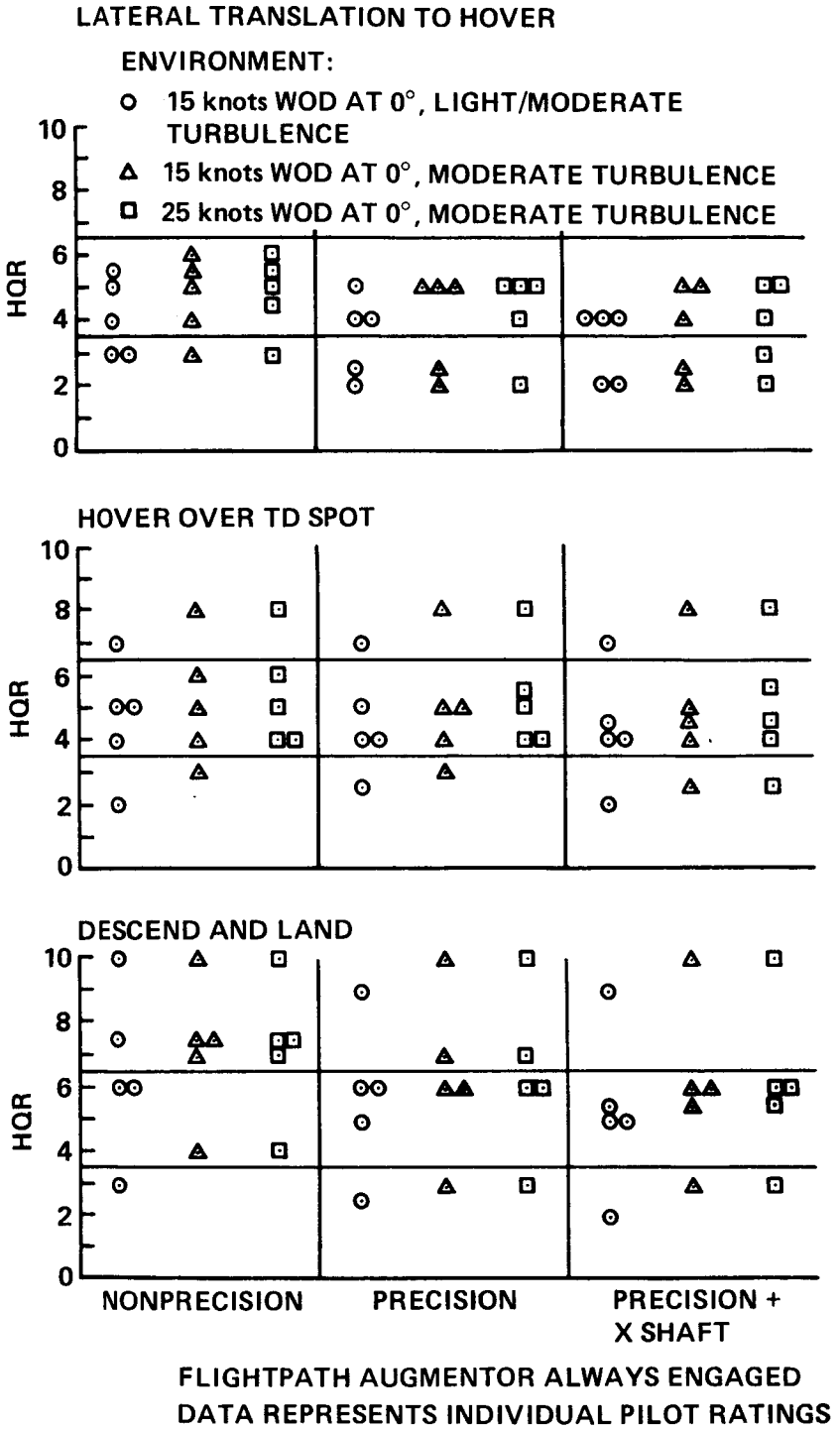

Figure 16.- Individual pilot ratings for inbound transition to an LPH: non-precision vs precision vs precision and cross-shafting--phase II.

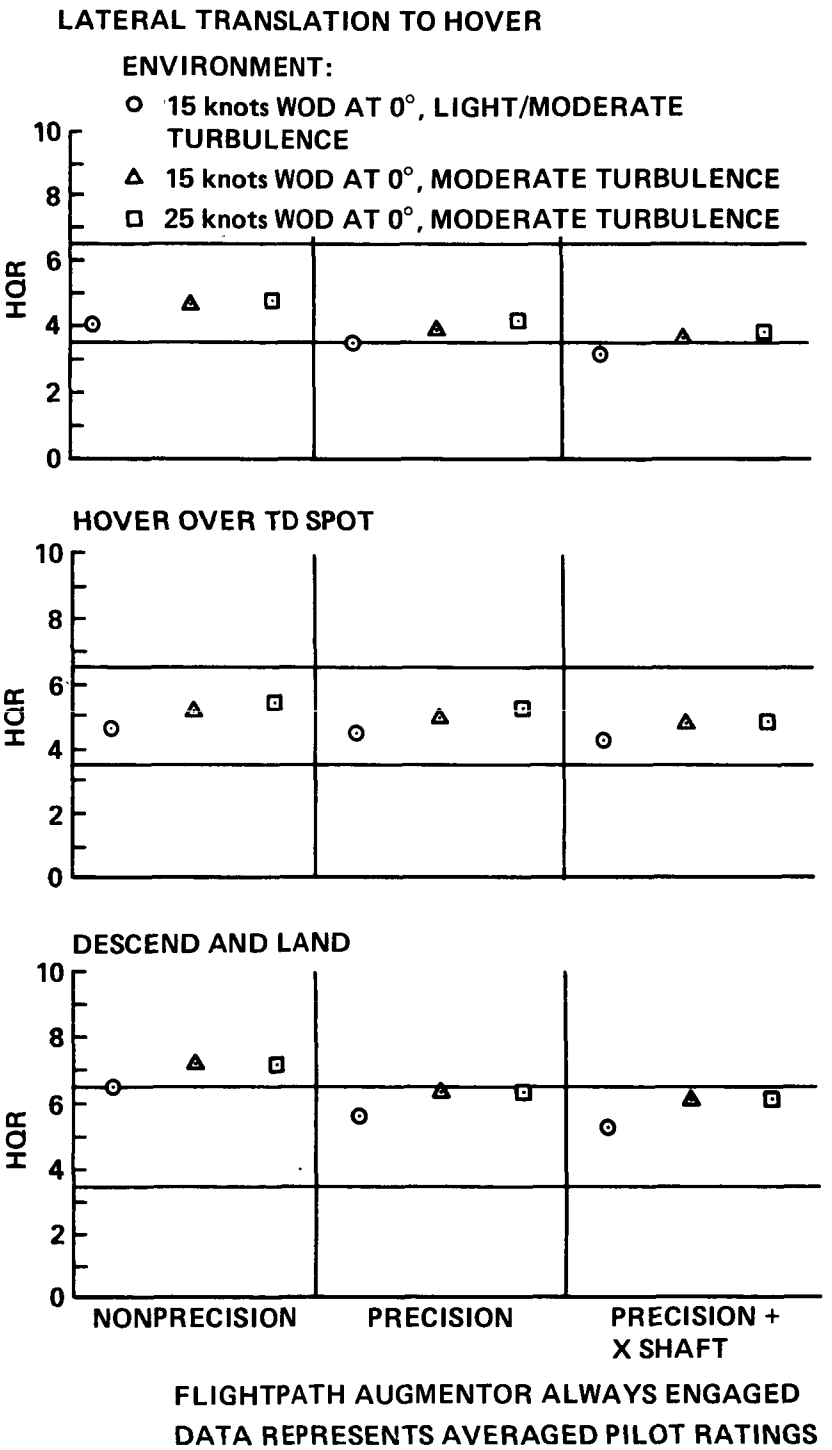

Figure 17.- Averaged pilot ratings for inbound transition to an LPH: non-precision vs precision vs precision and cross-shafting--phase II.

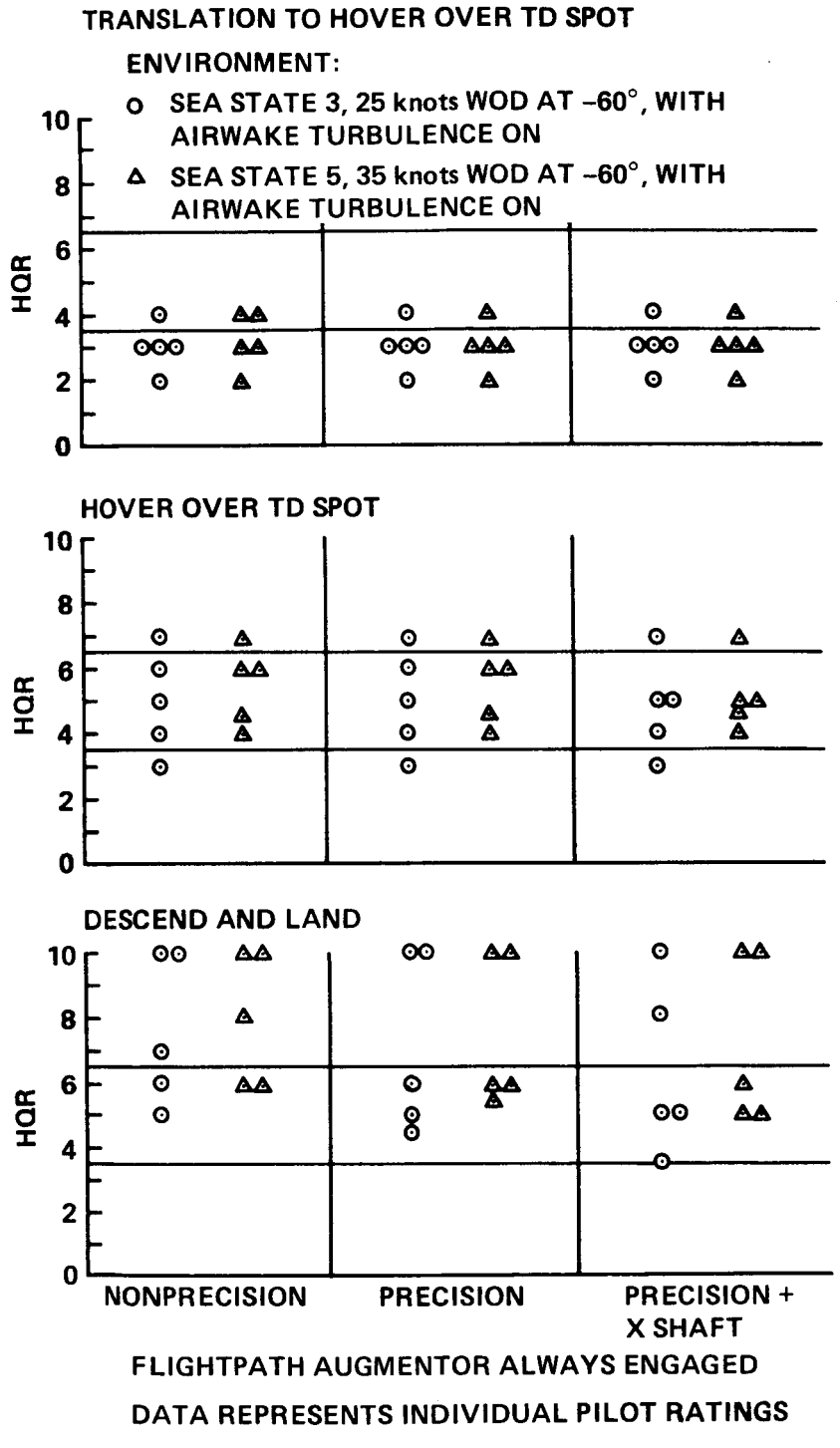

Figure 18.- Individual pilot ratings for inbound transition to a DD-963: non-precision vs precision vs precision and cross-shafting--phase II.

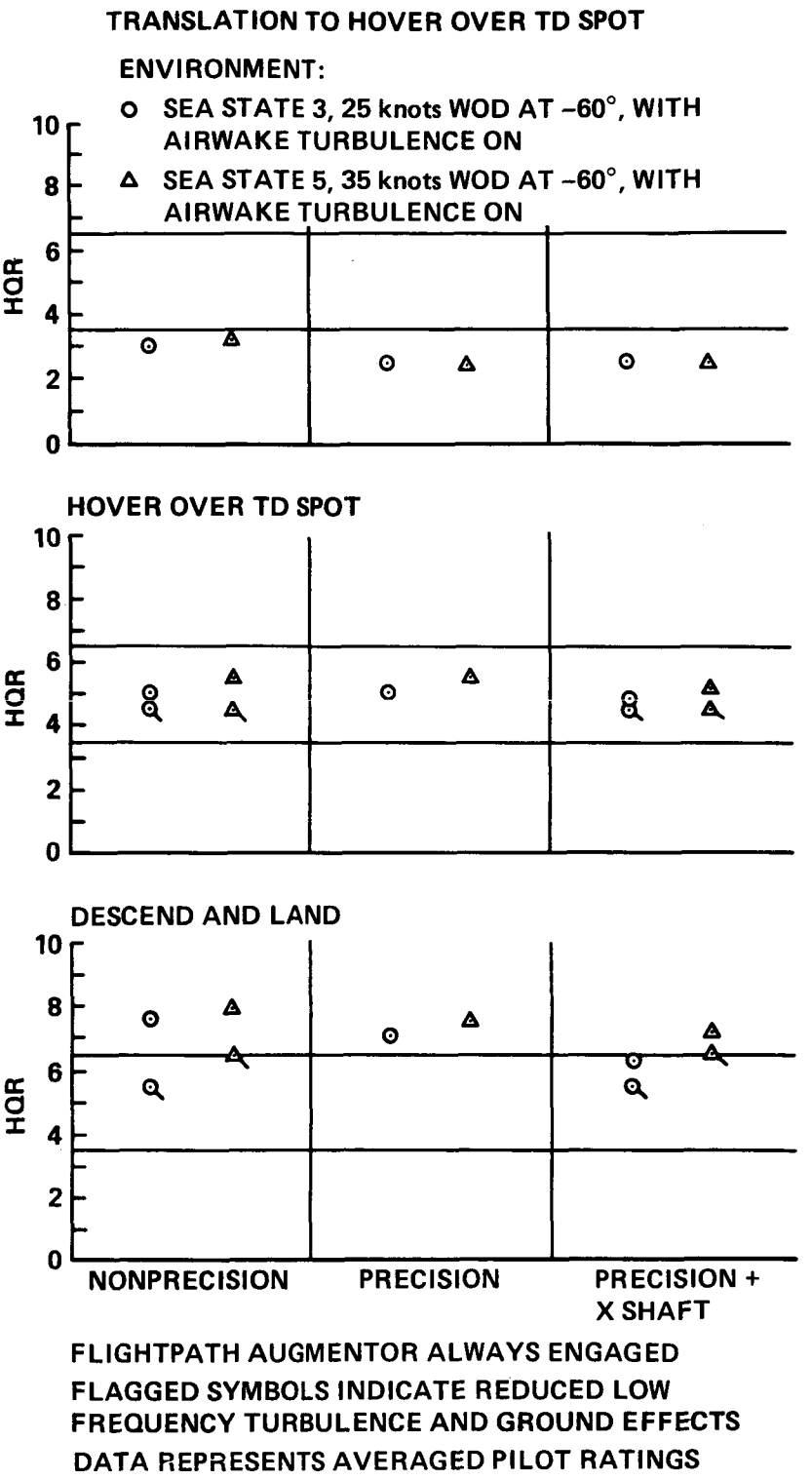

Figure 19.- Average pilot ratings for inbound transition to a DD-963: non-precision vs precision vs precision and cross-shafting--phase II.

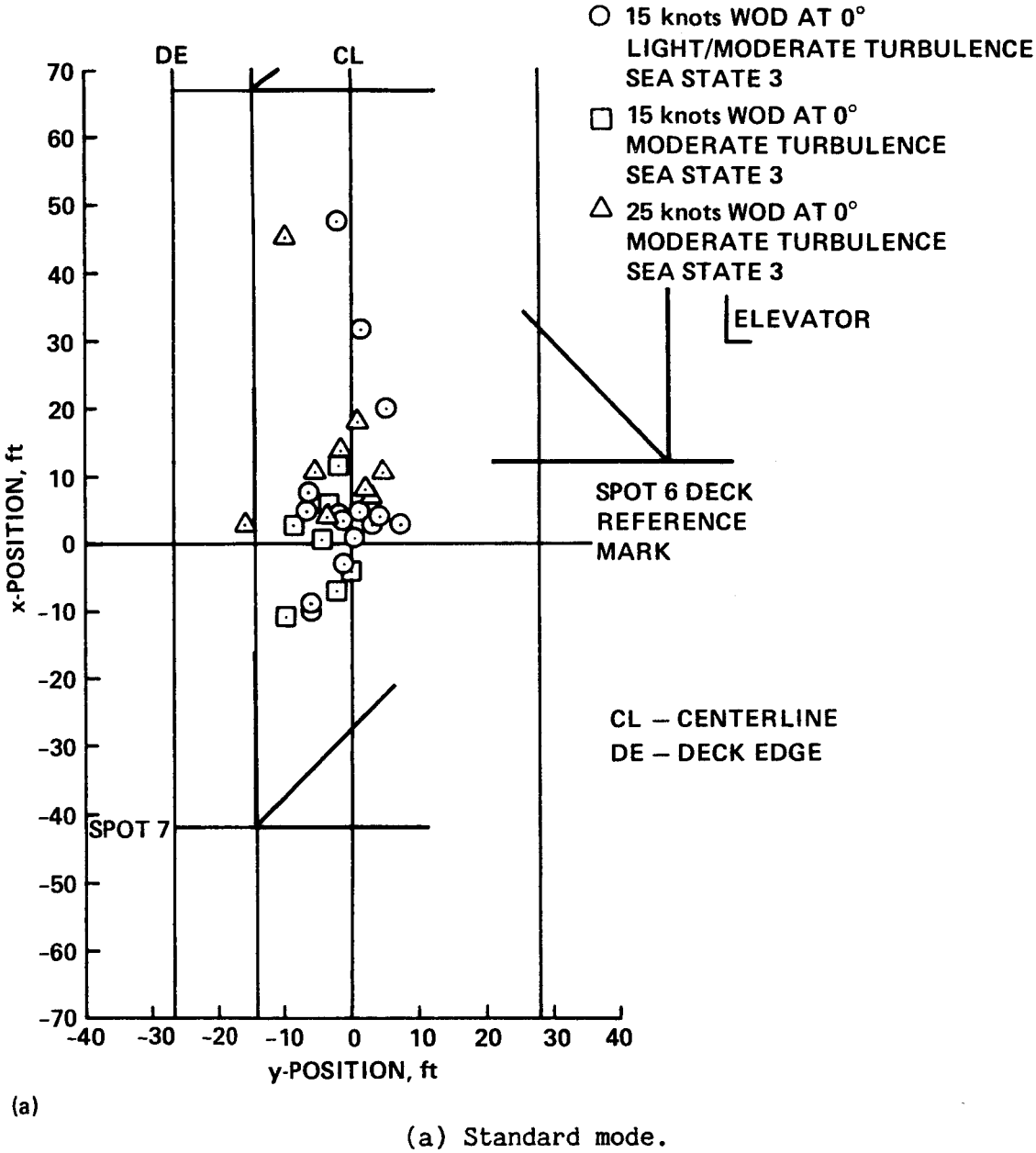

(a) Standard mode.

Figure 20.- Landing distribution on an LPH--phase II.

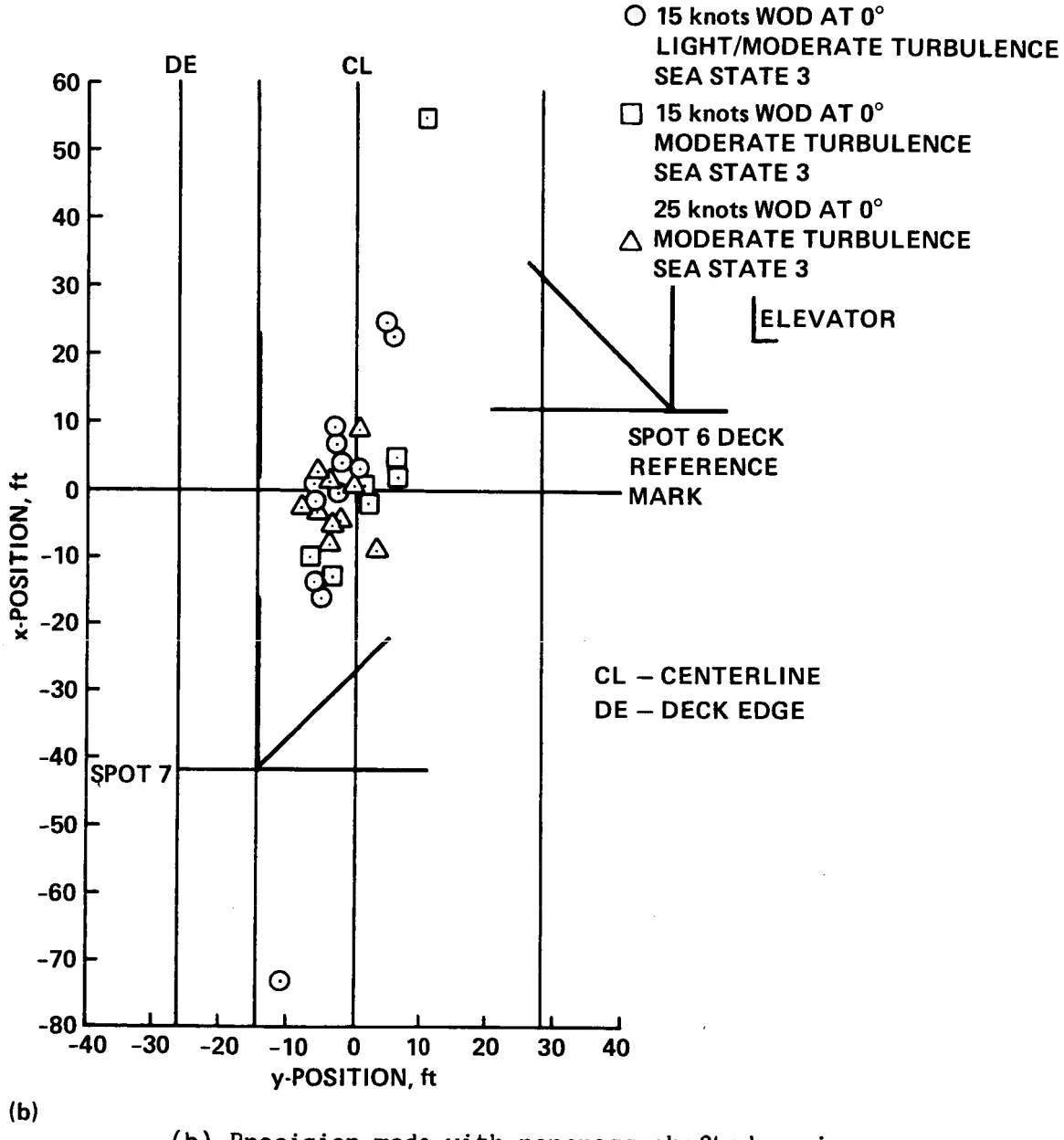

(b) Precision mode with noncross-shafted engines.

Figure 20.- Continued.

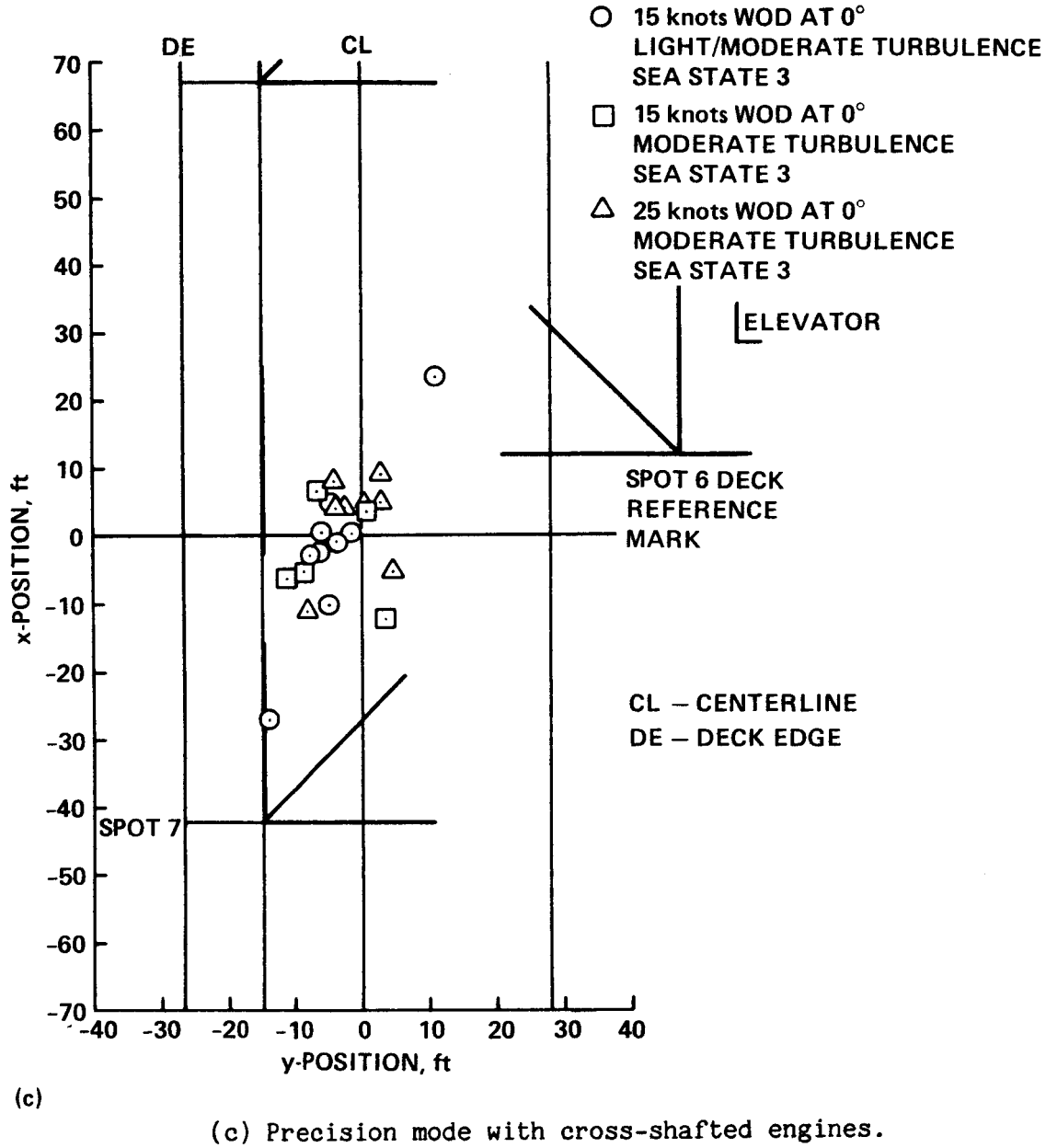

(c)

(c) Precision mode with cross-shafted engines.

Figure 20.- Concluded.

C-2

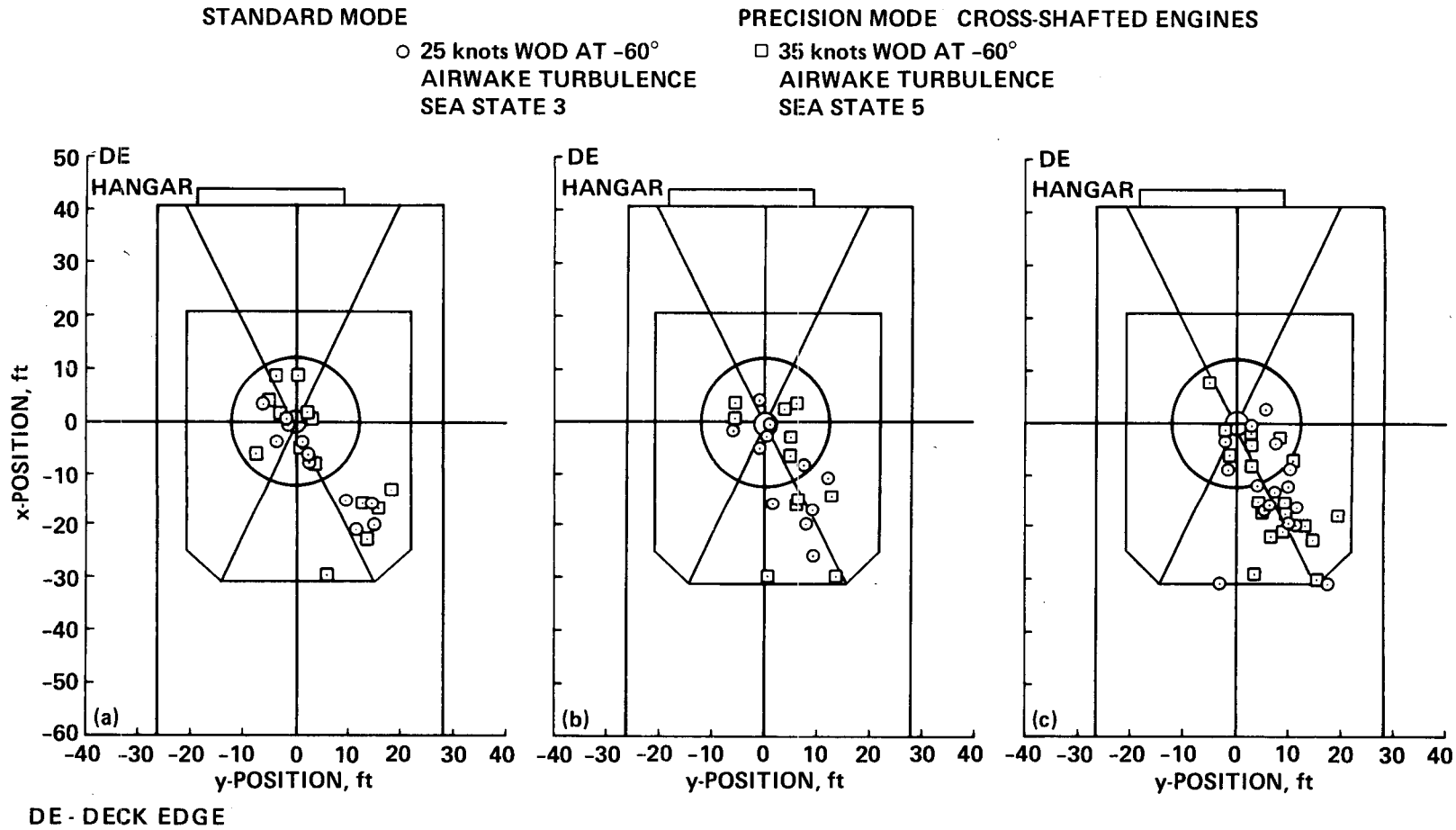

Figure 21.- Landing distribution on a DD--963-phase II.

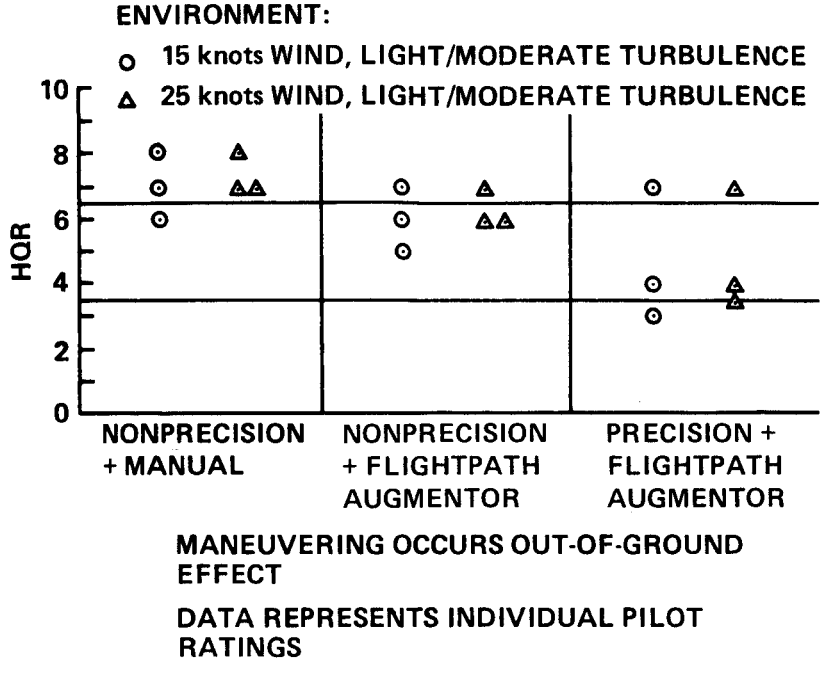

Figure 22.- Spot turns above a VTOL pad: individual pilot ratings--phase II.

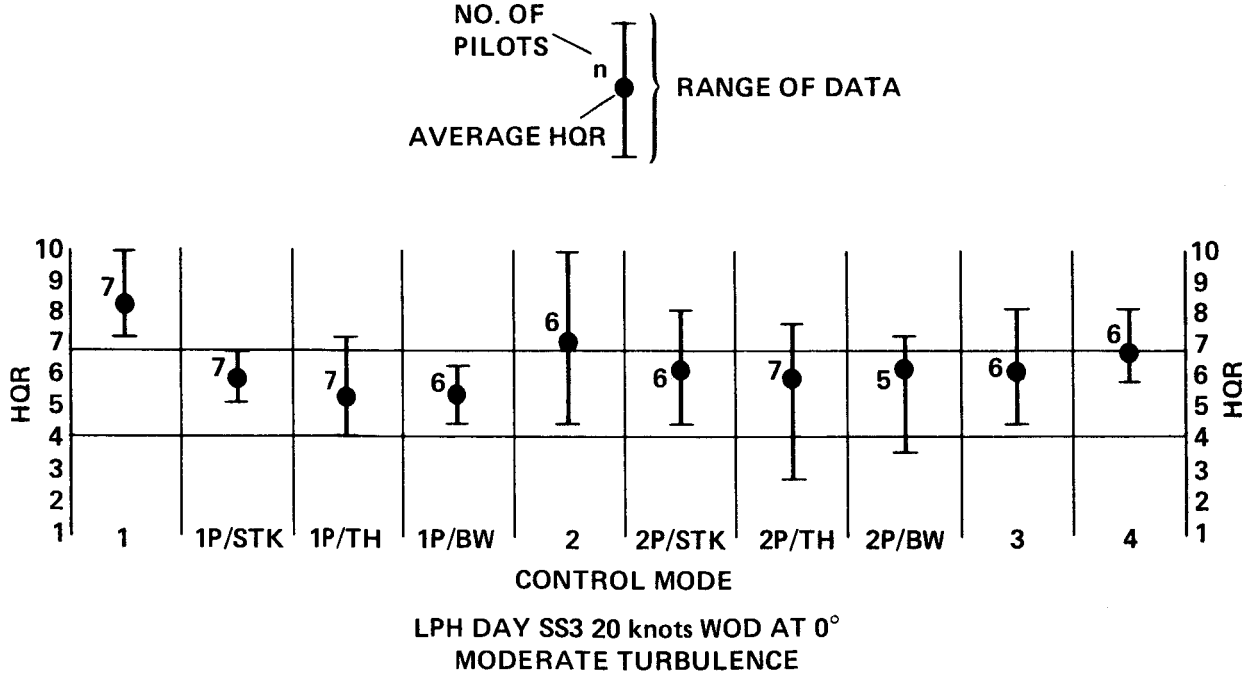

Figure 23.- General control mode comparison: pilot ratings--phase III.

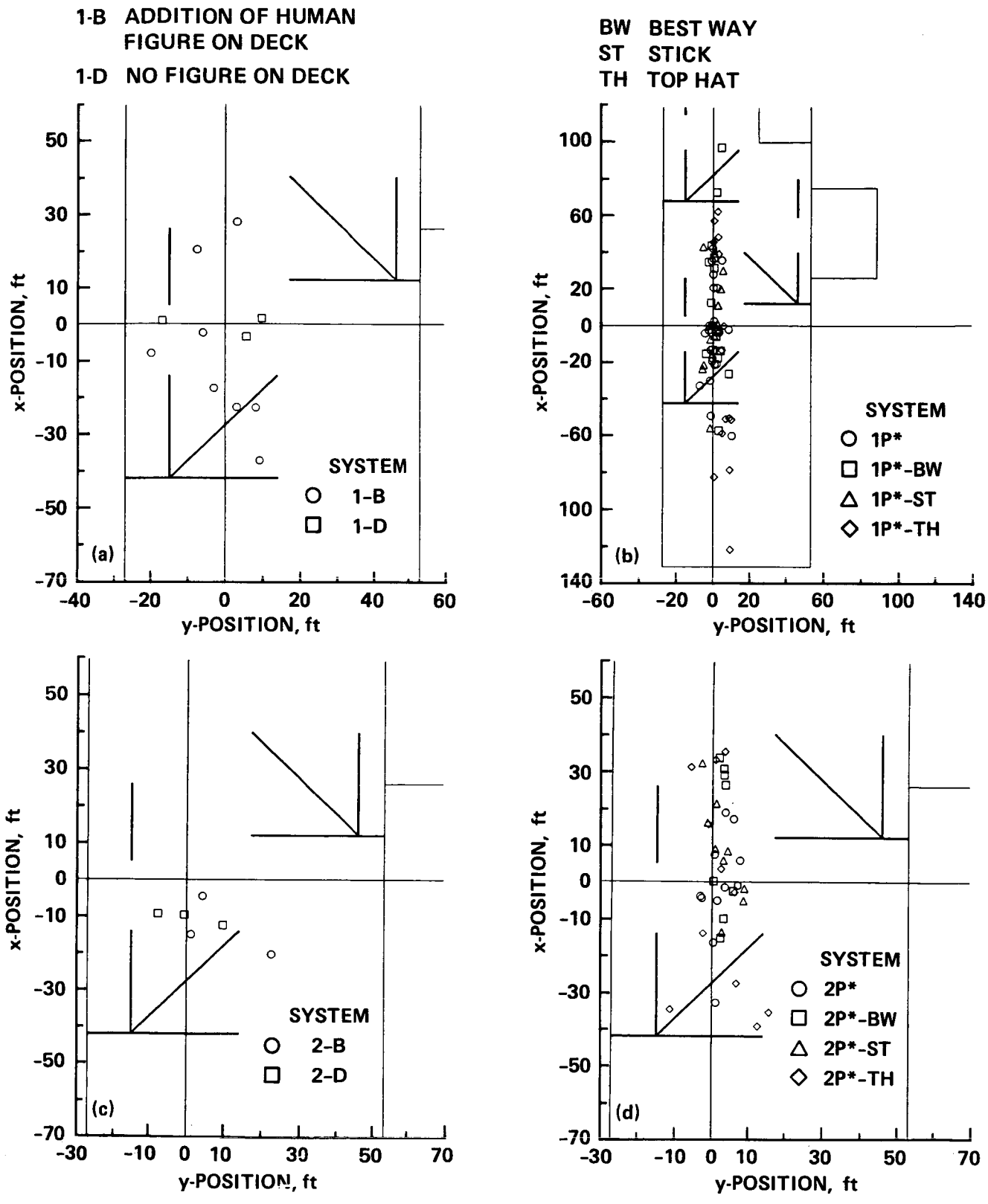

Figure 24.- LPH TD Dispersions. (a) Control mode 1, Sea State (SS) 3. (b) Control mode 1P*, SS 3. (c) Control mode 2, SS 3. (d) Control mode 2P*, SS 3.

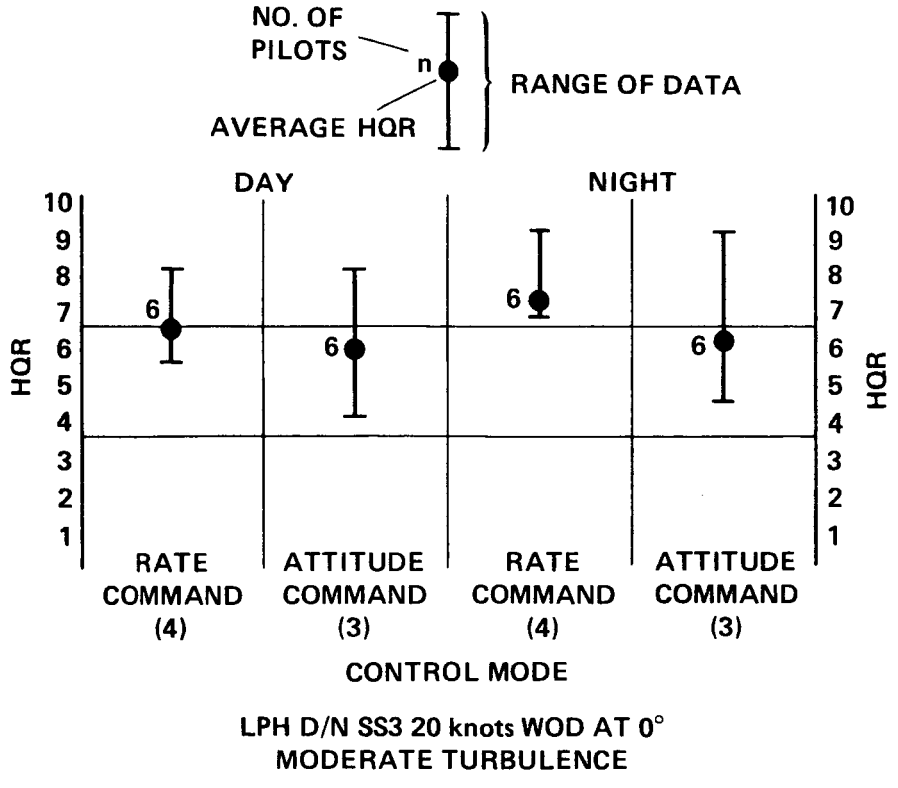

Figure 25.- Day vs night. Rate command vs attitude command: pilot ratings--phase III.

N FLOWN IN NIGHT CONDITIONS
B DAYTIME LANDING WITH HUMAN FIGURE

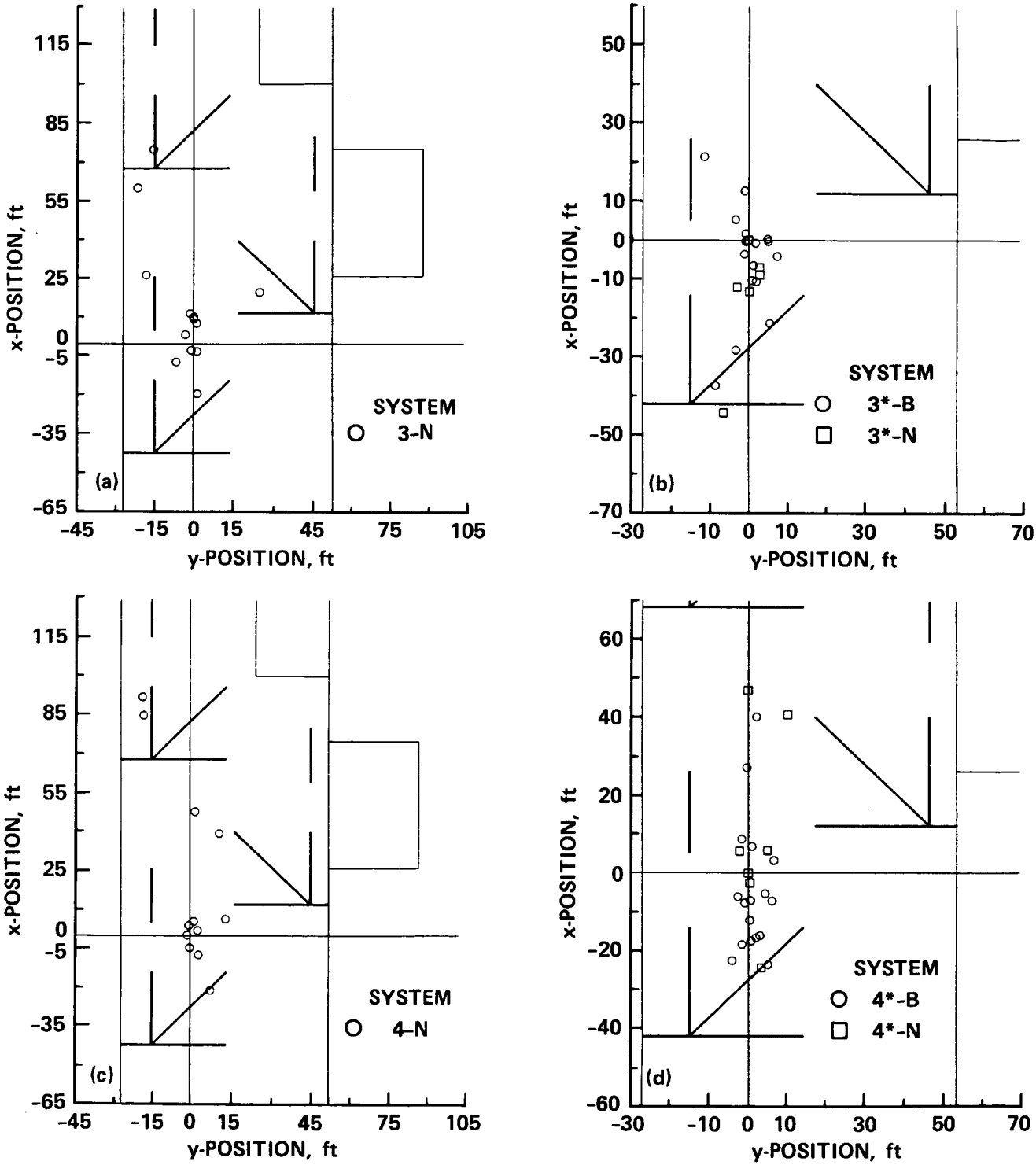

Figure 26.- LPH TD Dispersions. (a) Control system 3 SS 3. (b) Control system 3*, SS 3. (c) Control system 4, SS 3. (d) Control system 4*, SS 3.

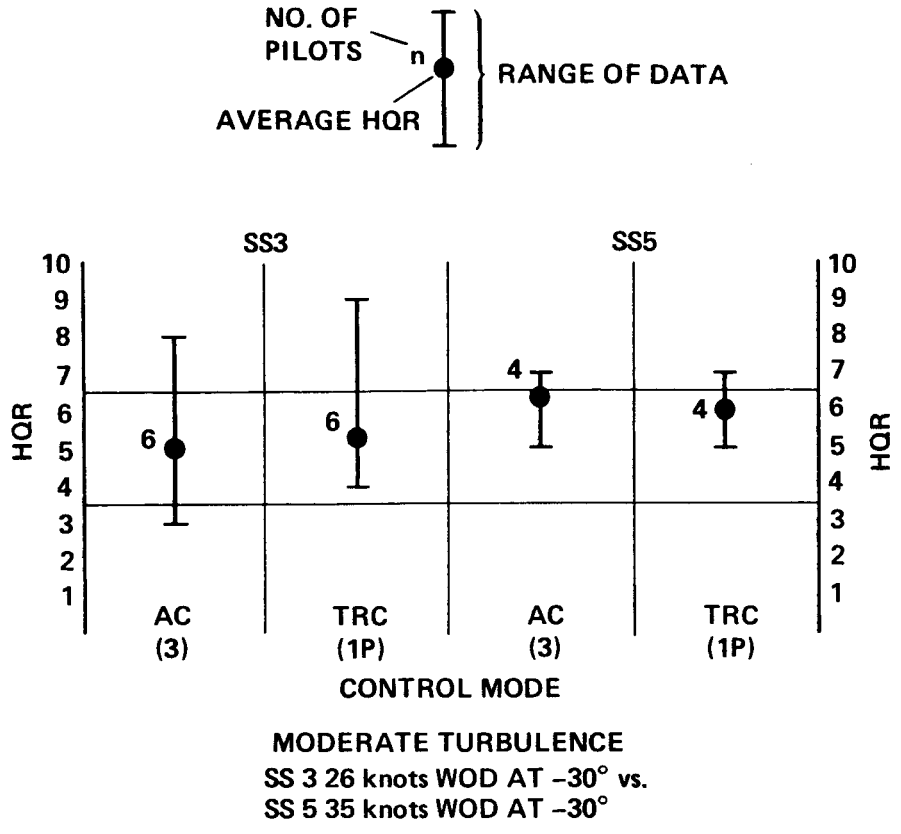

Figure 27.- SS 3 vs SS 5. Rate command vs attitude command: pilot ratings--phase III.

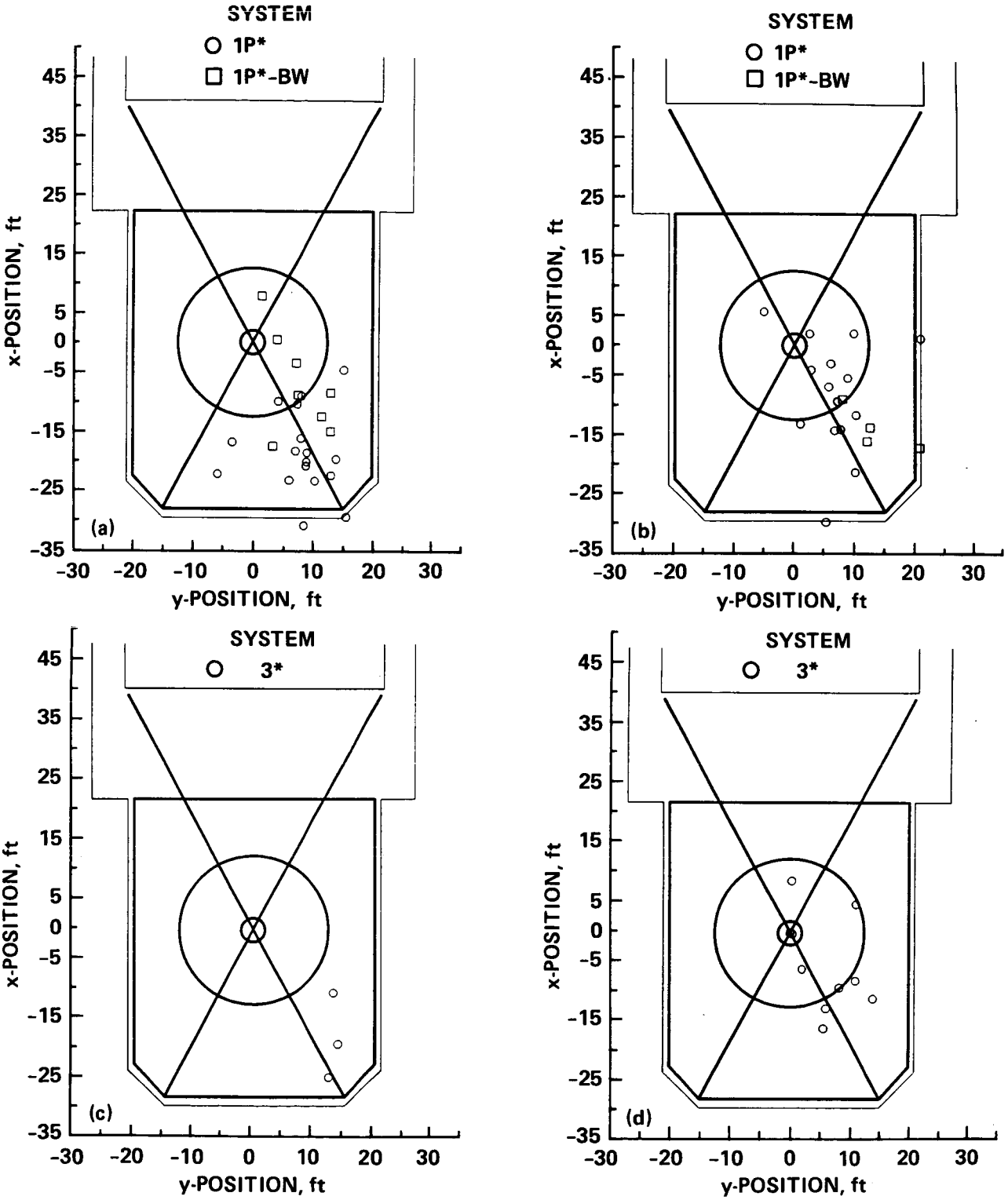

Figure 28.- DD-963 TD Dispersions. (a) Control system 1P, SS 3. (b) Control system 1P*, SS 5. (c) Control system 3*, SS 3. (d) Control system 3*, SS 5.

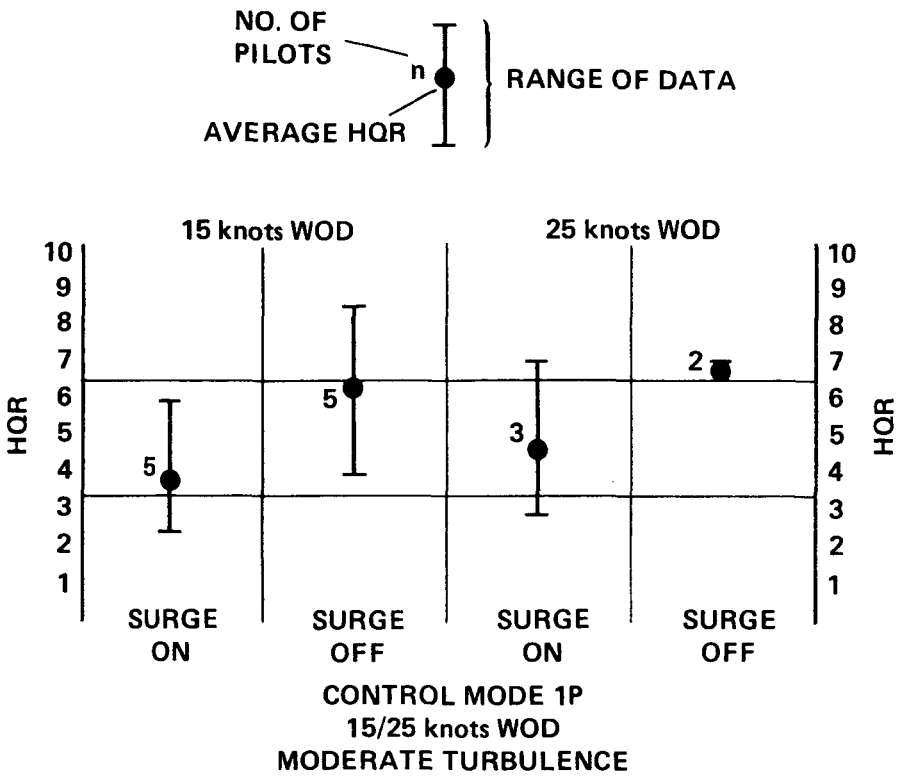

Figure 29.- Spot turns: surge control--phase III.

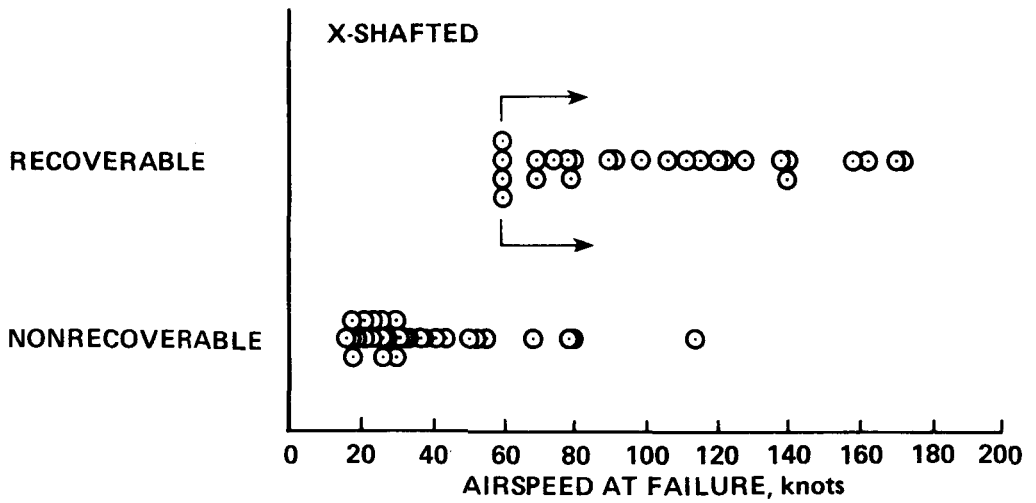

Figure 30.- Minimum recovery speed: cross-shafted engines--phase III.

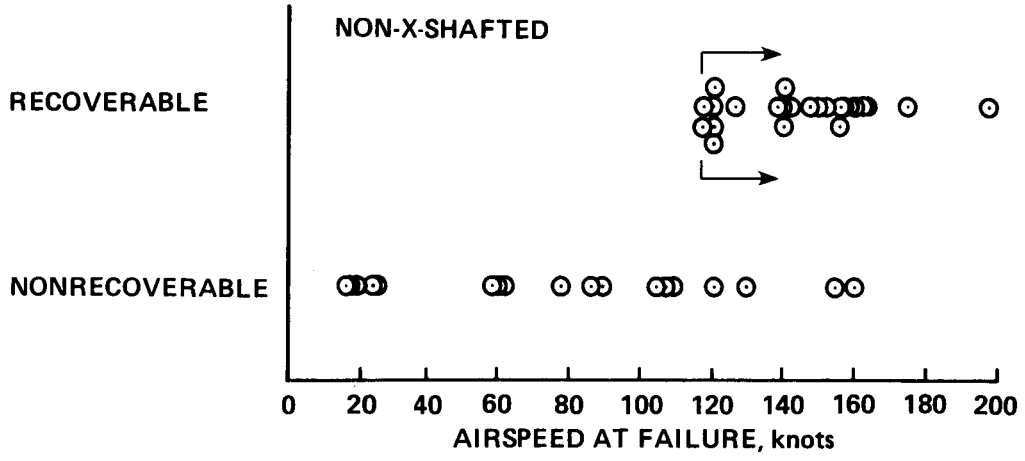

Figure 31.- Minimum recovery speed: noncross-shafted engines--phase III.

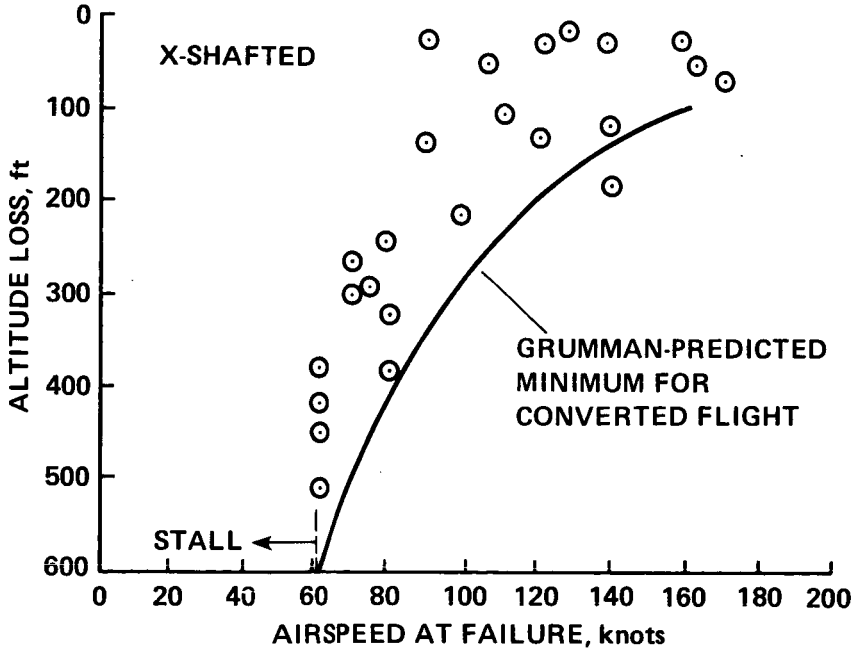

Figure 32.- Altitude loss following an engine failure: cross-shafted engines--phase III.

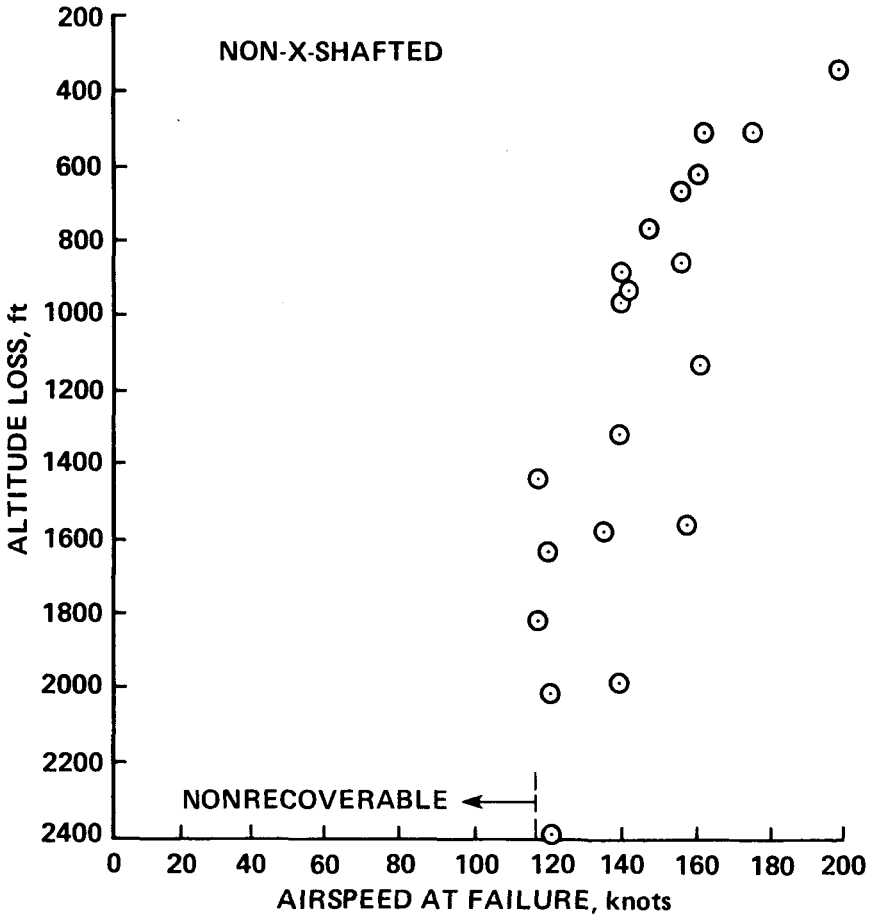

Figure 33.- Altitude loss following an engine failure: noncross-shafted engines--phase III.

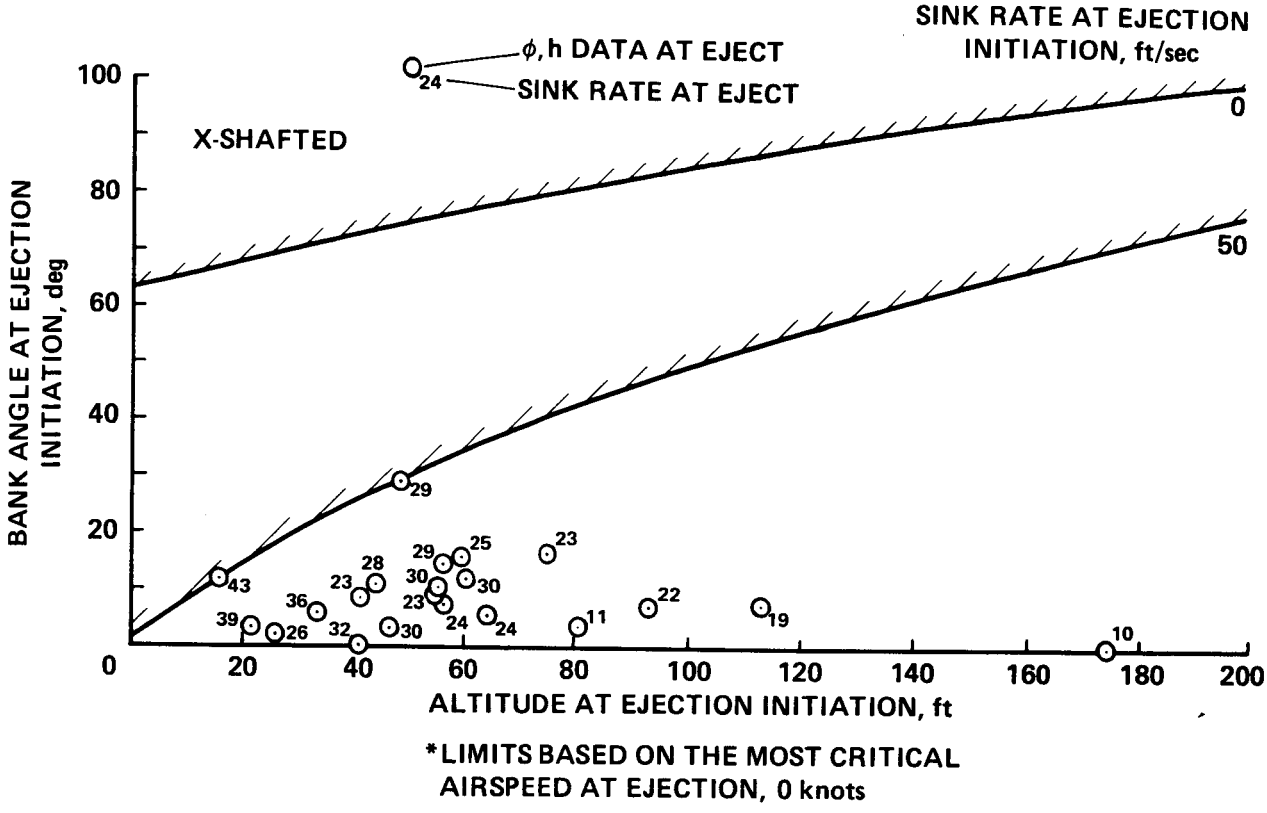

Figure 34.- Simulated ejections vs MK 10 ejection seat envelope: cross-shafted engines--phase III.

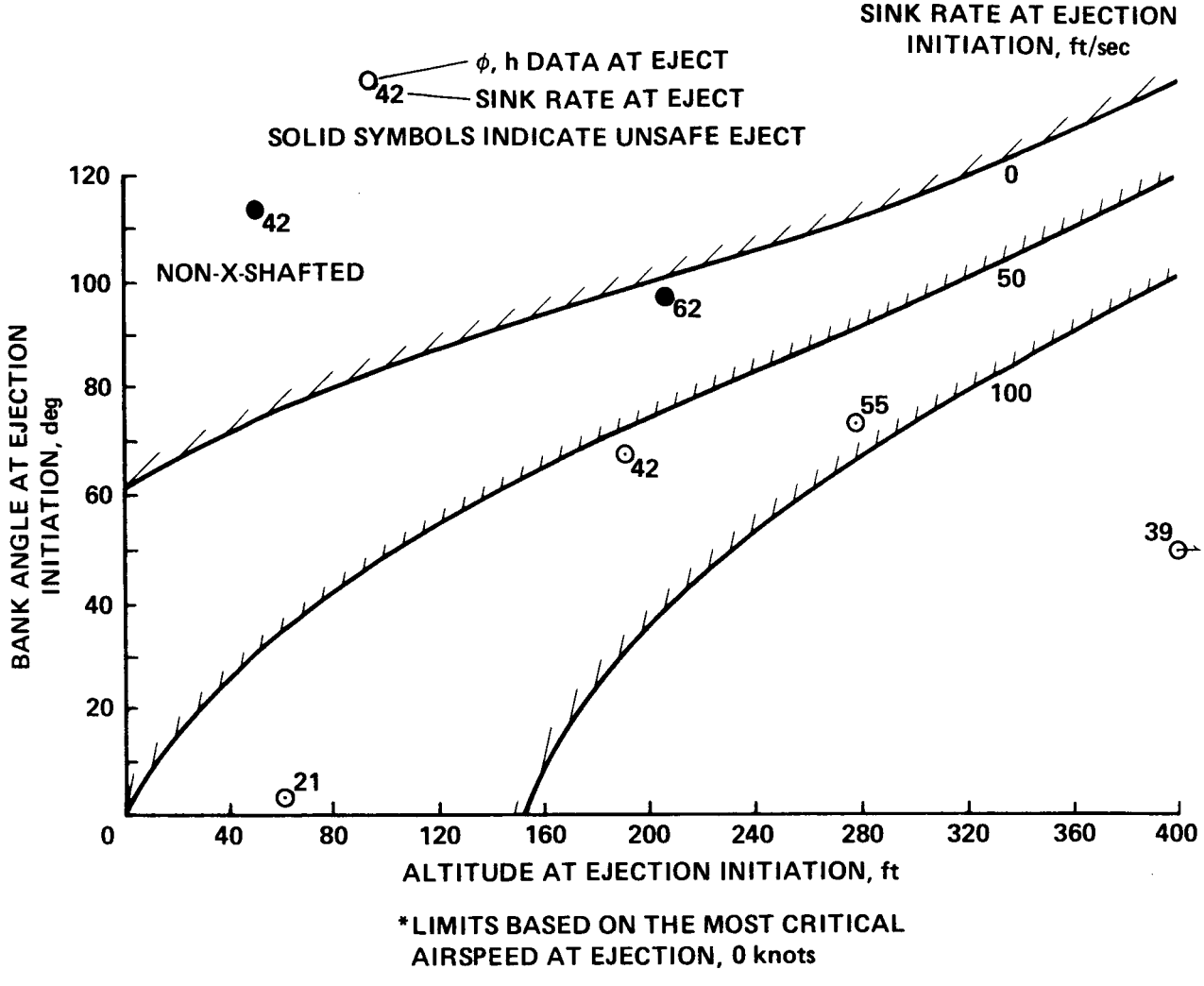

Figure 35.- Simulated ejections vs MK 10 ejection seat envelope: noncross-shafted engines--phase III

1. Report No.	2. Government Accession No.	3. Recipient's Catalog No.
NASA TM-86785		

4. Title and Subtitle	5. Report Date
THE HANDLING QUALITIES AND FLIGHT CHARACTERISTICS OF THE GRUMMAN DESIGN 698 SIMULATED TWIN-ENGINE TILT NACELLE V/STOL AIRCRAFT	June 1986
	6. Performing Organization Code

7. Author(s)	8. Performing Organization Report No.
Megan A. Eskey and Samuel B. Wilson, III	A-85361
	10. Work Unit No.

9. Performing Organization Name and Address	11. Contract or Grant No.
Ames Research Center Moffett Field, CA 94035	

12. Sponsoring Agency Name and Address	13. Type of Report and Period Covered
National Aeronautics and Space Administration Washington, DC 20546	Technical Memorandum
	14. Sponsoring Agency Code 505-43-01

15. Supplementary Notes

Point of Contact: Samuel B. Wilson, III, Ames Research Center, M/S 237-3
Moffett Field, CA 94035 (415) 694-5903 or FTS 464-5903

16. Abstract

This paper describes three government-conducted, piloted flight simulations of the Grumman Design 698 vertical and short takeoff and landing (V/STOL) aircraft. Emphasis is placed on the aircraft's handling qualities as rated by various NASA, Navy, and Grummand Aerospace Corporation pilots with flight experience ranging from conventional takeoff and landing (CTOL) to V/STOL aircraft. Each successive simulation incorporated modifications to the aircraft in order to resolve the flight problems which were of most concern to the pilots in the previous simulation. The objective of the first simulation was to assess the basic handling qualities of the aircraft with the noncross-shafted propulsion system. The objective of the second simulation was to examine the effects of incorporating the cross-shafted propulsion system. The objective of the third simulation was to examine inoperative-single-engine characteristics with and without cross-shafted engines.

17. Key Words (Suggested by Author(s))	18. Distribution Statement
Medium speed tilt-nacelle V/STOL aircraft Handling qualities ratings Flight simulations investigation	Unlimited Subject Category - 05

19. Security Classif. (of this report)	20. Security Classif. (of this page)	21. No. of Pages	22. Price*
Unclassified	Unclassified	110	A06

*For sale by the National Technical Information Service, Springfield, Virginia 22161